UNIVERSIDADE FEDERAL DE SÃO CARLOS
CENTRO DE CIÊNCIAS EXATAS E DE TECNOLOGIA
DEPARTAMENTO DE QUÍMICA
PROGRAMA DE PÓS-GRADUAÇÃO EM QUÍMICA

“Flow Chemistry:
From assembly to the application”

Gabriel dos Santos Scatena*

Tese apresentada como parte dos requisitos para obtenção do título de DOUTOR EM CIÊNCIAS, área de concentração: QUÍMICA ORGÂNICA.

Orientador: Prof. Dr. Márcio Weber Paixão

Coorientadora: Prof. Dr. Quezia Bezerra Cass

*** bolsista CNPq**

São Carlos – SP

2018

UNIVERSIDADE FEDERAL DE SÃO CARLOS

Centro de Ciências Exatas e de Tecnologia
Programa de Pós-Graduação em Química

Folha de Aprovação

Assinaturas dos membros da comissão examinadora que avaliou e aprovou a Defesa de Tese de Doutorado do candidato Gabriel dos Santos Scatena, realizada em 17/12/2018:

Prof. Dr. Márcio Weber Paixão
UFSCar

Prof. Dr. Ricardo Samuel Schwab
UFSCar

Prof. Dr. Leandro Helgueira de Andrade
USP

Prof. Dr. Joel Savi dos Reis
USP

Prof. Dr. Jean Marcel Ribeiro Gallo
UFSCar

Acknowledgements

Primeiramente gostaria de agradecer aos meus pais, pois sem eles nada disso seria possível, e a toda minha família, pela base criada, a qual me permitiu alcançar meus objetivos.

Gstaria de agradecer ao Professor Márcio Weber Paixão e Professora Quezia Bezerra Cass por me orientarem ao longo desses anos.

Aos colegas Alexander Fernandez de la Torre, Cassio da Silva Dias, Daniel Garcia, Gustavo Piva, Clarice Caiuby pela participação na minha formação científica e auxilio na produção dos resultados desta tese.

Ao laboratório SEPARARE e grupo CERSUSCHEM pelas sugestões, auxílios e participação direta ou indireta neste trabalho.

O presente trabalho foi realizado com apoio da Coordenação de Aperfeiçoamento de Pessoal de Nível Superior - Brasil (CAPES) - Código de Financiamento 001. Ao CNPQ pela bolsa concedida, CAPES, MES-CUBA e FAPESP pelo suporte financeiro.

A Karina Zaniolo, pelo carinho e suporte nos momentos difícies e companheirismo nos bons momentos.

A todos que de alguma forma colaboraram na realização deste trabalho e contribuíram para minha formação.

Abbreviations

ACCN: 1,1′-Azobis(cyclohexanecarbonitrile)

ACN: Acetonitrile

AIBN: Azobisisobutyronitrile

BET: Brunauer–Emmett–Teller

Boc: *tert*-butyloxycarbonyl

BZA: Benzylamine

Cbz: Carboxybenzyl

CFL: Compact fluorescent lamp

CuAAC: Copper(I)-catalyzed azide alkyne cycloaddition

DCM: Dichloromethane

DMF: Dimethylformamide

DMPU: *N,N*-Dimethylpropyleneurea

DMSO: Dimethylsulfoxide

EtOAc: Ethyl Acetate

FDA: Food and Drug Administration

FTIR: Fourier-transform infrared spectroscopy

HOMO: Highest Occupied Molecular Orbital

HPLC: High Performance Liquid Chromatography

LUMO: Lowest unoccupied Molecular Orbital

MCR: Multicomponent Reaction

MeOH: Methanol

PFA: Perfluoroalkoxy alkanes

pFA: polyFurfuryl alkanes

PTFE: Polytetrafluoroethylene

RT: Residence time

TBHP: *tert*-Butyl hydroperoxide

TFA: Trifluoroacetic acid

TGA: Thermogravimetric analysis

THF: Tetrahydrofuran

TTMSS: Tris(trimethylsilyl)silane

List of figures

List of schemes

Resumo

QUÍMICA DE FLUXO: DA MONTAGEM À APLICAÇÃO. Reações químicas vem sendo realizadas da mesma forma em vidrarias padronizadas por séculos. Em contrapartida, reações em fluxo contínuo vem ganhando interesse e seu "*hardware toolkit"* crescendo a cada dia. Para enfatizar isso, este trabalho descreve uma montagem de diferentes sistemas de reação em fluxo contínuo que possibilitaram: I. Síntese de 1,2,3-triazóis trissubstituídos usando peneira molecular como catalisador sólido; II. Aplicações organocatalíticas de pseudopeptídeos de prolina derivados de reações multicomponentes suportados em polímero renovável aplicado a adição assimétrica de Michael; III. Processo fotoquímico para a síntese de indóis e indolinas. Além disso, foi criada uma configuração instrumental que combina as vantagens da cromatografia e análise online dos parâmetros reacionais.

Abstract

FLOW CHEMISTRY: FROM THE ASSEMBLY TO THE APPLICATION. Over the centuries, chemical reactions have been carried out in the same way in standardized glassware. On the other hand, continuous flow reactions are gaining interest regularly and demand for the related hardware toolkit is also increasing every day. In this scenario, the current work describes assembly of different continuous flow reaction systems that enable: I. Synthesis of trisubstituted 1,2,3-triazoles using molecular sieve as a solid catalyst; II. Organocatalytic applications of multicomponent reaction-derived prolyl pseudo-peptide catalysts supported on the renewable polymer applied to asymmetric Michael addition; III. Photochemical process for the synthesis of indoles and indolines. Moreover, an instrumental setup configuration was created that combines the advantages of chromatography and online analysis of the reactional parameters.

Keywords: • Flow Chemistry • Catalysis • Molecular Sieve • Triazole • Organocatalysis • Asymmetric Michael addition • Renewable Polymer • Photocatalysis • Indoles • Indolines • TTMSS

Summary

1. Introduction

1.1. General Concepts

The extraordinary development of synthetic organic chemistry in the 20th century is unquestionable, in particular, due to its contribution to medicine, agriculture, and the polymeric materials industry. Historically, synthetic chemists have been using nature as a source of inspiration for the development of molecules with desired properties, such as antibiotic, antitumoral, agrochemical applications, etc. These successful strategies have based on millions of years of evolution that have led many organisms to produce stocks of chemical defenses for adaptation and survival.[1,2]

Accordingly, natural products are of fundamental importance for medicinal chemistry and its correlated areas. Evidence of this is that in the areas of antimicrobial and anticancer agents, between 35-40% of all commercial drugs are derived from natural products, while 70% are natural products or its synthetic analogues.,[3,4]

However, natural products are frequently isolated in small amounts using large amounts of biomass or microbial sources, thereby limiting their availability and their development as drugs and therapeutic agents. Traditionally, the solution to this problem is chemical synthesis, which has shown to be quite efficient in obtaining important natural products.[5,6]

Nowadays, there is a conceptual change in the synthetic strategies of molecules with high synthetic complexity. Previously, most strategies for obtaining these compounds have based on long synthetic linear sequences of high costs and very low overall yields. In fact, for the synthesis, researchers are continuing to employ mainly the techniques, resources, and types of equipment that have used for more than one hundred years. For example, the rounded bottom flasks (batch process) as glassware has mostly used for laboratory scale synthesis. There is nothing wrong in using this kind of glassware or the old fashioned techniques. However, in the modern era, we have a new and extensive

collection of techniques that allow us to obtain better results in terms of yield, reaction time and other aspects that have combined in a new term that is currently known as Green Chemistry. Thus, the use of techniques that allow real-time monitoring of the reaction medium has been fundamental in the development of new ways (such as continuous flow reactions) of doing organic synthesis. The flow reactions have become increasingly common in organic synthesis laboratories, since they allow quick achieving optimal reaction conditions, particularly when coupled with an analytical technique, such as UV, IR, MS, etc..[7–9]

1.2. Flow Chemistry: principles and key parameters

A continuous flow chemical system usually consists of three parts: a flow-promoting device that consists of a syringe pump, peristaltic pump or even a gravitational force, a reactor where the reaction actually occurs that could be heated, cooled, filled with catalyst, light irradiated while the third part is a fraction collector or analyzer where sample could be manually collected and analyzed by thin-layer chromatography or automated with an online analysis such as infrared technique.The reactor is the heart of the system, providing fast mixing and energy transfer mainly due to the small channel diameter. These reactors can be made locally or purchased and can be of the order of 10 to 1000 μm, thus called microreactors (reactors greater than 1000 μm are called meso-reactor). Nowadays, reactors are widely commercially available in the most diverse form of materials, depending on the specific application and sometimes budget constraint. Materials such as glass, quartz, stainless steel, fluoropolymers (e.g. Polytetrafluoroethylene, PTFE; and Perfluoroalkoxy alkanes, PFA) has broadly applied due to its chemical and physical resistance, optical transparency, and in some cases, flexibility. Therefore, for each reaction, a particular choice of reactor material could be applied. For example, a reaction involving high temperature and pressure, the material of choice may be stainless steel, while for a photocatalyzed reaction, PFA is the most appropriate material to be used.[10,11]

In addition, there are many types of reactors such as chip (a), columns (b,c), coil-type or tubular (d,e) and each type of reactor can be used for a specific purpose.**Figure 1**.

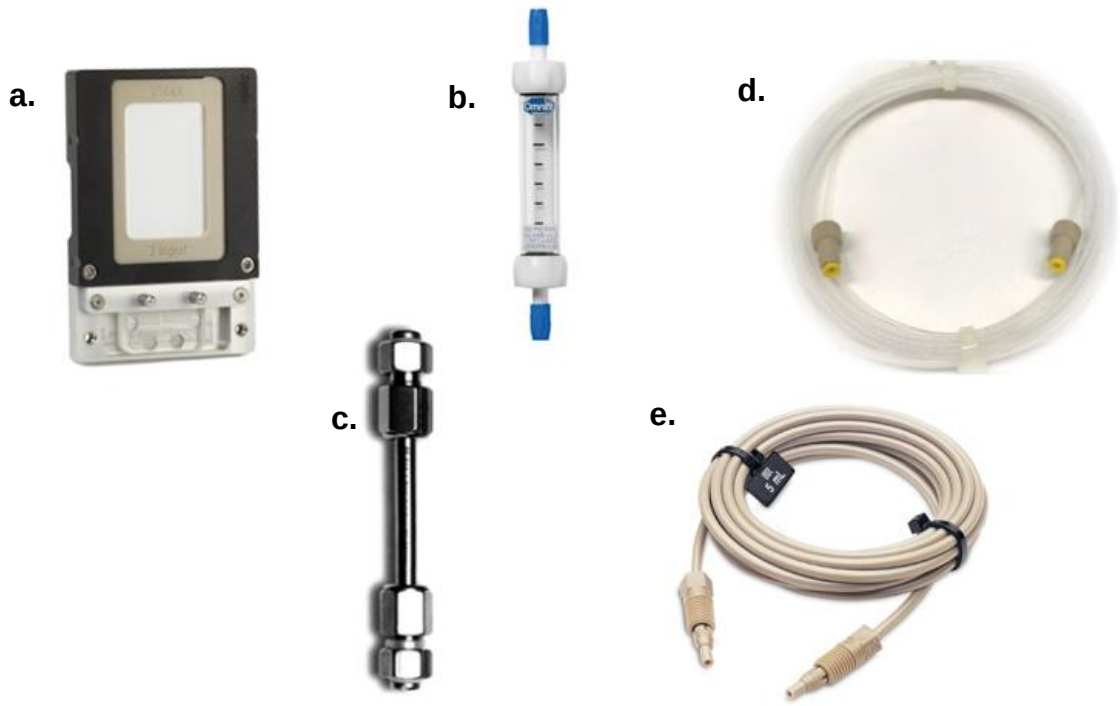

Figure 1. Types of flow reactors: chip, column, and tubular.

The construction of such systems in the laboratory could easily be achieved by the use of tubular reactors or columns, as most of the outfit used for the assembly are coming from HPLC connections (e.g.: T-split, Y-split, backpressure regulator, end fittings, and stainless steel, etc).Another important factor is that the system becomes easily pair with the HPLC and thus can be connected directly to a detector, e.g., a UV-Vis detector to the chromatographic system so that the desired compounds could be isolated with high purity and maximum quantity.[12,13]

In order to use the flow chemistry, some key parameters should be considered. The main parameter of a continuous flow reaction is the **Residence Time (RT)**, which is the ratio of the total reactor volume to the total flow rate.

$$RT\ (\mathrm{min}) = reactor\ volume\ (\mu L)/\ total\ flow\ rate\ (\mu l/\mathrm{min})$$

Productivity (mg/mg/day): The mass of product obtained using a determined mass of the catalyst per day.

$$Productivity = mass\ of\ product\ (mg)/\ mass\ of\ catalyst\ (mg)/day$$

Productivity (for a non-catalyzed reaction): The mass of the product obtained per day.

$$Productivity = mass\ of\ product\ (mg)/day$$

TON (turnover number): The number of substrate moles for which one mole of catalyst can transform before becoming inactivated. An ideal catalyst would have an infinitely large TON. In practice this number varies between10^2 and 10^6.

TOF (turnover frequency): The turnover number (TON) divided by time.

The rate of the flow which depends on the nature of the sample is an important factor of fluidic in pipes or tubes, which is imperative to know before begin running the setup. The Reynolds number (Re) explain this that it is the ratio of inertial forces to viscous force in a determinate reactor or tube.[14–16] Therefore, the reactor dimensions and fluid velocity are used for calculations:

$$Re = \frac{puL}{\mu} = \frac{uL}{v}$$

where:

ρ: density of the fluid

u: velocity of the fluid

L: linear dimension

μ: dynamic viscosity of the fluid

v: kinematic viscosity of the fluid .

The equation, which can be rearranged for flow in reactor or tube, is given bellow:

$$Re = \frac{puD}{\mu} = \frac{uD}{v} = \frac{QD}{vA}$$

where:

D: diameter of the tube

Q: volumetric flow rate

A: tube cross-sectional area

u: mean velocity of the fluid

μ: dynamic viscosity of the fluid

v: kinematic viscosity (*v = μ/ρ*)

ρ: density of the fluid.

There are three types of flow:

- **Laminar,** soft and smooth flow, generally occurs in small tubes and low flow velocities, the innermost fluid flows faster: *Re < 2300.*
- **Transient,** flow regime between the laminar and turbulent: *2300 < Re < 4000.*
- **Turbulent,** uneven flow regime, produce chaotic eddies and vortices. Generally, occurs in high flow velocities: *4000 < Re.*

Turbulent flow provides a better mixing and energy transfer in microreactors and should be considered as an option for organic reactions.

The Reynolds number can also be used for predicting the type of flow packed reactor with approximately spherical particles:

$$Re = pv_s D/\mu$$

Where:

D: diameter

***ε**: voidage; porosity*

ρ: density of the fluid

v_s*: superficial velocity.*

In this case, Laminar flow Re < 10, fully turbulent flow Re > 2000.

Most of the reactors uses **laminar flow** because small tubes and low flow velocities are commonly used. Therefore, if the Re is lower than 2300, the flow is laminar. For packed bed reactors the Re should be lower than 10, for that reason most of the tubular reactors must use a pre-mixer to increase the homogeneity of the reaction. For a packed bed reactor, it is important to take into account the shape and porosity of the particles.

One example of of such technique is to determine total porosity of a solid catalyst, ***ε,*** is Pycnometry.[17] This method comprises in filling the microreactor sequentially with two distinct miscible solvents that have different densities, (for example ethanol and *n*-hexane) and then accurately weighting the filled microreactor with each solvent. The difference between the masses of a filled reactor divided by the differences of solvent densities permits to calculate the microreactor void volume (V_0 - dead volume). This feature is important because it provides an idea of the volume not utilized in the microreactor, i.e. the total porosity of the reactor bed. Also, the final total amount of packed material in the reactor can be determined by pycnometry.

$$V_0 = (w_{s2} - w_{s1})/(d_2 - d_1)$$

$$V_G = \pi h r^2$$

$$V_{Bed} = V_G - V_0$$

$$\varepsilon = V_0 / V_G$$

Where:

h: Length of reactor

r: Radius of reactor

V_0: Dead volume

V_G: Geometric volume

V_{bed}: Catalyst Volume

d: Density of the solvent

ε: Total porosity.

Another technique that is broadly applied to determine total porosity of a solid catalyst and also the total surface area is Brunauer–Emmett–Teller (BET). [18] It consists of the physical adsorption of gas molecules (usually nitrogen) on the solid surface.

1.3. Catalysis and flow chemistry

Catalysis is the most important subject to large-scale production of chemicals, polymers, and pharmaceuticals. It is involvedin the production of the vast majority of the products we consume today and represents a market that moves trillions of dollars a year. In this way, it is vital to use the catalysts in the most efficient way, that is to achieve maximum productivity with minimum deactivation.

In this context, a good strategy to turn the process more efficient and productive is through allying catalysis with continuous flow regime. In organic chemistry, most reactions are carried out in the liquid phase, so if the catalyst specie is in the same phase as that of the solvent and reagents, it is called homogeneous. On the other hand, if it is insoluble solid, the catalytic condition is heterogeneous.

A broad range of heterogeneous catalysts have used nowadays, metals like platinum for hydrogenation, cracking of gas oil by zeolites, olefin polymerization Ziegler–Natta by titanium (III) chloride. Those materials are effective catalysts and its performance depends on its shape, size, crystalline structure, among other properties.[19]

Another possibility is, to tether the functional groups of organic catalyst to the surface of a material, that act as support, i.e. organic supports (resins, polymers) or inorganic supports (zeolites, silica).[20–23] Each support have unique characteristics. In general it is ideal that they have high physical (abrasion, pressure, temperature) and chemical stability (pH, leaching, and solubility).

The process of tethering, grafting, supporting or immobilizing or even using a material with different phase of the reaction media, is known as “catalyst heteregenization”. A physical process (i.e. adsorption) or a chemical process (i.e. covalently bond) could be used to get a heterogeneous catalyst from a solid support.

In terms of heterogeneous catalysis, another important factor required for the catalyst is the maximum possible surface area for a maxium quantity of material, maximizing the mass and energy transfer, and consequently the reaction rate. For this reason, it is convenient to use the particles of reduced size and a high area to volume or weight ratio. Generally, these particles containing a well-defined porous structure to maximize surface area, mimicing the homogeneous catalysis.[24]

Once the heterogeneous catalyst is obtained and selected for a given reaction then the selection of appropriate synthetic technique is of paramount importance. Most of the laboratory chemical processes are still based on batch reactions, although new techniques are being implemented and produced. In this

regards, rounded bottom flasks and bench column isolation product remain the most recurrent form of work. The main disadvantage of the traditional bench technique is that the optimization of the reaction is slow and tedious. Generally, Each reaction parameter is independently modified in order to obtain the ideal reaction condition, increasing the expended time, reagent expenses and the cost of the whole process.[25]

Continuous flow reactions can be used to overcome this problem. The flow reactions have a number of advantages such as: better mass and heat transfer efficiency, ease of hyphenation to purification and analysis, reaction scaling through numbering-up, and the possibility of multiple sequential reactions. In addition, the ease of product purification and recovery/recycling of the catalyst from the reaction medium for further reuse, makes the continuous flow reactions an important ally for the synthesis of organic chemicals. Some of the leading advantages of flow techniques are given bellow.

- ✓ **Safety:** Usually the flow reactor could be considered as an isolated system, dealing with smaller volumes that permits easy handling and also make easy to work under anhydrous, sensitive air or dangerous conditions.[26]
- ✓ The use of several reactors in parallel and numbering up, allow achieve the same residence time by just recalculating the total flow rate, multiplying the initial flow rate by the total number of columns that allows obtaining exactly the same results. It is also possible to design a bigger reactor that has the same residence time. So, the **scaling up** of reaction become straightforward.[27]
- ✓ Many techniques can be coupled to the flow systems such as precipitation, liquid/liquid extraction, solid phase scavenging, and chromatographic separation. All these coupling are helpful in avoiding the time consuming and laborious **purification** steps.[28]
- ✓ Practically, reaction temperature can be well controlled due to the small channels and the large area to volume ratio mixing and heat/cooling occurs instantly. **Heat and mass transfers** are much efficient.[29]
- ✓ The system could be arranged in a continuous sequence, in other words, **multistep reactions** could be done in a single system.[30]

- ✓ The reaction progress online monitoring systems is less efforting, facilitating operational and experimental planning, thus reaction parameters (concentration and proportional of reagents, temperature, pressure and flow rate) can be easily improved. It gives a better knowledge of reactional system (kinetics and thermodynamic). **Automated system** presents a decrease in costs in terms of solvents, reagents, and in reactional time.[31,32]

However, some disadvantages are inherent in using continuous flow chemistry. If maximum yield is desired, the instrumental setup should generally be optimized for each synthesis of a new compound. Though for the synthesis of analogues, standard condition could be used to save time and reagents. Moreover, there are a number of ways to perform reactions using solids and suspensions as reagents, but their use is not trivial, usually requires specifically developed equipment or setup for this purpose. Also, the cost of a commercially available equipment could be discouraging.

Despite this, in recent years there is a considerable growth in the use of "home-made" continuous flow setups. This allows students and researchers to learn the conceptual and practical modern flow chemistry with a broad range of applications. Using an old HPLC pump and some inexpensive hardware, Czarnocki et al. describes a flow photochemistry setup for total synthesis of (+)-Epigalcatin **Scheme 1.**[33]

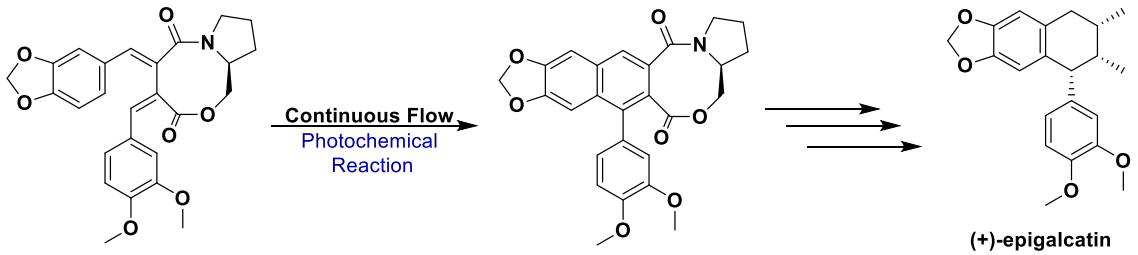

Scheme 1. Flow photochemistry as a tool for the total synthesis of (+)-epigalcatin.

1.4. Photochemistry

Each hour our planet receives more than $4x10^{20}$ Joules of energy from the Sun. To have a better notion, that was the total amount of energy used in the world during the whole year in 2013.[34]

Very recently, the human being initiated to use the sun light as a way to obtain energy effectivelyInspiring the plants and algae that already uses the process of photosynthesis, a natural process, for over 700 million years.

Using an ordered array of light-harvesting pigments, those organisms are capable of getting energy efficiently in a series of cascading electron transfers of pigment compounds from lower to higher energy states. Finally, they reduce carbondioxide (CO_2) to sugars, which are converted into several organic compounds of interest.[35]

The sunlight comes to Earth's surface in different wavelengths and energy, most of them are in the infrared reagion (700 nm, 54%), visible (400-700 nm, 42%) and ultraviolet (below 400 nm, 4%). [36] The radiation from the Sun could be used for the energy generation on Earth as an inexhaustible and sustaintable resource. For example, infrared could be applied for thermic heat, as well, ultraviolet and visible light can be use as energy source to chemical light-harvesting.

Different energy sources give different results in terms of reaction efficiency and selectivity (i.e. thermic heat, light, ultrasound, etc.). The use of light could be advantageous since the energy can be precisely selected by the wavelength. The energy and wavelength are correlated by Plank's Equation:

$$\boldsymbol{E = h\upsilon = hc/\lambda}$$

Where:

E: energy of a photon,

$\boldsymbol{\upsilon}$: frequency of radiation,

h: Planck's constant,

c: speed of light,

λ: wavelength of the radiation.

The Plank's Equation combined with UV-Vis absorbance spectrometry could be used to estimate the difference between the highest-energy occupied molecular orbital (HOMO) and the lowest energy unoccupied molecular orbital (LUMO). Therefore, the specific wavelenght of the reaction setup could be estimated to ensure the reaction selectivity.

A Photochemistry process starts with a photoexcitation, which is the absorption of energy by a chemical compound to reach a higher energy state. Those process follow two rules:

-The first law (Grotthuss–Draper law)

States that light must be absorbed by a chemical substance so that a photochemical reaction occurs.

-The second law of photochemistry (Stark-Einstein law)

States that in a chemical system, no more than one molecule is activated for each photon of light absorbed. It could be defined numerically as Quantum Yield.

A photochemical process can lead to the formation of various energy states and transitions between them. In order to summarize, generally an energy diagram or Jablonski diagram is used to describe these states, which can be divided into radiative transitions (indicated by straight arrows) or non-radiative transitions (indicated by wavy arrows) figure 2.

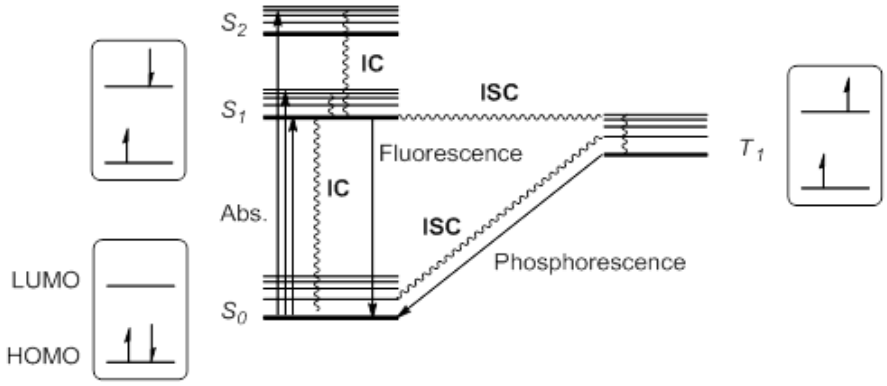

Figure 2. Jablonski diagram: IC – internal conversion, ISC – intersystem crossing.

The Jablonski diagram represents vertically the energy level and horizontally the spin multiplicity. Thicker horizontal lines represent vibrational fundamental states of each electronic state, while thinner lines represent higher vibrational states.

If one electron excited from the ground state (S_0) to a higher orbital, it maintains its spin according to the spin rule selection, other transitions would violate the law of conservation of angular momentum.

There are two decays transitions, fluorescence and phosphorescence:

Fluorescence is the process where the emission of radiation of the formed species has the same spin multiplicity as the excited state, most often from S_1 to S_0 for instance. Time scale: 10^{-9} - 10^{-7} s.

Whereas, in the phosphorescence, the multiplicity of spin is changed, which is forbidden by spin selection rules, generally from T_1 to S_0. Triplet state usually are less energetic and have longer lifetime than singlet. Time scale: 10^{-4} - 10^{-1} s.

In the non-radiative transitions, represented by curly waves in the diagram where the energy is released as heat. The internal conversion occurs very fast, between 10^{-14} and 10^{-11} seconds and the spin state remains the same (S_1 to S_0, S_2 to S_1). While in the intersystem crossing, the spin multiplicity is changed from an excited singlet state S_1 to the excited triplet T_1 state. This transition is forbidden by electronic selection rules, but it slowly occurs by vibrational coupling, competing with the time scale of fluorescence.

Importantly, once an excited state with distinc eletronic distribution is reached, the reactivity of the ground state molecule is altered. that might result in a different chemical reactivity. [37,38]

A range of photochemical reactions using visible or ultraviolet light has been described: such as eliminations, photodegradation, rearrangements, isomerizations, additions, among other reactions. Different activation processes may occur in order to promote the photoreaction such as direct excitation, energy transfer through photosensitization and photo-induced electron transfer processes.[39–42]

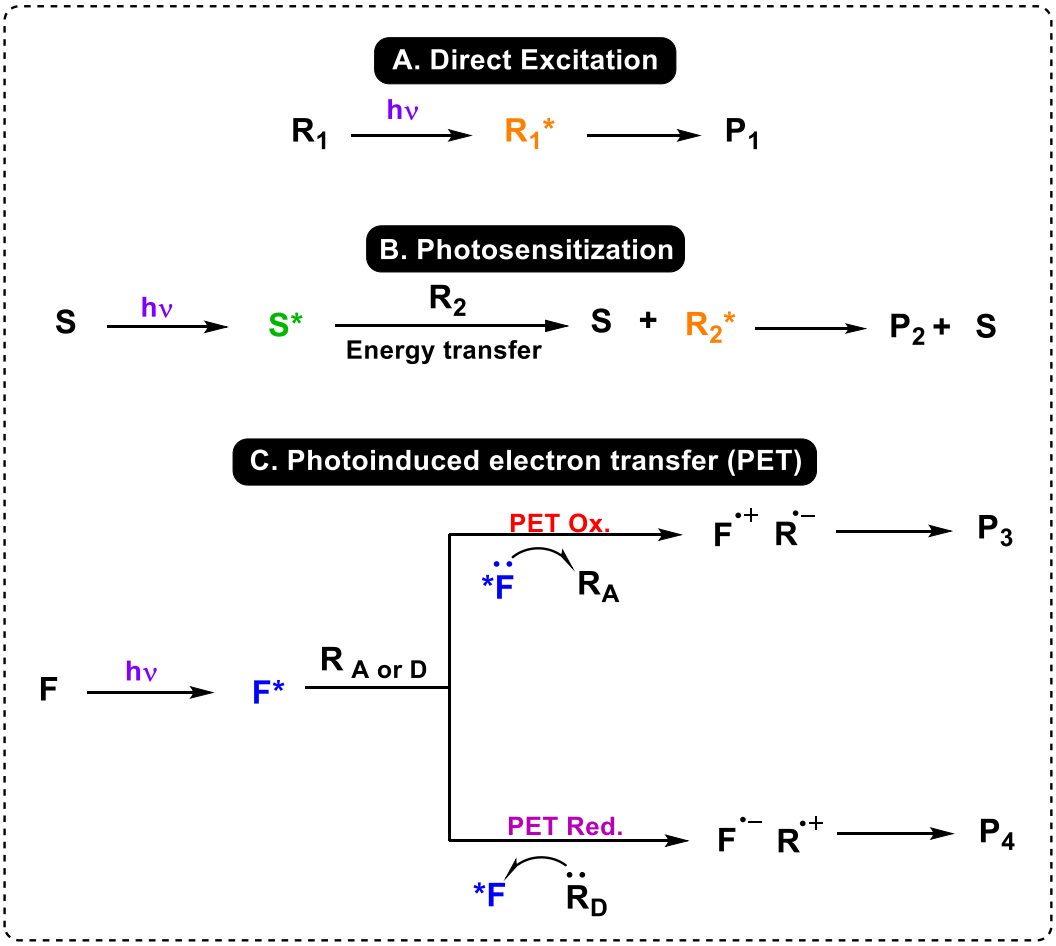

Scheme 2. General mechanisms of photochemical reactions -. R = Substrate or cocatalyst. P = Product. S = Photosensitizer. F = Photoredox molecule. A = Electron acceptor. D = Electron donor.

In the direct excitation process (**Scheme 2A**), the molecule that absorbs light, directly participates in the reaction to convert into product. However, a drawback of this methodology is that many organic compounds could not be directly photoexcited because there is no absorption take palce in the range of visible spectrum. As the use of more energetic radiation in the ultraviolet range could lead to the degradation of the substrate. To overcame this drawback of energy transfer, a process of photosensitization can be used (**Scheme 2B**). In this mechanism reactions can occur through an easily excitable chemical species that allowing the reaction to proceed by bringing it to an excited state, for example a dye, present in the reaction medium, which can transfer the energy to a substrate or co-catalyst in its fundamental state. Other possible mechanism is photoinduced electron transfer - PET (**Scheme 2C**). It consists of an excited state

electron transfer process from donor to acceptor that resulting in the chemical transformations. The excited species may return to the ground electronic state without being consumed or acting as the initiator of the photochemical reactions and not necessarily are restored at the end of the reaction.[43]

The increasing recognition due to the chemical and environmental benefits, has stimulated the scientific community in the search for photoinduced methodologies in the field of new synthetic strategies development. Photochemical reactions are more efficiently energetic as compared to the conventional thermal methods due to the narrow energy distribution.

Heterocyclic compounds constitute an important chemical class encompassing more than half of all known organic compounds and are presented as key structural units in pharmaceuticals and agrochemicals. In organic synthesis, these compounds are extremely relevant because they can be used in several synthetic strategies, acting as protecting groups, chiral auxiliaries, asymmetric catalysts as well as important building blocks for total synthesis.

Thus, the combination of photochemistry and strategies for the production of nitrogenous heterocyclic compounds is extremely important. Taking into account the sustainability of the process, the TTMSS - Tris(trimethylsilyl)silane reagent appears as a sustainable alternative for the production of these compounds and it can be used as a substitute for Bu_3SnH, in radical reactions.

TTMSS is generally applied in reduction reactions but it can also be used in a wide range of transformations, such as dehalogenation, decarboxylation, addition to the double and triple bonds, formation of inter- and intramolecular C-C bonding. Generally, those reactions involve radical initiators such as AIBN or ACCN in solvents like toluene. Thus, it is imperative that TTMSS can be effectively exploited as alternative radical source to develop sustainable methodologies in organic synthesis.

The ability of TTMSS is of generating radicals through atmospheric air or by light absorption substitutes using the radical initiators and represent a greener alternative to the other methods that involving dangerous or toxic reagents. For example, the reductive dehalogenation reaction that generate molecular oxygen

in atmospheric air, react with the silane to form silicon radicals and subsequent reductive dehalogenation of the substrate take place[44] (**Scheme 3B**). Moreover, the reaction could also proceed photochemically, using the white compact fluorescent lamp. The radical can be formed at the aryl bromide specie and then can abstract hydrogen from the TTMSS, which will form silyl radical that is necessary for the chain propagation step of the reaction (**Scheme 3A**).[45] The latter mentioned mechanism needs further investigation in order to confirm as the homolytic cleavage of the Si-H bond by visible light does not occurs, since the TTMSS has no significant absorbance above the 210 nm which is not very likely to happen.

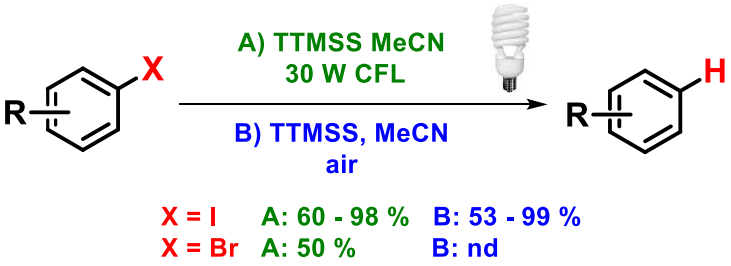

Scheme 3. Radical dehalogenation of aryl compounds using TTMSS.

1.5. References

(1) POHNERT, G. Chemical Defense Strategies of Marine Organisms. In *Topics in current chemistry*; 2004;Vol.239, pp 179–219.

https://doi.org/10.1007/b95453.

(2) MITHÖFER, A.; BOLAND, W. Plant Defense Against Herbivores: Chemical Aspects. *Annu. Rev. Plant Biol.* **2012**, *63* (1), 431–450.

https://doi.org/10.1146/annurev-arplant-042110-103854.

(3) LAM, K. S. New aspects of natural products in drug discovery. *Trends Microbiol.* **2007**, *15* (6), 279–289.

https://doi.org/10.1016/J.TIM.2007.04.001.

(4) GORDON M. CRAGG; DAVID J. NEWMAN, AND; SNADER, K. M. Natural Products in Drug Discovery and Development. **1997**.

https://doi.org/10.1021/NP9604893.

(5) MAIER, M. E. Design and synthesis of analogues of natural products. *Org. Biomol. Chem.* **2015**, *13* (19), 5302–5343.

https://doi.org/10.1039/C5OB00169B.

(6) M. CARREIRA, E. Natural Products Synthesis: A Personal Retrospective and Outlook. *Isr. J. Chem.* **2018**, *58* (1–2), 114–121.

https://doi.org/10.1002/ijch.201700127.

(7) DALLINGER, D.; KAPPE, C. O. Why flow means green – Evaluating the merits of continuous processing in the context of sustainability. *Curr. Opin. Green Sustain. Chem.* **2017**, *7*, 6–12.

https://doi.org/10.1016/J.COGSC.2017.06.003.

(8) MCQUADE, D. T.; SEEBERGER, P. H. Applying Flow Chemistry: Methods, Materials, and Multistep Synthesis. *J. Org. Chem.* **2013**, *78* (13), 6384–6389. https://doi.org/10.1021/jo400583m.

(9) FITZPATRICK, D. E.; BATTILOCCHIO, C.; LEY, S. V. A Novel Internet-Based Reaction Monitoring, Control and Autonomous Self-Optimization Platform for Chemical Synthesis. *Org. Process Res. Dev.* **2016**, *20* (2), 386–394. https://doi.org/10.1021/acs.oprd.5b00313.

(10) PLUTSCHACK, M. B.; PIEBER, B.; GILMORE, K.; SEEBERGER, P. H. The Hitchhiker's Guide to Flow Chemistry. *Chem. Rev.* **2017**, *117* (18), 11796–11893. https://doi.org/10.1021/acs.chemrev.7b00183.

(11) BRITTON, J.; RASTON, C. L. Multi-step continuous-flow synthesis. *Chem. Soc. Rev.* **2017**, *46* (5), 1250–1271. https://doi.org/10.1039/C6CS00830E.

(12) CAPEL, A. J.; WRIGHT, A.; HARDING, M. J.; WEAVER, G. W.; LI, Y.; HARRIS, R. A.; EDMONDSON, S.; GOODRIDGE, R. D.; CHRISTIE, S. D. R. 3D printed fluidics with embedded analytic functionality for automated reaction optimisation. *Beilstein J. Org. Chem.* **2017**, *13*, 111–119.

https://doi.org/10.3762/bjoc.13.14.

(13) FITZPATRICK, D. E.; MUTTON, R. J.; LEY, S. V. In-line separation of multicomponent reaction mixtures using a new semi-continuous supercritical fluid chromatography system. *React. Chem. Eng.* **2018**, *3* (5), 799–806. https://doi.org/10.1039/C8RE00107C.

(14) PEDRAS, M. H. J.; DE LEMOS, M. J. S. Macroscopic turbulence modeling for incompressible flow through undeformable porous media. *Int. J. Heat Mass Transf.* **2001**, *44* (6), 1081–1093. https://doi.org/10.1016/S0017-9310(00)00202-7.

(15) HORTON, N. A.; POKRAJAC, D. Onset of turbulence in a regular porous medium: An experimental study. *Phys. Fluids* **2009**, *21* (4), 045104. https://doi.org/10.1063/1.3091944.

(16) SEGUIN, D.; MONTILLET, A.; COMITI, J. Experimental characterisation of flow regimes in various porous media—I: Limit of laminar flow regime. *Chem. Eng. Sci.* **1998**, *53* (21), 3751–3761. https://doi.org/10.1016/S0009-2509(98)00175-4.

(17) SCATENA, G. S.; DE LA TORRE, A. F.; CASS, Q. B.; RIVERA, D. G.; PAIXÃO, M.

W. Multicomponent Approach to Silica-Grafted Peptide Catalysts: A 3 D Continuous-Flow Organocatalytic System with On-line Monitoring of Conversion and Stereoselectivity. *ChemCatChem* **2014**, *6* (11), 3208–3214. https://doi.org/10.1002/cctc.201402501.

(18) LEOFANTI, G.; PADOVAN, M.; TOZZOLA, G.; VENTURELLI, B. Surface area and pore texture of catalysts. *Catal. Today* **1998**, *41* (1–3), 207–219. https://doi.org/10.1016/S0920-5861(98)00050-9.

(19) LLOYD, L. *Handbook of Industrial Catalysts*; Springer Science + Business Media, 2006.

(20) RODRÍGUEZ-ESCRICH, C.; PERICÀS, M. A. Catalytic Enantioselective Flow Processes with Solid-Supported Chiral Catalysts. *Chem. Rec.* **2018**. https://doi.org/10.1002/tcr.201800097.

(21) LIANG, J.; LIANG, Z.; ZOU, R.; ZHAO, Y. Heterogeneous Catalysis in Zeolites, Mesoporous Silica, and Metal-Organic Frameworks. *Adv. Mater.* **2017**, *29* (30), 1701139. https://doi.org/10.1002/adma.201701139.

(22) SHEN, G.; OSAKO, T.; NAGAOSA, M.; UOZUMI, Y. Aqueous Asymmetric 1,4-Addition of Arylboronic Acids to Enones Catalyzed by an Amphiphilic Resin-Supported Chiral Diene Rhodium Complex under Batch and Continuous-Flow Conditions. *J. Org. Chem.* **2018**, *83* (14), 7380–7387. https://doi.org/10.1021/acs.joc.8b00178.

(23) CHEN, X.; JIANG, H.; HOU, B.; GONG, W.; LIU, Y.; CUI, Y. Boosting Chemical Stability, Catalytic Activity, and Enantioselectivity of Metal–Organic Frameworks for Batch and Flow Reactions. *J. Am. Chem. Soc.* **2017**, *139* (38), 13476–13482. https://doi.org/10.1021/jacs.7b06459.

(24) TANIMU, A.; JAENICKE, S.; ALHOOSHANI, K. Heterogeneous catalysis in continuous flow microreactors: A review of methods and applications. *Chem. Eng. J.* **2017**, *327*, 792–821.

https://doi.org/10.1016/J.CEJ.2017.06.161.

(25) REIZMAN, B. J.; JENSEN, K. F. Feedback in Flow for Accelerated Reaction Development. *Acc. Chem. Res.* **2016**, *49* (9), 1786–1796.

https://doi.org/10.1021/acs.accounts.6b00261.

(26) FANELLI, F.; PARISI, G.; DEGENNARO, L.; LUISI, R. Contribution of microreactor technology and flow chemistry to the development of green and sustainable synthesis. *Beilstein J. Org. Chem.* **2017**, *13*, 520–542. https://doi.org/10.3762/bjoc.13.51.

(27) NAGAKI, A.; HIROSE, K.; TONOMURA, O.; TANIGUCHI, S.; TAGA, T.; HASEBE, S.; ISHIZUKA, N.; YOSHIDA, J. Design of a Numbering-up System of Monolithic Microreactors and Its Application to Synthesis of a Key Intermediate of Valsartan. *Org. Process Res. Dev.* **2016**, *20* (3), 687–691. https://doi.org/10.1021/acs.oprd.5b00414.

(28) HOHMANN, L.; KURT, S. K.; SOBOLL, S.; KOCKMANN, N. Separation units and equipment for lab-scale process development. *J. Flow Chem.* **2016**, *6* (3), 181–190. https://doi.org/10.1556/1846.2016.00024.

(29) HUNT, G.; TORABI, M.; GOVONE, L.; KARIMI, N.; MEHDIZADEH, A. Two-dimensional heat and mass transfer and thermodynamic analyses of porous microreactors with Soret and thermal radiation effects—An analytical approach. *Chem. Eng. Process. - Process Intensif.* **2018**, *126*, 190–205. https://doi.org/10.1016/J.CEP.2018.02.025.

(30) SAHOO, H. R.; KRALJ, J. G.; JENSEN, K. F. Multistep Continuous-Flow Microchemical Synthesis Involving Multiple Reactions and Separations. *Angew. Chemie Int. Ed.* **2007**, *46* (30), 5704–5708. https://doi.org/10.1002/anie.200701434.

(31) FABRY, D. C.; SUGIONO, E.; RUEPING, M. Online monitoring and analysis for autonomous continuous flow self-optimizing reactor systems. *React. Chem. Eng.* **2016**, *1* (2), 129–133. https://doi.org/10.1039/C5RE00038F.

(32) BORTOLINI, O.; CAVAZZINI, A.; GIOVANNINI, P. P.; GRECO, R.; MARCHETTI, N.; MASSI, A.; PASTI, L. A Combined Kinetic and Thermodynamic Approach for the Interpretation of Continuous-Flow Heterogeneous Catalytic Processes. *Chem. - A Eur. J.* **2013**, *19* (24), 7802–7808. https://doi.org/10.1002/chem.201300181.

(33) LISIECKI, K.; CZARNOCKI, Z. Flow Photochemistry as a Tool for the Total Synthesis of (+)-Epigalcatin. *Org. Lett.* **2018**, *20* (3), 605–607. https://doi.org/10.1021/acs.orglett.7b03974.

(34) JACOBSON, M. Z.; DELUCCHI, M. A.; BAUER, Z. A. F.; GOODMAN, S. C.; CHAPMAN, W. E.; CAMERON, M. A.; BOZONNAT, C.; CHOBADI, L.; CLONTS, H. A.; ENEVOLDSEN, P.; ET AL. 100% Clean and Renewable Wind, Water, and Sunlight All-Sector Energy Roadmaps for 139 Countries of the World. *Joule* **2017**, *1* (1), 108–121. https://doi.org/10.1016/J.JOULE.2017.07.005.

(35) BARBER, J. Photosynthetic energy conversion: natural and artificial. *Chem. Soc. Rev.* **2009**, *38* (1), 185–196. https://doi.org/10.1039/B802262N.

(36) 2000 ASTM Standard Extraterrestrial Spectrum Reference E-490-00 | Grid Modernization | NREL https://www.nrel.gov/grid/solar-resource/spectrum-astm-e490.html (accessed Nov 16, 2018).

(37) OELGEMÖLLER, M. Solar Photochemical Synthesis: From the Beginnings of Organic Photochemistry to the Solar Manufacturing of Commodity Chemicals. *Chem. Rev.* **2016**, *116* (17), 9664–9682. https://doi.org/10.1021/acs.chemrev.5b00720.

(38) LEVIN, M. D.; KIM, S.; TOSTE, F. D. Photoredox Catalysis Unlocks Single-Electron Elementary Steps in Transition Metal Catalyzed Cross-Coupling. *ACS Cent. Sci.* **2016**, *2* (5), 293–301. https://doi.org/10.1021/acscentsci.6b00090.

(39) HOFFMANN, N. Photochemical Reactions as Key Steps in Organic Synthesis. **2008**. https://doi.org/10.1021/CR0680336.

(40) MAURIZIO FAGNONI; DANIELE DONDI; DAVIDE RAVELLI; ANGELO ALBINI. Photocatalysis for the Formation of the C−C Bond. **2007**. https://doi.org/10.1021/CR068352X.

(41) SKUBI, K. L.; BLUM, T. R.; YOON, T. P. Dual Catalysis Strategies in Photochemical Synthesis. *Chem. Rev.* **2016**, *116* (17), 10035–10074. https://doi.org/10.1021/acs.chemrev.6b00018.

(42) DE KEUKELEIRE, D.; HE, S. L. Photochemical strategies for the construction

of polycyclic molecules. *Chem. Rev.* **1993**, *93* (1), 359–380. https://doi.org/10.1021/cr00017a017.

(43) ANSLYN, E. V.; DOUGHERTY, D. A. *Modern Physical Organic Chemistry*; University Science, 2006.

(44) ZABOROVSKIY, A. B.; LUTSYK, D. S.; PRYSTANSKY, R. E.; KOPYLETS, V. I.; TIMOKHIN, V. I.; CHATGILIALOGLU, C. A mechanistic investigation of (Me3Si)3SiH oxidation. *J. Organomet. Chem.* **2004**, *689* (18), 2912–2919. https://doi.org/10.1016/J.JORGANCHEM.2004.06.030.

(45) JIANG, H.; BAK, J. R.; LÓPEZ-DELGADO, F. J.; JØRGENSEN, K. A. Practical metal- and additive-free methods for radical-mediated reduction and cyclization reactions. *Green Chem.* **2013**, *15* (12), 3355. https://doi.org/10.1039/c3gc41520a.

Chapter 1

Molecular Sieves: a highly efficient and greener catalyst for the synthesis of trisubstituted 1,2,3-triazoles under batch and continuous flow regimes

Abstract: Substituted 1,2,3-triazoles are important heterocyclic scaffolds that possess several applications in all most every field of life. The 1,3-Dipolar cycloaddition of azides and enolizable carbonyl compounds are a straightforward approach for the assembly of highly substituted 1,2,3-triazoles. However, many methodologies have already been reported that has different features such as some include long reaction time, utilization of risky/hazardous reagents, and harmful solvents etc. In this chapter we have demonstrated an innovative condition for the preparation of trisubstituted-1,2,3-triazoles using different aryl azides and carbonyl compounds. The reaction was evaluated under batch and continuous flow regimes. Therefore, another major goal of this project has to develop a continuous flow system for online monitoring of this reactions. Thus, to develop a technology with improved energy, material and time saving as well as increased security, scalability and reproducibility.

Keywords: Catalysis • Molecular Sieve • Triazole • Flow Chemistry

2.1. Introduction

Nowadays the search and synthesis of compounds with biological activity is imperative. In this regard, heterocycles containing nitrogen atoms in their molecular architecture have served as privileged scaffold in organic chemistry, drug discovery and material science.[1]

As highly valuable *N*-containing heterocycles, the triazoles[2,3] have gained intensive interest due to their prominent applicability (**Scheme 4**), e.g., antibiotic,[4] anticancer,[5–7] antifungal,[8] anti-HIV[9,10] and antituberculotic abalities.[11]

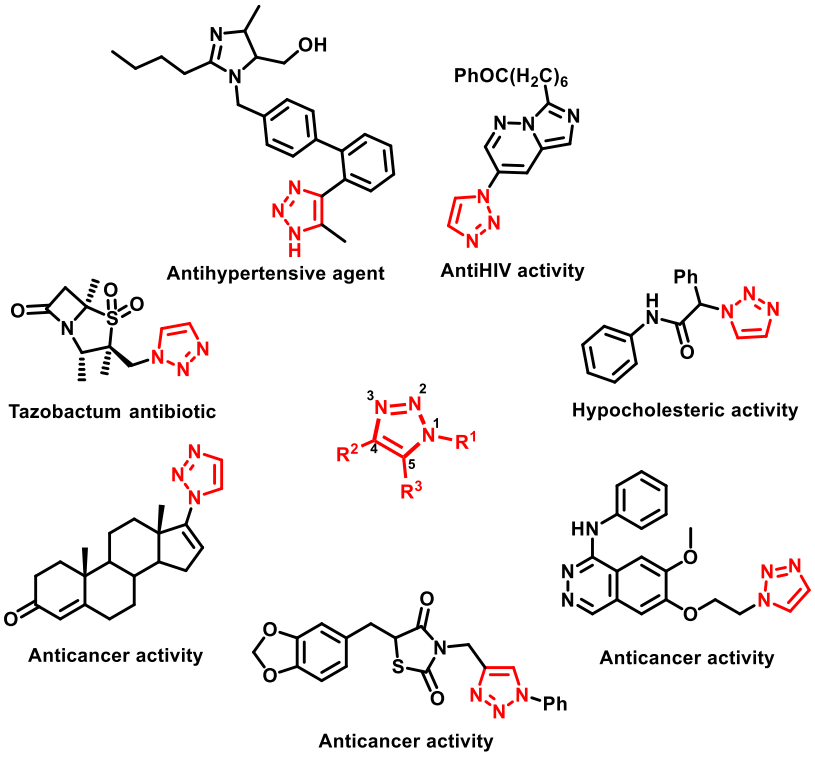

Scheme 4. Some examples of 1,2,3-triazole containing commercial drugs and bioactive molecules.

The 1,2,3-triazole core was first synthesized using the established Huisgen 1,3-dipolar cycloaddition reaction of an azide with alkynes.[12] However, the Huisgen's protocol requires high temperatures to promote the reaction. As consequence, this methodology suffers with the poor selectivity, being the desired triazole formed as a mixture of the 1,4 and 1,5-adducts (**Scheme 5**).[13]

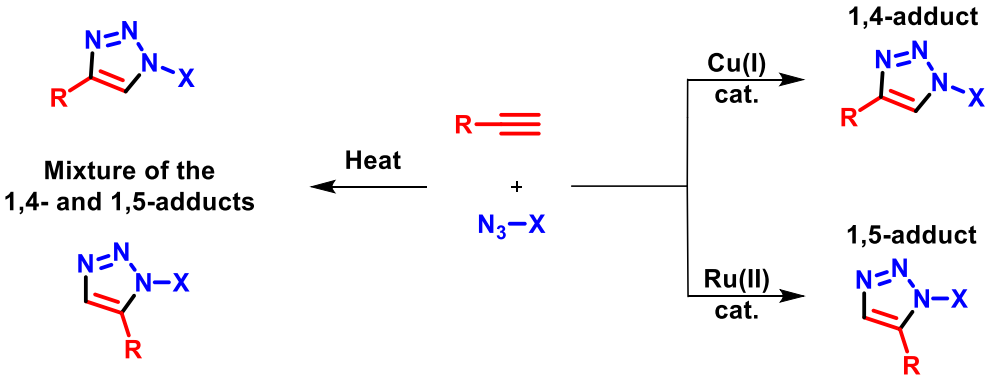

Scheme 5. Classical and catalyzed reaction of Huisgen's 1,3-dipolar cycloaddition of azide with alkynes.

On the other hand, the metal catalyzed versions (Cu and Ru)[14,15] were developed for the selective construction of the 1,4 and 1,5-adduct. This reaction could be performed under milder reaction conditions and consequently numerous applications were reported. Nevertheless, this procedure undergoes with the limitations of either narrow substrate scope or restriction of its application in chemical biology.

Triazoles can also be achieved by (3+2) cycloaddition reaction of azides and active carbonyl compounds. One-pot synthesis is a possible option to reduce operational steps, solvent amount and consequently obtaining a greener process. Kannan and co-workers applied such approach to generate a variety of 1,4,5-trisubstituted-1,2,3-triazoles with different substituents. The aforementioned synthesis applied potassium carbonate as a base to promote the reaction of aromatic azides and acetylacetone through the enol formation. The need of three equivalents of base and the laborious work-up to achieve the desired product could be faced as a drawback of this methodology (**Scheme 6**).[16]

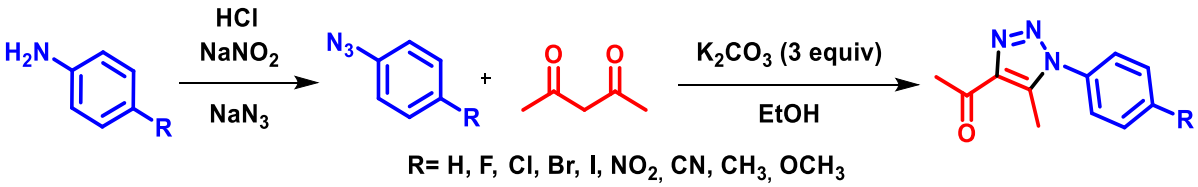

Scheme 6. Synthesis of the 4-acetyl-5-methyl-1,2,3-triazole.

In the past few decades, great progress has been made in regards of addressing environmental concerns of important chemical transformations. In this regard, continuous flow chemistry could direct contribute into the development of sustainable chemical synthesis - especially when combined with online monitoring system of the reaction protocol. Thus, flow-strategy became a powerful tool for the design of “greener processes” by several characteristics: such as improvement of product selectivity, energy saving, waste minimization, and reduction of time-consuming purification steps, etc.[17,18]

Combining catalysis and continuous flow seems to be an ideal situation to maximize the benefits of both techniques. In this scenario, heterogeneous catalysis is of great interest since it is confined in the reactor, allowing easy recovery and reuse of the catalyst. Moreover, it allows the fast isolation of the desired product.

In this context, some important reports were recently made. Silvana and coworkers evaluate the advantages of continuous flow over batch conditions of Cu(I)-catalyzed 1,3-dipolar cycloaddition (CuAAC) using the respective terminal alkynes and azides. Ultrasonic irradiation and flow microreactor were combined to provide optimal conditions and avoid clogging. Also, a BZA resin, polymer supported benzylamine, was used as copper-scavenger resin and to stop the reaction. Thus, the reactional time was reduced from hours to minutes and an enhancement of yield was also observed. Using this methodology new hybrids of ascorbic acid and 1,2,3-triazole units were produced that is an important moiety for bioactivity applications (**Scheme 7**). [19]

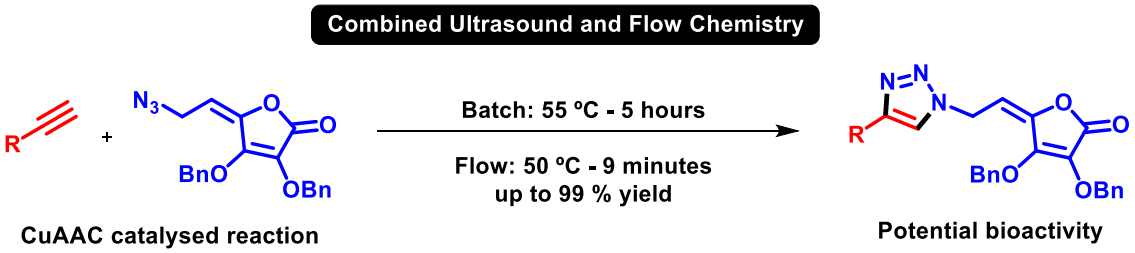

Scheme 7. A Cooper catalyzed 1,3-dipolar cycloaddition reaction using combined ultrasonic irradiation and flow microreactor protocol.

The use of heterogeneous catalysts can result in more effective and economic reactional systems. Wang et al. described an efficient method for the synthesis *N*-unsubstituted 4-aryl-1,2,3-triazoles using Amberlyst 15 (**Scheme 8**). The polymeric catalyst is a strongly acidic ion exchange resin, containing a phenyl sulfonic acid moiety. The catalyst was removed by simple filtration and reused upon 4 times without significant loss of activity. A wide range of functional groups were evaluated and very good yields ranging from 80 to 95 % were obtained,.[20]

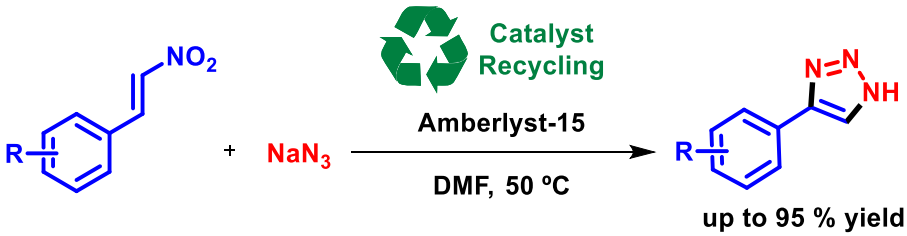

Scheme 8. Amberlyst 15 as recyclable catalyst for the synthesis of *N*-unsubstituted 4-aryl-1,2,3-triazoles.

More recently, Zhang and collaborators synthesized *N*-unsubstituted 4-aryl-1H-1,2,3-triazoles via acetic acid promoted cycloaddition. The transition-metal-free protocol was compared under batch and flow condition. Also, a scale-up of reaction was done successfully and reaction up to 70 mmol scale was performed that maintained the same reaction yield. Furthermore, a multicomponent approach was developed and b-nitrostyrenes that was generated by the corresponding aldehyde and nitromethane. Continuous flow conditions showed better yields for reactions evaluated and most of the cases had an increase of 10 % compared to batch conditions. Moreover, continuous flow provides a safe environment for the use of nitromethane and sodium azide, allowing the scaling up of the reaction (**Scheme 9**).[21]

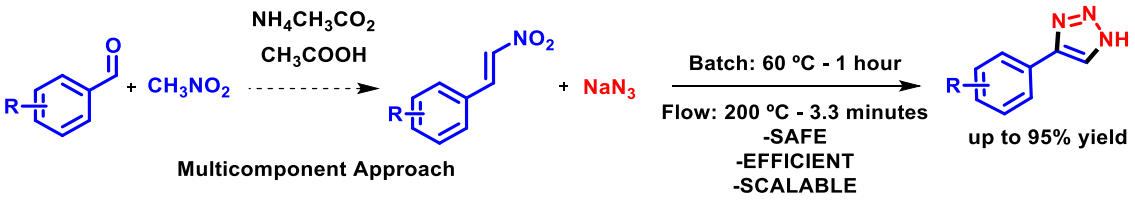

Scheme 9. Comparison of batch and flow conditions for synthesis of *N*-unsubstituted 4-aryl-1H-1,2,3-triazoles.

A multi-step continuous-flow synthesis could be used not only to achieve higher yield in short time but it also can increase production capacity as well as the use of lower amount of solvent during the purification step. An interesting example is the synthesis of rufinamide precursor that is a 1,2,3-triazole antiepileptic drug used to treat the Lennox-Gastaut syndrome. Hessel et al. reported a 5-stage 3-step continuous-flow synthesis counting the purification steps, for example, the azide was use in the subsequent step without purification, reducing organic solvent consumption, giving a total yield of 82 % with productivity of 9 g/h (11.5 $mol.h^{-1}L^{-1}$) of rufinamide precursor. The process minimizes the handling of dangerous reagents, increasing safety and better sustainability(**Scheme 10**).[22]

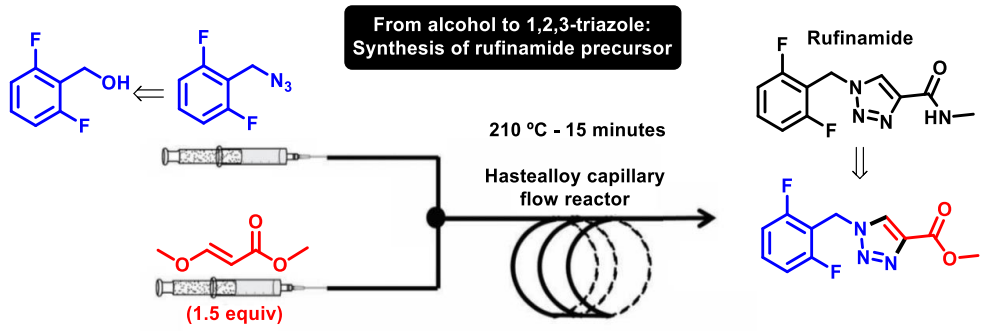

Scheme 10. Multi-step continuous-flow synthesis of rufinamide precursor from the respective alcohol.

Another remarkably example of the application of multistep synthesis using continuous flow microreactors is the formation of 1,4-disubstituted 1,2,3-triazoles in two-steps described by Guo et al. (**Scheme 11**). The methodology consists of a metal and azide-free condition using easily available starting materials. In the first step acetophenones were reacted with tosylhydrazine at 50 ºC while in the second step the stream was mixed with the respective aniline, iodine (10 mol %) and TBHP (*tert*-Butylhydroperoxide). A broad range of acetophenones (15 in total) and 3 different anilines were used, giving the desired product in good to excellent yields.[23]

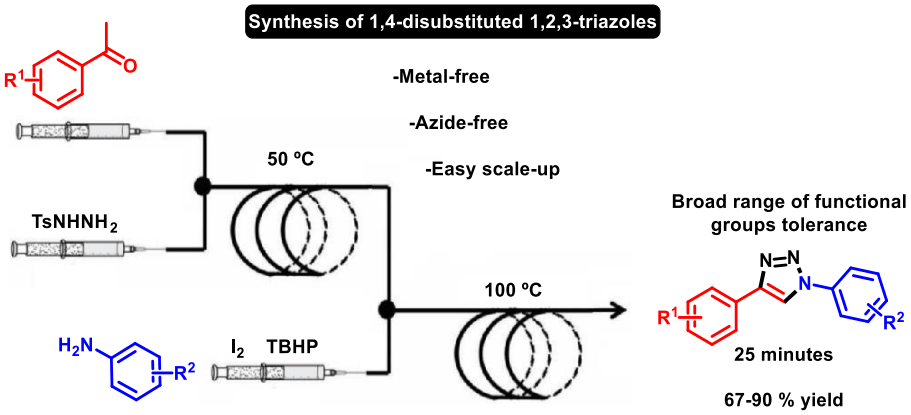

Scheme 11. Efficient multistep synthesis of 1,4- disubstituted 1,2,3-triazoles.

2.2. Results and Discussion

Herein, we report the 1,3-dipolar cycloaddition of azides with enolizable carbonyl compounds to generate 1,4,5-trisubstituted 1,2,3-triazoles using a solid catalyst in batch or under continuous-flow conditions with online monitoring. These hyphenated techniques permit the determination of conversion of the starting material, yield and isolation of the product.

Many materials could be applied as heterogeneous catalyst. In general, it is ideal that they have high physical (abrasion, pressure, temperature) and chemical (pH, leaching, solubility) stability. A material with high surface area, chemical and mechanical stability is desirable for the application in flow chemistry. Furthermore, the knowledge of chemical properties as acidity and basicity are imperative for the optimization of reaction conditions. In our endeavor to find the best heterogeneous catalyst, we started by screening different materials that could catalyze the reaction between 4-azidobenzonitrile and acetylacetone delivering 4-acetyl-5-methyl-1,2,3-triazole (**Table 1**). In this study, we started evaluating a broad range of materials with different characteristics under batch conditions, e.g. Lewis acid (entries 1-5), Brønsted-acid (entry 6) and amphoteric (entries 10-12) species were evaluated. Almost all evaluated catalysts are commercially available. By using commercial silicate material with different sizes, furnished the 1,2,3-triazole in low yields (entries 1-3). When the Stober silica was used, the desired triazole could be obtained in moderate yield. However, the use of HPLC grade silica furnished the triazole scaffold in a very low yield while in the case of sulfonated silica the reaction was inhibited (entry 6). These results gave us a very important hint that HPLC grade Silica (entry 5) has the highest surface area, lower in acidic behavior and has highest purity. Other silicas may have higher level of metals contamination, contributing to an increase in acidity of the silica, thus those metals could act as catalyst.

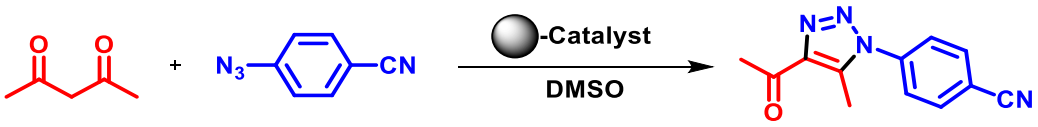

Table 1. Evaluation of solid catalysts for 1,3-Dipolar cycloaddition of azides and acetylacetone under batch condition.

Entry[a]	Catalyst	Yield (%)[b]
1	Silica 60 Å – 32-63 µm	48
2	Silica 60 Å – 63-200 µm	38
3	Silica 60 Å – 200-425 µm	28
4	Silica Stober	62
5	Silica 10 µm 100 Å (HPLC grade)	8
6	Silica Sulfonated (HPLC grade)	Traces
7	Celite	7
8	Montmorillonite K10	15
9	Montmorillonite KSF	Traces
10	Molecular Sieve 3 Å	95%
11	Molecular Sieve 4 Å	> 99%
12	Molecular Sieve 5 Å	92%

[a] Reactions conducted in 0.25 mmol scale using: catalyst (25 mg), carbonyl compound (1.2 equiv.), azide in DMSO (1.0 mL) at room temperature. [b] Isolated yield.

Furthermore, we turned our attention to the use of different heterogeneous catalysts. Molecular sieves are commercially available catalyst and own a distinct and well-known structure, being physically and chemically stable under the reaction conditions. To our delight, all molecular sieves used without previous activation that presented excellent catalytic behavior (entries 10-12).

In order to understand the catalytic activity of molecular sieves in case of this reaction, we investigated some of its properties. It is reported that a slurry (5%) raises the pH of solution to 10.5,[24] suggesting that is a basic catalyst. To confirm, a titration was performed using HCl with phenolphthalein as indicator. A 6 $\mu mol.g^{-1}$ amount of base was slowly released during the process. Furthermore, the molecular sieve was used without previous activation, so the hypothesis of water removal of the reaction media was rejected. Another important factor observed was that neither the azide nor carbonyl compound nor even DMSO could access the pores of this zeolite, because all of them have a critical diameter greater than 4 Å.

Next, we turned our attention to study the scope and limitation of this reaction protocol. In the initial screening, a series of aryl azides and carbonyl compounds were evaluated. The standard reaction under batch conditions comprises the use of catalyst (25 mg), azide (0.25 mmol, 1.0 M), carbonyl compound (1.2 equiv.), and DMSO (250 µL) as solvent at room temperature (**Scheme 11**).

The conversion of the azide was monitored off-line by the reverse phase HPLC, which gave us an idea of the reaction time as well as the total azide consumption. Thus, facilitates the transfer of the method to continuous flow.

From this study, we could observe that the electronic nature of the substituents attached at the aryl azide moiety are crucial as the electron-withdrawing group (EWG), e.g. nitrile, attached at the *para*-position afforded the products in a short reaction time with total conversion of the azide, **1a, 1d, 1g**. These results could be explained by frontier molecular orbitals, HOMO and LUMO. The reactivity is controlled by the LUMO of the dipole, the azide with electron-withdrawing group, lower the LUMO energy, favoring the reaction to occurs.

Therefore, for the total reaction conversion, when electron-neutral azide were used, longer reaction times required were observed (**Scheme 11**, entries **1b, 1e, 1h**).

Moreover, azide bearing the para-methoxy group did not provide total conversion when reacted with acetylacetone and methyl acetoacetate, even after 120h (compounds **1c** and **1f**).

In general, acetylacetone and methyl acetoacetate represents a very similar reactivity, probably due to the similarity in acidity. The 4-(2-cyanoacetyl) benzonitrile has the most acidic proton and was excepted to have the lowest reaction time as compared with acetylacetone and methyl acetoacetate. It could be explained by the reaction sensibility to the steric effects of the phenyl group in this case. Besides, product **1g** precipitation was observed that could cause a slightly deactivation of the catalyst, resulting in a prolong reaction time.

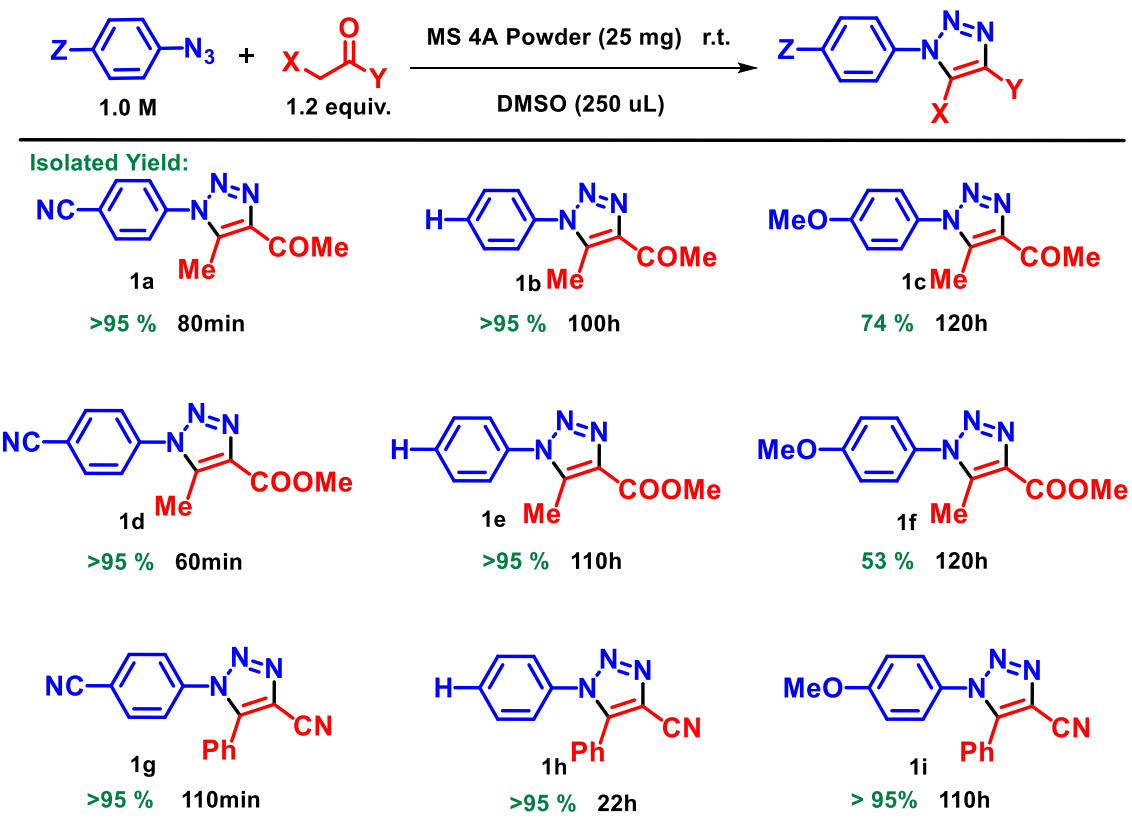

Scheme 12. Batch reaction: Reactions conducted in 0.25 mmol scale using: catalyst (25 mg), carbonyl compound (1.2 equiv.) and azide in DMSO (250 µL) at room temperature. Isolated yield.

In the light of those encouraging results we envisioned and apply this reactional strategy in the continuous-flow regime, planning to use a HPLC as base to the system setup. Nowadays, HPLC is considered as common equipment in most of the synthetic organic chemistry laboratories. In this regard, our home-made flow system was assembled for the simultaneous production and analysis. In the search of optimal reaction conditions, it permits the real time monitoring of the reaction and helps in controlling parameters such as flow rate and temperature. By using the HPLC oven as reactor heater, a stainless-steel column as the packed-bed microreactor manually compressed with catalyst (molecular sieve 4 Å) (Ø = 0.46 cm (diameter), l = 1,0 cm (length), particle size =< 3 µm, ~150 mg), a syringe pump to introduce the reagents in packed-bed microreactor and a switching-valve system (**Figure 3-4**).

Figure 3. Reactional flow system for the simultaneous production and analysis of Triazoles. A-Pump, B-Auto Sample, C-Oven, D-UV-Vis Detector, E-Injection Valve, S.P.-Syringe Pump.

Figure 4. Open oven with the reactor inside (Left). Syringes (midlle). Injection Valve (Right).

In addition, the system comprises two valves, valve one (injection) in which the outcome of the reaction is stored in a loop (2 µl) and changing the valve position

coupled the loop to the chromatographic column for the analysis. In the valve two (collection) - during the chromatographic analysis the compound of interest can be collected with high purity. In this way, monitoring of the reaction progress allowed the determination of the maximum flow rate during the reaction in order to achieve maximum conversion. Also, it is possible to monitor the reaction selectivity. Therefore, changes in the reaction conditions can be made to minimize the formation of undesirable products. If necessary, it is possible to collect the side product for eventual characterization and better comprehension of reaction mechanism. In order to transfer the batch method to continuous flow conditions for avoiding problems that could stop the system, clogging or detector saturation, a dilution of reagents was performed that is reducing the concentration from 1.0 M (batch condition), to 0.1 M (flow condition). Using this amount of powdered 4 Å molecular sieve i.e. 150 mg, up to 10 mmol can be produced without losing catalytic efficiency.

One drawback of this system is that the maximum temperature of oven could only be maintained up to 80 ºC as where full conversion of disactivated substrates, such as 4-methoxy aryl azides, could be observed.

Initially, for a comparison propose, the same substrates used in the batch conditions were evaluated in the flow conditions. To our delight, a significant improvement in terms of reactional time and conversion was achieved. The azides containing *4*-cyano group, reacted at least 4 times faster than in the batch protocol along with full conversion using higher temperatures i.e. 80 ºC and allow to obtain the desired product only in 3.4 minutes, **1a, 1d** (**Scheme 12**)**.** Also, the reaction with 4-(2-cyanoacetyl)benzonitrile for the synthesis of product **1g**, was completed much faster as compare the batch conditions. The flow reaction completed in 5.7 minutes as compared to batch conditions which took place in 80 minutes. This corroborates the hypothesis of precipitation of **1g** on catalyst surface, under batch condition, and catalyst deactivation as mentioned previously.

It is noteworthy that the isolated yield of **1a** was the same as compared to the HPLC yield, determined by the calibration curve using the pure product as an external standard. Using the same amount of catalyst, 150 mg, up to 4 mmol of the final product was produced. In addition, the reaction was successfully performed in a 10 mmol scale, with no observed decrease in the chemical yield. Products with no substituents in para position were obtained in lower reactional time, **1b** (from 100 hours to 85 minutes), **1e** (from 110 hours to 85 minutes), and **1h** (from 22 hours to 42.5 minutes). Moreover, for para-methoxy substituted compounds an improvement in the conversion was achieved. Previously under batch conditions, **1c** and **1f** were afforded only with 74% and 53% yield, respectively in 120 hours of reaction time while under the flow conditions it was possible to achieve 85% and 75%isolated yield in 170 minutes. Furthermore, the product **1i** was also obtained with full conversion at the same time.

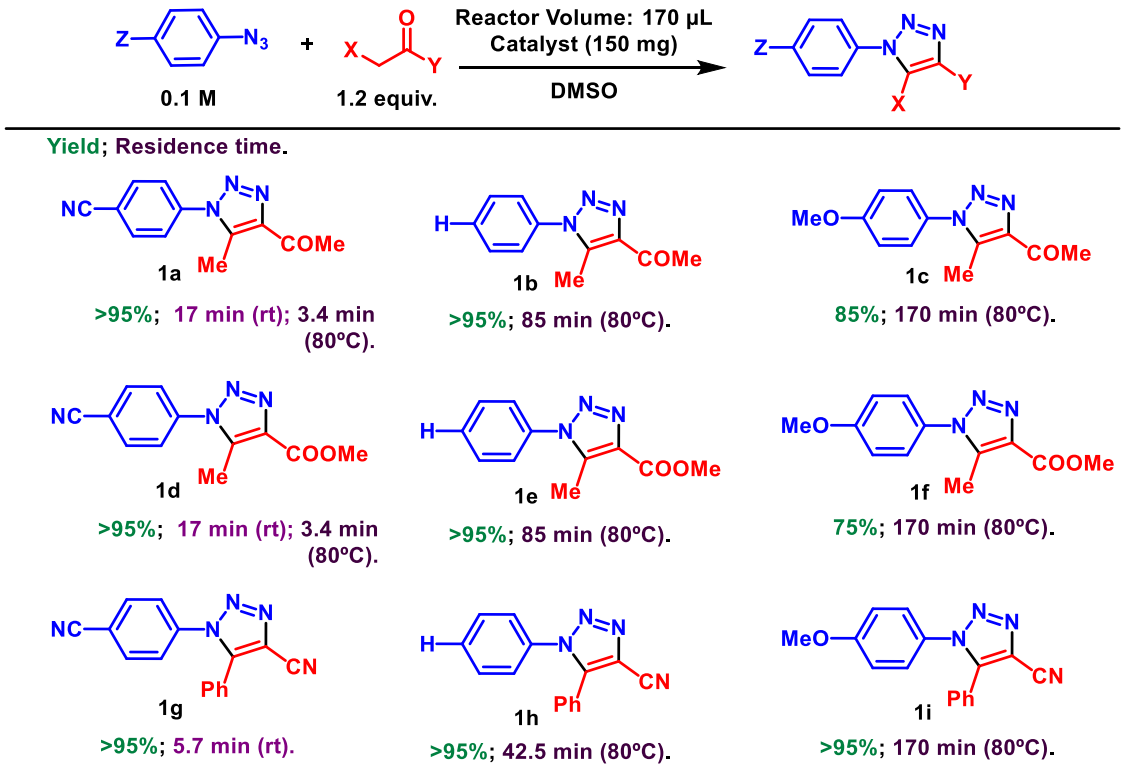

Scheme 13. Continuous Flow reaction - Reactions conducted using: catalyst (150 mg), carbonyl compound (1.2 equiv) and azide (0.1 M) in DMSO (2 mL) at the specified temperature (rt: room temperature). HPLC Yield.

In the light of these encouraging results, different azides and carbonyl compounds were evaluated under flow conditions starting with para, ortho and meta trifluoromethyl substituted azides. The product **1k** was obtained in 3.4 minutes and **1l** in 6.8 minutes. Unfortunatelly, the ortho-substituted **1m** underwent degradation. Regrettably, this metodolhogy was not sucessfull in order to generat the products derived from benzyl azide **1o**, neither from pycolyl azide **1s**.

Morvere, the reaction with acetoacetanilide, an amide, generated the product **1n** in 17 minutes and full conversion was observed. An analogue of 1,2,4 triazole precussor of Rimonabant, CB1 receptor antagonists **1p** that is important in the human obesity treatment, was also synthesized. In this case full conversion was achieved only in 17 minutes. Also, by using this methodology, a very polar and bulk carbonyl groups, like cinchona alkaloid derivative could be used for the products decore. Although, there is much higher steric hindrance, the product **1r**

could be obtained only in 3.4 min, suggesting that an autocatalysis reaction may occurs.

Moreover, by the use of very non-polar groups, like cholesterol derivatives, afforded the product **1q** in good yield. In this specific case a change in the solvent system and dillution was necessary to to made in oder to solubilize the starting material and avoid clogth a mixture of DMPU/DMSO (3:1, 4 mL) was used(**Scheme 14**).

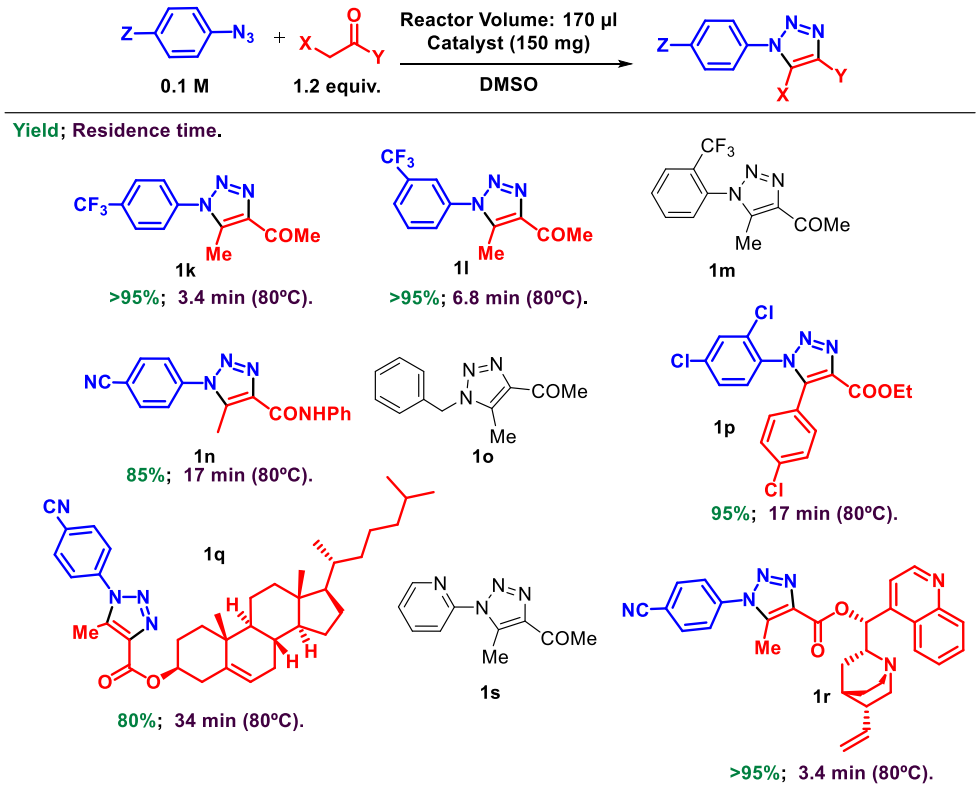

Scheme 14. Continuous Flow reaction: Reactions conducted in 0.20 mmol scale, using: catalyst (150 mg), carbonyl compound (1.2 equiv.) and azide (0.1 M) in DMSO (2 mL) at the specified temperature (rt: room temperature). HPLC Yield. Product **1q**: azide (0.025 M), solvent DMPU/DMSO 3:1 (4 mL).

Regarding the mechanism of this newly developed approach, the reaction procedes through a (3+2) cycloaddition between azide and active carbonyl compound. The latter could have a base-catalyzed enolate formation. The water elimination is the final step, furnishing the desired product that is 1,4,5-trisubstituted 1,2,3-triazoles. A stepwise addition-cyclisation route is another

plausible possibility, although more studies need to be done in order to understand the (this) mechanism (**Scheme 15**).

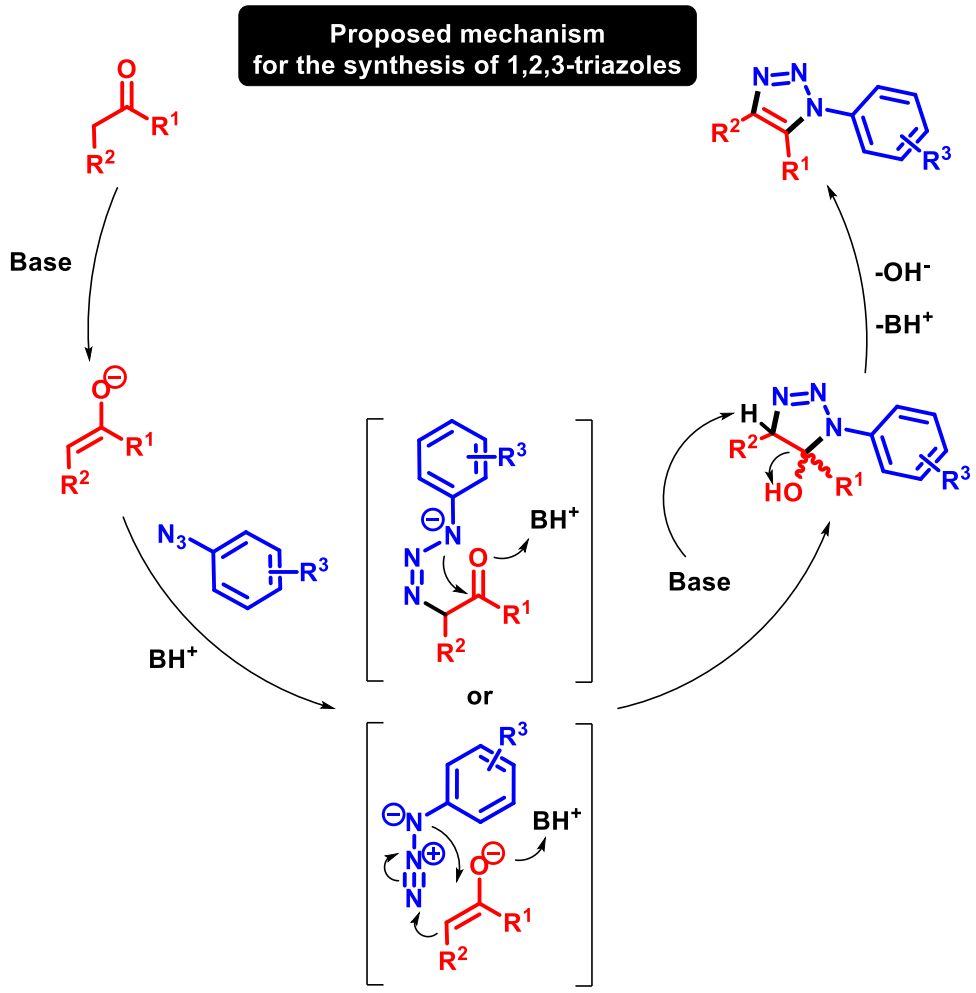

Scheme 15. Pausible mechanism for synthesis of 1,4,5-trisubstituted 1,2,3-triazoles.

2.3. Conclusion

The exploration of molecular sieve as catalyst for the synthesis of 1,4,5-trisubstituied 1,2,3-triazole was observed to be very efficient. The combination of heterogeneous catalysis under continuous-flow regime permits the fast optimization and rapid access to a small library of triazoles. Molecular sieves are the cheap catalyst, alternative, giving lower reaction time and similar selectivity, compared to the homogeneous catalyst methodology. They also avoid the use of large excess of base and harsh reaction conditions. The utilization of microreactors coupled to the HPLC device permits the on-line monitoring of stream constantly, allowing a quicker improvement of the response parameters. The instrumental setup can be modulated in different ways in order to achieve high throughput screening of new catalysts, multiple steps reactions or purification of product.

Molecular Sieves: a highly efficient and greener catalyst for the synthesis of trisubstituted 1,2,3-triazoles under batch and continuous flow regimes

2.4. Experimental Section

All reagents and solvents were purchased well reputed chemical industries and used as received without any further purification. Flash column chromatography was carried out using silica gel 60 (F_{254} 230-400 mesh) and analytical thin layer chromatography (TLC) was performed using silica gel aluminium sheets (0.2 mm F_{254}), which were developed using visualizing agents: UV fluorescence (254 nm), iodine, potassium permanganate/Δ. ^{1}H NMR and ^{13}C NMR spectrum were recorded at 400 MHz for ^{1}H and 100 MHz for ^{13}C, respectively. Chemical shifts (δ) are reported in parts per million (ppm) relative to the residual solvent signals chemical shifts are given relative to tetramethylsilane (TMS) and coupling constants (*J*) are reported in Hertz. High resolution mass spectrum (HRMS) were recorded using electron spray ionization (ESI) (Hybrid linear ion trap–orbitrap FT-MS and QqTOF/MS – Microtof – QII models). HPLC chromatograms were obtained on an apparatus with two LC-10AT Pumps, FCV-10ALvp Low Pressure Gradient Valve, DGU-14A degasser unit, CTO-10A oven, SIL-10ADvp, SPD-10A UV-Vis Detector, SCL-10Avp System Controller, using a Phenyl-Hexyl Phenomenex (4,6 mmØ $\times$ 100 mmL, particle size 10 µm) under reported conditions. Two valves of six port *VICI* Valco.

General procedure for batch synthesis of triazole.

In a plastic vial tube (2.0 mL), the azide (0.25 mmol), enolizable compound (0.30 mmol, 1.2 equiv.), DMSO (250 µL), and the catalyst (25 mg, 0.1 mol%) were

added. The reaction mixture was mechanically stirred at room temperature until completion of the reaction (monitored by HPLC). The crude reaction mixture was purified by column chromatography using hexane/ ethyl acetate (100:0 to 70:30).

General procedure for flow synthesis of triazole.

To a stainless-steel syringe, the azide (0.2 mmol, 0.1 M), the enolizable compound (0.24 mmol, 1.2 equiv.), DMSO (2.0 mL) were added and passed through a stainless reactor containing catalyst (150 mg, reactor volume: 170 µL) at the appropriate temperature. The flow rate/residence time was adjusted to achieve conversion of the azide >95 %, monitored by HPLC. The crude reaction mixture was purified by column chromatography using hexane/ ethyl acetate (100:0 to 70:30).

Reaction under flow condition

Representative example: The residence time (hold-up volume divided by the flow rate) is expressed as multiple of V. The residence time of 17 min (flow rate = 10 µl.min^{-1})

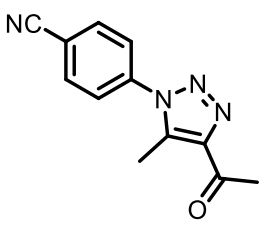

4-(4-acetyl-5-methyl-1*H*-1,2,3-triazol-1-yl)benzonitrile (1a): Yield: 95 %; white solid; m.p.: 153-155 °C; **^{1}H NMR** (400 MHz, $CDCl_3$, 25°C) δ = 7.91 (d, *J* = 8.7 Hz, 2H), 7.65 (d, *J* = 8.7 Hz, 2H), 2.76 (s, 3H), 2.66 (s, 3H) ppm. **^{13}C NMR** (100 MHz, $CDCl_3$, 25°C) δ = 194.3, 144.2, 138.9, 137.4, 133.8, 125.8, 117.5, 114.2, 28.1, 10.4 ppm.

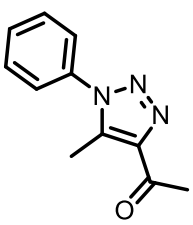

1-(5-methyl-1-phenyl-1*H*-1,2,3-triazol-4-yl)ethenone (1b): Yield: 95 %; white solid; m.p.: 99-100 °C; **^{1}H NMR** (400 MHz, $CDCl_3$, 25°C) δ = 7.61-7.55 (m, 3H), 7.47-7.42 (m, 2H), 2.76 (s, 3H), 2.59 (s, 3H) ppm. **^{13}C NMR** (100 MHz, $CDCl_3$, 25°C) δ = 194.8, 144.0, 137.7, 135.7, 130.4, 130.0, 125.6, 28.2, 10.5 ppm.

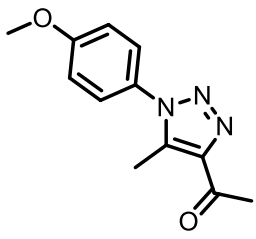

1-(1-(4-methoxyphenyl)-5-methyl-1*H*-1,2,3-triazol-4-yl)ethanone (1c): Yield: 74 %; white solid; m.p.: 121-122 °C; **^{1}H NMR** (400 MHz, $CDCl_3$, 25°C) δ = 7.35 (d, *J* = 9.0 Hz, 2H), 7.06 (d, *J* = 9.0 Hz, 2H), 3.89 (s, 3H), 2.75 (s, 3H), 2.55 (s, 3H) ppm. **^{13}C NMR** (100 MHz, $CDCl_3$, 25°C) δ = 194.5, 160.7, 143.5, 137.5, 128.1, 126.7, 114.8, 55.7, 27.8, 10.1 ppm.

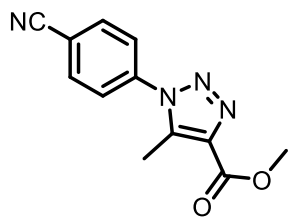

methyl 1-(4-cyanophenyl)-5-methyl-1*H*-1,2,3-triazole-4-carboxylate (1d): Yield: 95 %; white solid; m.p.: 171-172 °C; **^{1}H NMR** (400 MHz, $CDCl_3$, 25°C) δ = 7.91 (d, *J* = 8.8 Hz, 2H), 7.67 (d, *J* = 8.8 Hz, 2H), 4.00 (s, 3H), 2.67 (s, 3H) ppm. **^{13}C NMR** (100 MHz, $CDCl_3$, 25°C) δ = 161.9, 139.0, 138.9, 137.3, 133.8, 125.9, 117.5, 114.24, 52.4, 10.2 ppm.

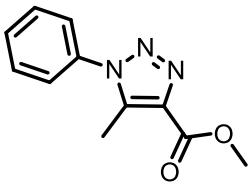

methyl 5-methyl-1-phenyl-1*H*-1,2,3-triazole-4-carboxylate (1e): Yield: 95 %; **NMR ^{1}H** (400 MHz, $CDCl_3$, 25°C) δ 7.60 – 7.55 (m, 3H), 7.47 – 7.44 (m, 2H), 3.99 (s, 3H), 2.60 (s, 3H) ppm. **NMR ^{13}C** (100 MHz, $CDCl_3$, 25°C) δ 162.5, 139.3, 136.8, 135.7, 130.4, 130.0, 125.7, 52.4, 10.3 ppm.

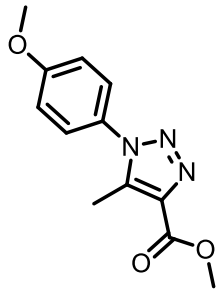

methyl 1-(4-methoxyphenyl)-5-methyl-1H-1,2,3-triazole-4-carboxylate (1f): Yield: 53 %; **NMR ^{1}H** (400 MHz, $CDCl_3$, 25°C) δ 7.34 (d, *J* = 8.9 Hz, 2H), 7.04 (d, *J* = 9.0 Hz, 2H), 3.97 (s, 3H), 3.87 (s, 3H), 2.54 (s, 3H) ppm. **NMR ^{13}C** (100 MHz, $CDCl_3$) δ 162.2, 160.7, 139.1, 136.2, 128.2, 126.7, 114.7, 55.6, 52.0, 9.8 ppm.

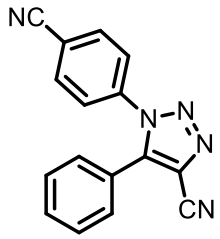

1-(4-cyanophenyl)-5-phenyl-1H-1,2,3-triazole-4-carbonitrile (1g): Yield: 95 %; **NMR ^{1}H** (400 MHz, $CDCl_3$, 25°C) δ 7.80 – 7.76 (m, 2H), 7.59 – 7.55 (m, 1H), 7.53 – 7.48 (m, 4H), 7.36 – 7.32 (m, 2H) ppm. **NMR ^{13}C** (100 MHz, $CDCl_3$, 25°C) δ 142.56, 137.8, 133.0, 131.0, 129.2, 128.3, 124.8, 122.0, 120.7, 116.5, 113.6, 110.8 ppm.

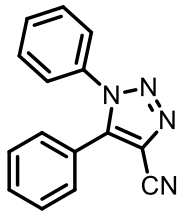

1,5-diphenyl-1H-1,2,3-triazole-4-carbonitrile (1h): Yield: 95 %; **RMN ^{1}H** (400 MHz, $CDCl_3$, 25°C) δ 7.54 – 7.42 (m, 6H), 7.36 – 7.33 (m, 4H), ppm. **RMN ^{13}C** (100 MHz, $CDCl_3$, 25°C) δ 143.4, 135.6, 131.4, 130.6, 130.1, 129.7, 129.3, 125.5, 123.6, 120.9, 112.4 ppm.

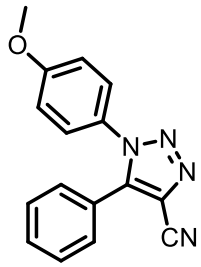

1-(4-methoxyphenyl)-5-phenyl-1*H*-1,2,3-triazole-4-carbonitrile (1i): Yield: 95 %; **^{1}H NMR** (400 MHz, $CDCl_3$, 25°C) δ 7.51 – 7.42 (m, 3H), 7.36 – 7.33 (m, 2H), 7.26 (d, *J* = 9.0 Hz, 2H), 6.95 (d, *J* = 9.0 Hz, 2H), 3.86 (s, 3H), ppm. **^{13}C NMR** (100 MHz, $CDCl_3$, 25°C) δ 161.1, 143.3, 131.3, 129.7, 129.2, 128.4, 126.9, 123.8, 120.67, 115.2, 112.5, 55.9 ppm.

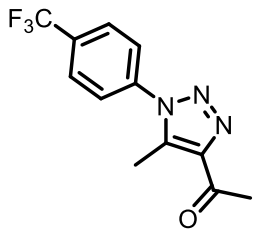

1-(5-methyl-1-(4-(trifluoromethyl)phenyl)-1H-1,2,3-triazol-4-yl)ethanone (1k): Yield: 86 %; white solid; m.p.: 77.5-78.5 °C; **^{1}H NMR** (400 MHz, $CDCl_3$, 25°C) δ = 7.85 (d, *J* = 8.4 Hz, 2H), 7.62 (d, *J* = 8.5 Hz, 2H), 2.72 (s, 3H), 2.62 (s, 3H) ppm. **^{13}C NMR** (100 MHz, $CDCl_3$, 25°C) δ = 194.5, 144.2, 138.5, 137.7, 132.4 (q, *J* = 33 Hz), 127.3 (q, *J* = 3.3 Hz), 125.9, 123.7 (q, *J* = 272 Hz), 28.2, 10.5 ppm.

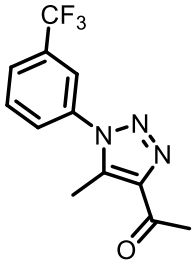

1-(5-methyl-1-(3-(trifluoromethyl)phenyl)-1H-1,2,3-triazol-4-yl)ethan-1-one (1l): Yield: 95%. **^{1}H NMR** (400 MHz,$CDCl_3$, 25°C) δ = 7.85 (d, *J* = 7.97 Hz, 1H), 7.78-7.74 (m, 2H), 7.69 (d, *J* = 7.9x Hz, 1H) , 2.76 (s, 3H), 2.64 (s, 3H) ppm. **^{13}C NMR** (100 MHz, $CDCl_3$, 25°C) δ = δ 194.2, 143.8, 137.5, 135.8, 132.3, 130.5, 128.4, 126.9, 124.5, 122.4, 27.9, 10.1.ppm.

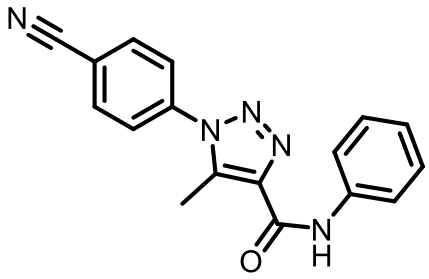

1-(4-cyanophenyl)-5-methyl-N-phenyl-1H-1,2,3-triazole-4-carboxamide (1n): Yield: 85%; white solid; m.p.: 231-231.5 °C; **^{1}H NMR** (400 MHz, $CDCl_3$, 25°C) δ 9.04 (s, 1H), 7.92 (d, *J* = 8.6 Hz, 2H), 7.70 (t, *J* = 7.9 Hz, 4H), 7.39 (t, *J* = 7.9 Hz, 2H), 7.17 (t, *J* = 7.4 Hz, 1H), 2.76 (s, 3H). **^{13}C NMR** (100 MHz, $CDCl_3$, 25°C) δ 158.8, 139.2, 138.9, 137.5, 137.3, 133.7, 129.1, 125.6, 124.6, 119.9, 117.3, 114.1, 10.0 (ppm).

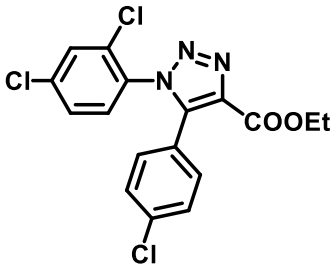

1-(5-(4-chlorophenyl)-1-(2,4-dichlorophenyl)-1H-1,2,3-triazol-4-yl)propan-1-one (1p): ^{1}H NMR (400 MHz,$CDCl_3$, 25°C) δ = 7.50 (d, *J* = 2.04 Hz, 1H), 7.40 - 7.22, (m, Hz, 6H) 4.39 (q, *J* = 7.13 Hz, 2H), 1.37, (t, *J* = 7.13 Hz, 3H) ppm. **^{13}C NMR** (100 MHz, $CDCl_3$, 25°C) δ = 160.7, 141.7, 137.7, 136.7, 136.5, 132.7, 132.0, 131.2, 130.6, 130.2, 128.7, 128.3, 123.3, 61.5, 14.2 ppm.

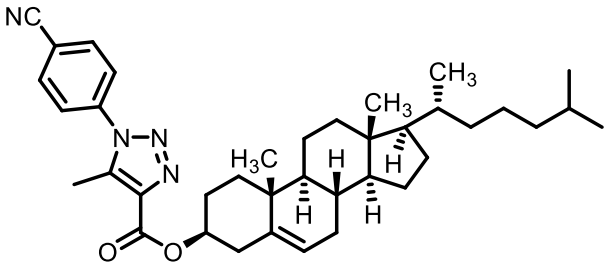

(3S,8S,9S,10R,13R,14S,17R)-10,13-dimethyl-17-((R)-6-methylheptan-2-yl)- 2, 3, 4, 7, 8, 9, 10, 11, 12, 13, 14, 15, 16, 17-tetradecahydro-1H-cyclopenta[a]phenan-thren-3-yl 1-(4-cyanophenyl)-5-methyl-1H-1, 2, 3-triazole-4-carboxylate (1q): Yield: 80%; white solid; m.p.: 239-242 °C; **^{1}H NMR** (400 MHz, $CDCl_3$, 25°C) δ =7.89 (d,

J = 8.4 Hz, 2H), 7.64 (d, *J* = 8.4 Hz, 2H), 5.43 (s, 1H), 4.98-4.90 (m, 1H), 2.64 (s, 3H), 2.57 (t, *J* = 12.3 Hz, 1H), 2.48 (dd, *J* = 13.2, 4.6 Hz, 1H), 2.03-1.80 (m, 6H), 1.57 (s, 3H), 1.53-1.44 (m, 4H), 1.38-1.30 (m, 3H), 1.24-1.08 (m, 7H), 1.05 (s, 3H), 1.02-0.94 (m, 3H), 0.91 (d, *J* = 6.5 Hz, 3H), 0.85 (d, *J* = 6.5 Hz, 6H), 0.68 (s, 3H) ppm. **^{13}C NMR** (100 MHz, $CDCl_3$, 25°C) δ = 161.0, 139.6, 139.0, 138.8, 137.7, 133.8, 125.9, 123.1, 117.5, 114.2, 75.4, 56.8, 56.3, 50.2, 42.5, 39.9, 39.6, 38.3, 37.2, 36.8, 36.3, 35.9, 32.1, 32.0, 28.4, 28.1, 28.0, 24.4, 24.0, 23.0, 22.7, 21.2, 19.5, 18.8, 12.0, 10.4 ppm.

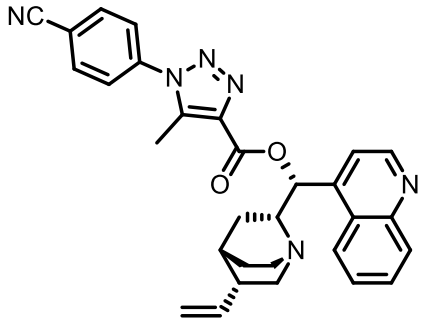

(R)-quinolin-4-yl((1S,2R,4S,5R)-5-vinylquinuclidin-2-yl)methyl 1-(4-cyanophenyl)-5-methyl-1H-1,2,3-triazole-4-carboxylate (1r): Yield: 95%; white solid; m.p.: 119-122 °C; **^{1}H NMR** (400 MHz, $CDCl_3$, 25°C) δ 8.87 (d, *J* = 4.5 Hz, 1H), 8.44 (d, *J* = 8.1 Hz, 1H), 8.13 (dd, *J* = 8.4, 1.0 Hz, 1H), 7.89 (d, *J* = 8.8 Hz, 2H), 7.77-7.73 (m, 1H), 7.70-7.66 (m, 1H), 7.63 (d, *J* = 8.8 Hz, 2H), 7.54 (d, *J* = 4.5 Hz, 1H), 7.03 (s, 1H), 5.78 (ddd, *J* = 17.4, 10.4, 7.3 Hz, 1H), 5.02 (dt, *J* = 9.6, 1.3 Hz, 1H), 4.99 (m, 1H), 3.55 (m, 1H), 3.43 (m, 1H), 3.18 (dd, *J* = 13.7, 10.4 Hz, 1H), 2.85-2.73 (m, 2H), 2.58 (s, 3H), 2.43-2.38 (m, 1H), 2.16-2.06 (m, 1H), 1.97 (m, 2H), 1.93-1.87 (m, 1H), 1.66 (m, 1H) ppm. **^{13}C NMR** (100 MHz, $CDCl_3$, 25°C) δ = 160.6, 150.2, 148.8, 144.4, 140.9, 140.3, 138.9, 136.9, 134.1, 130.8, 129.9, 127.8, 126.0, 125.7, 123.6, 118.6, 117.6, 115.6, 114.5, 74.3, 59.8, 56.7, 43.4, 39.4, 27.9, 27.1, 23.4, 10.4 ppm.

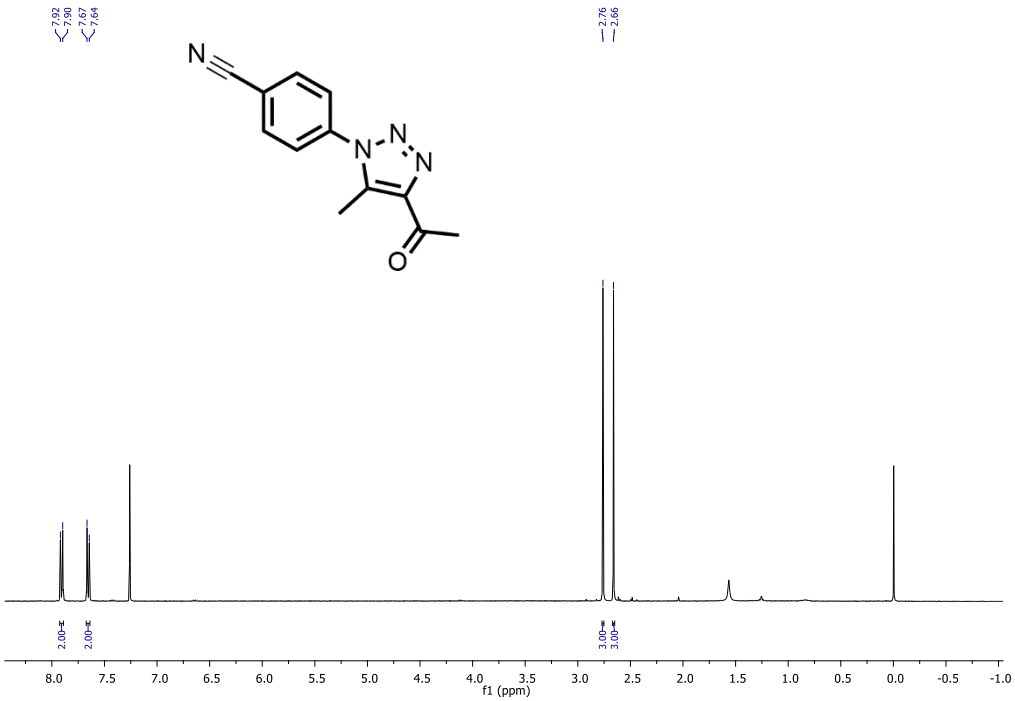

Figure 5: ^{1}H NMR (400 MHz, $CDCl_3$) Spectrum of compound **1a**.

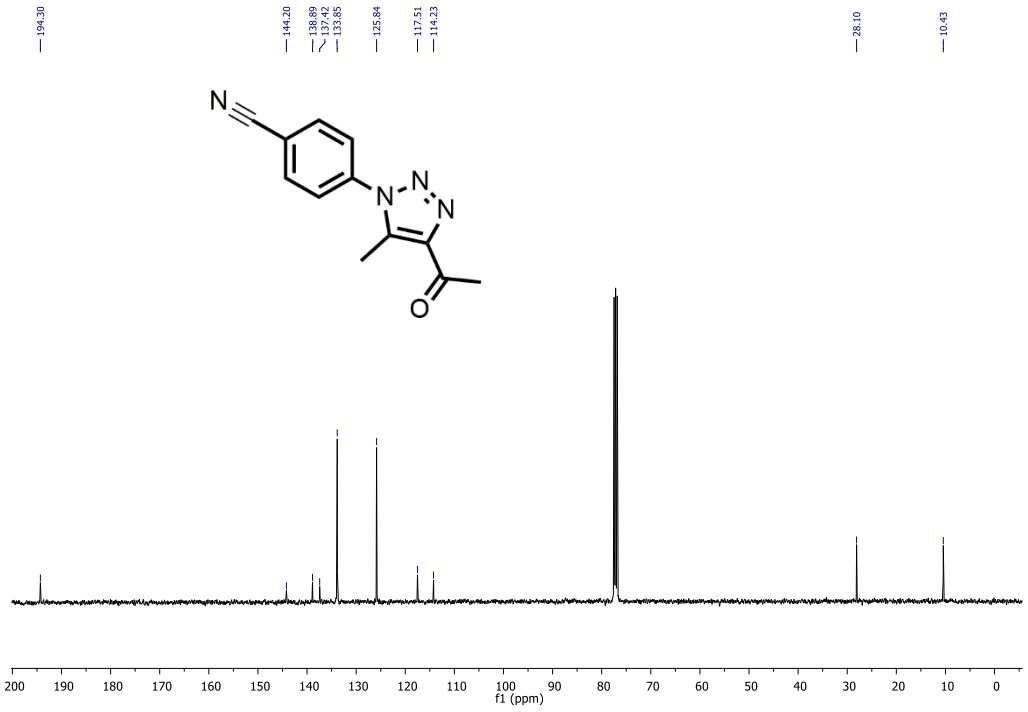

Figure 6: ^{13}C NMR (100 MHz, $CDCl_3$) Spectrum of compound **1a**.

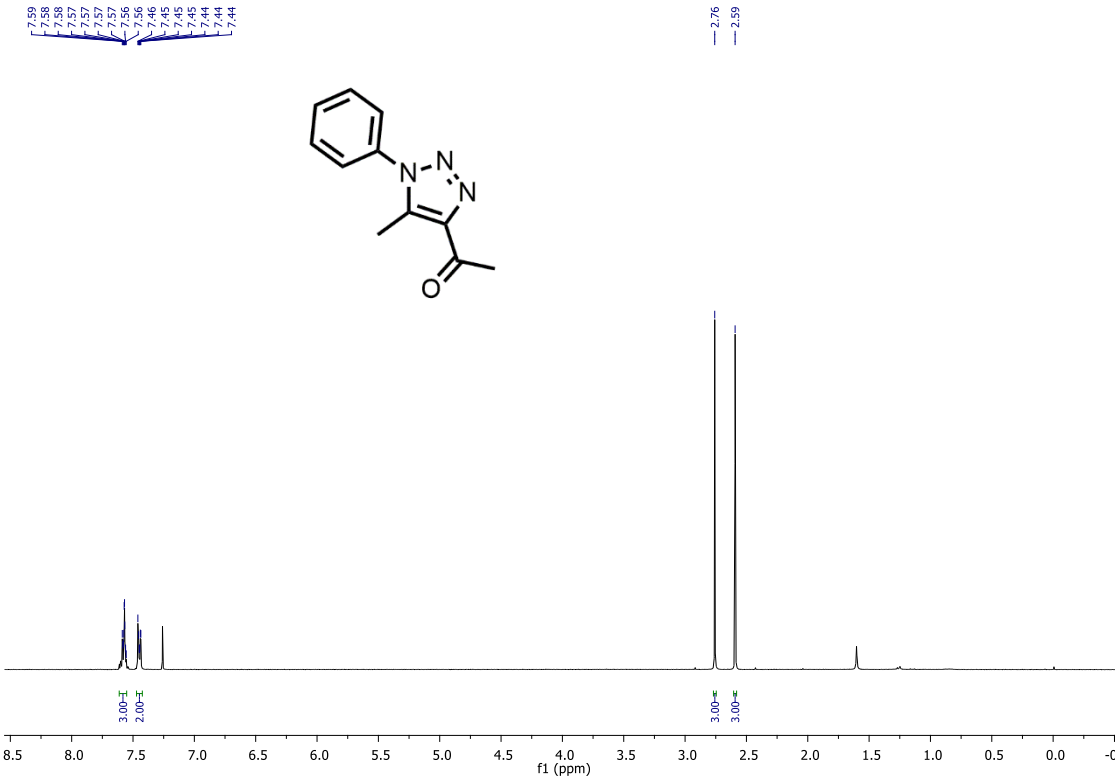

Figure 7: ^{1}H NMR (400 MHz, $CDCl_3$) Spectrum of compound **1b**.

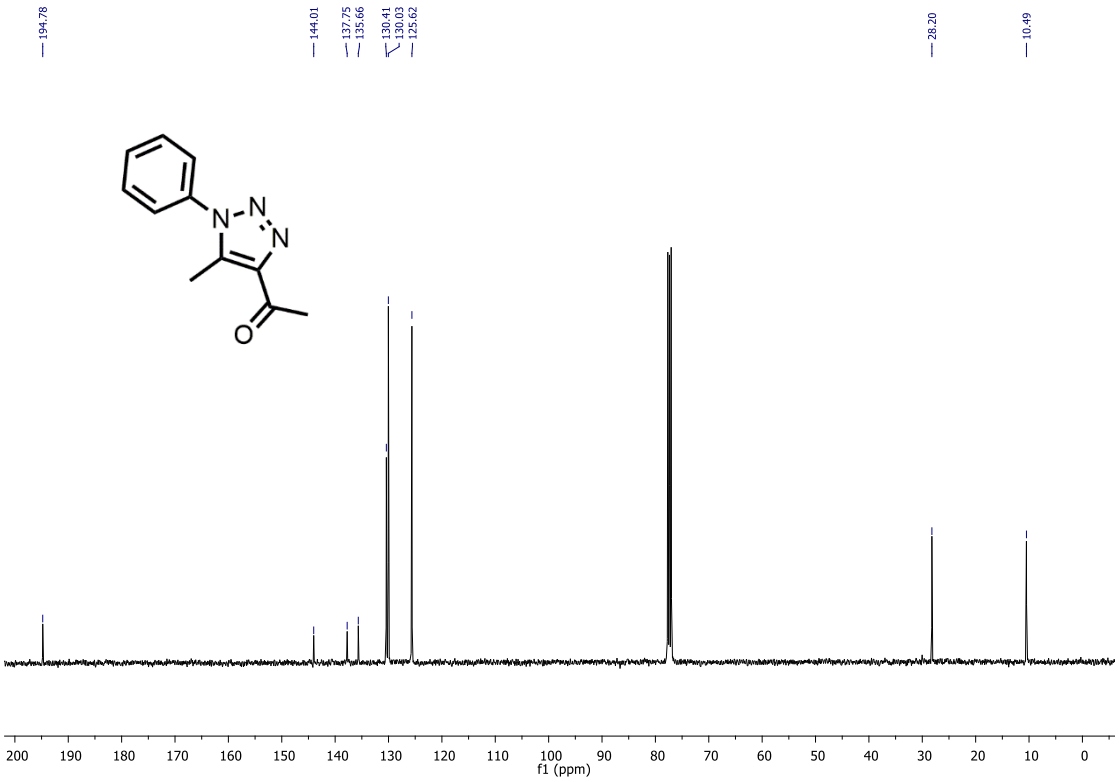

Figure 8: ^{13}C NMR (100 MHz, $CDCl_3$) Spectrum of compound **1b**.

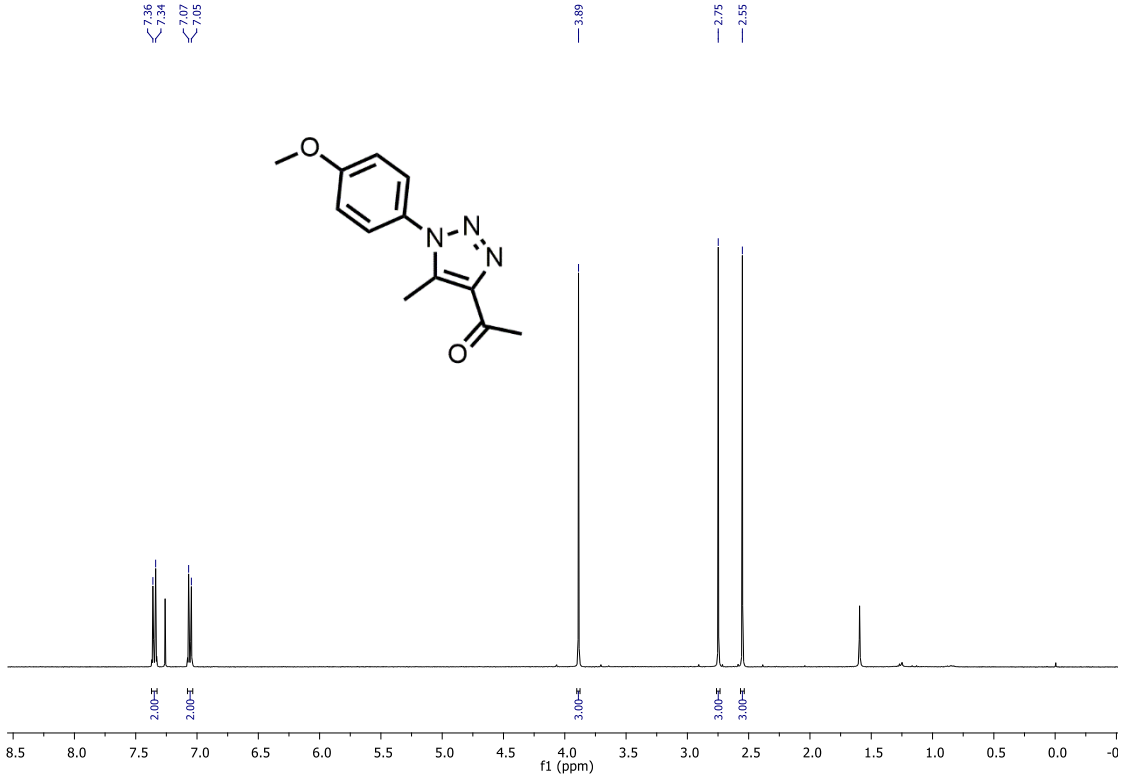

Figure 9: ^{1}H NMR (400 MHz, $CDCl_3$) Spectrum of compound **1c**.

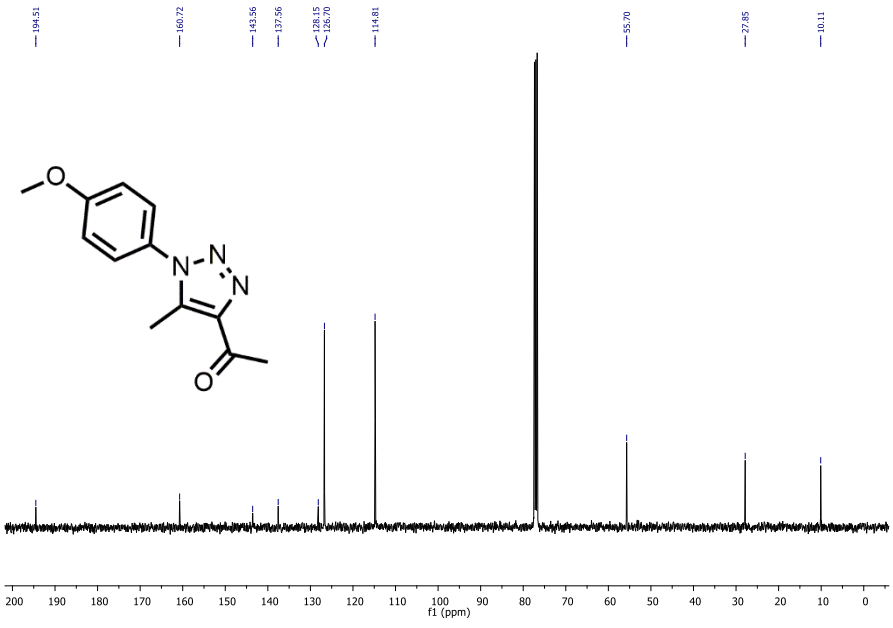

Figure 10: ^{13}C NMR (100 MHz, $CDCl_3$) Spectrum of compound **1c**.

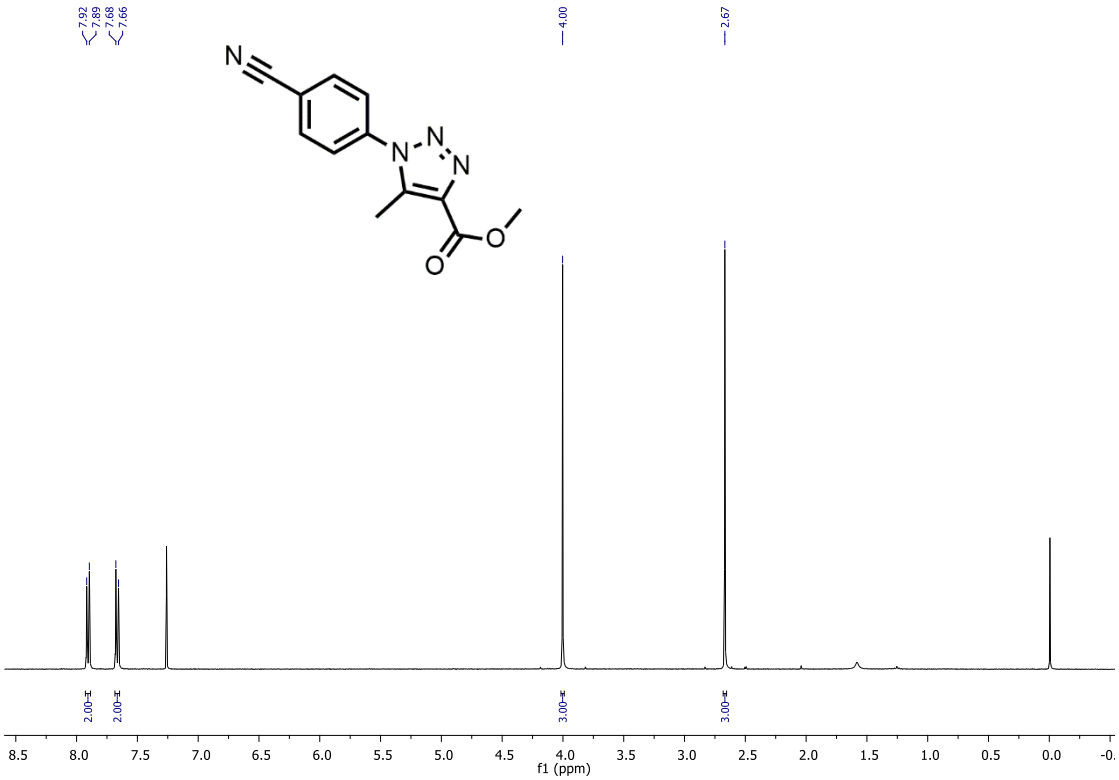

Figure 11: ^{1}H NMR (400 MHz, $CDCl_3$) Spectrum of compound **1d**.

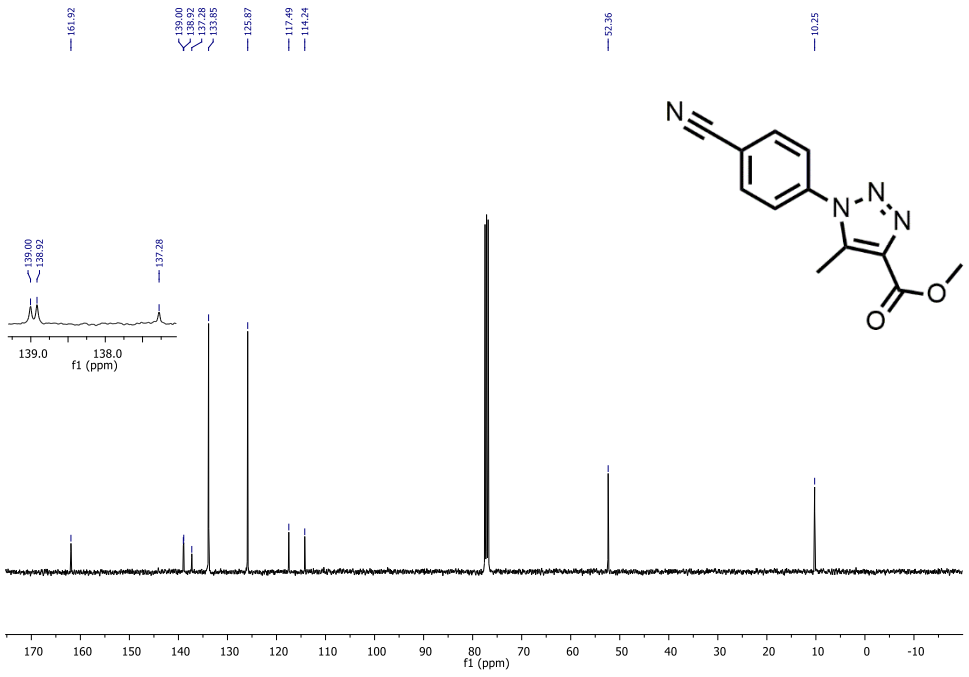

Figure 12: ^{13}C NMR (100 MHz, $CDCl_3$) Spectrum of compound **1d**.

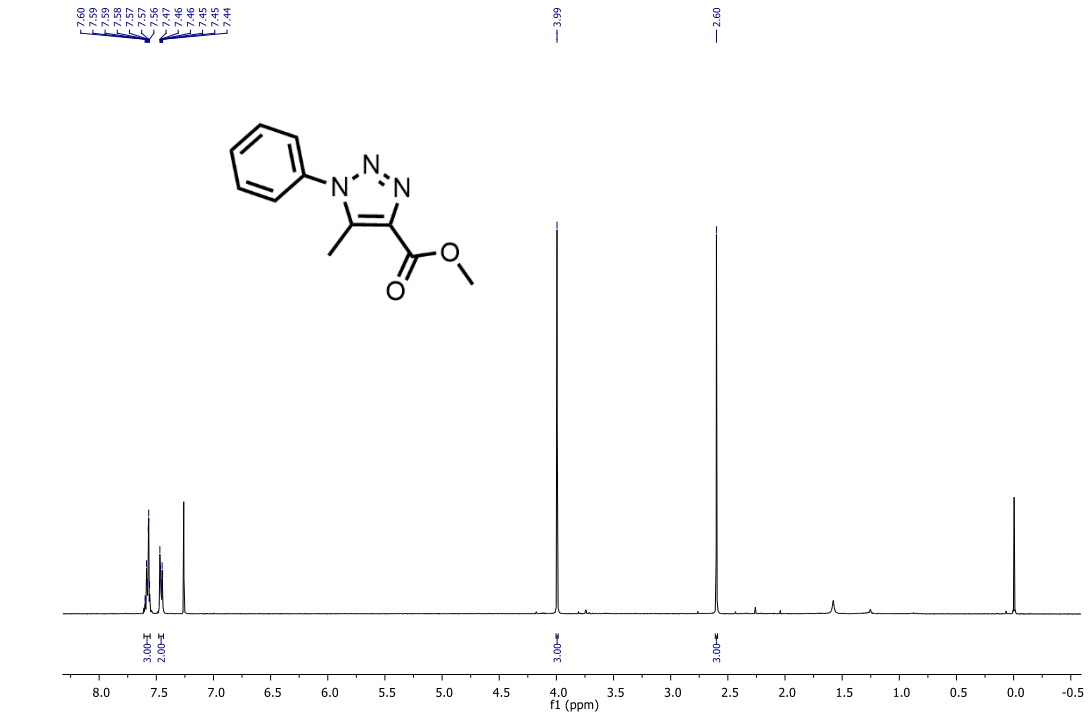

Figure 13: ^{1}H NMR (400 MHz, $CDCl_3$) Spectrum of compound **1e**.

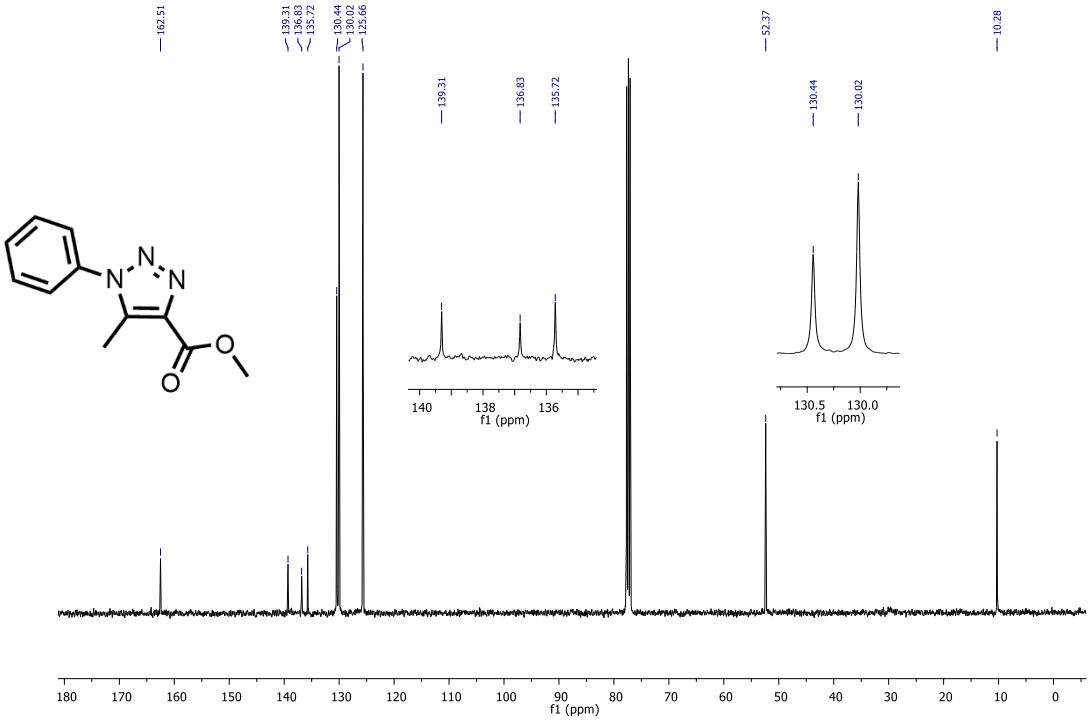

Figure 14: ^{13}C NMR (100 MHz, $CDCl_3$) Spectrum of compound **1e**.

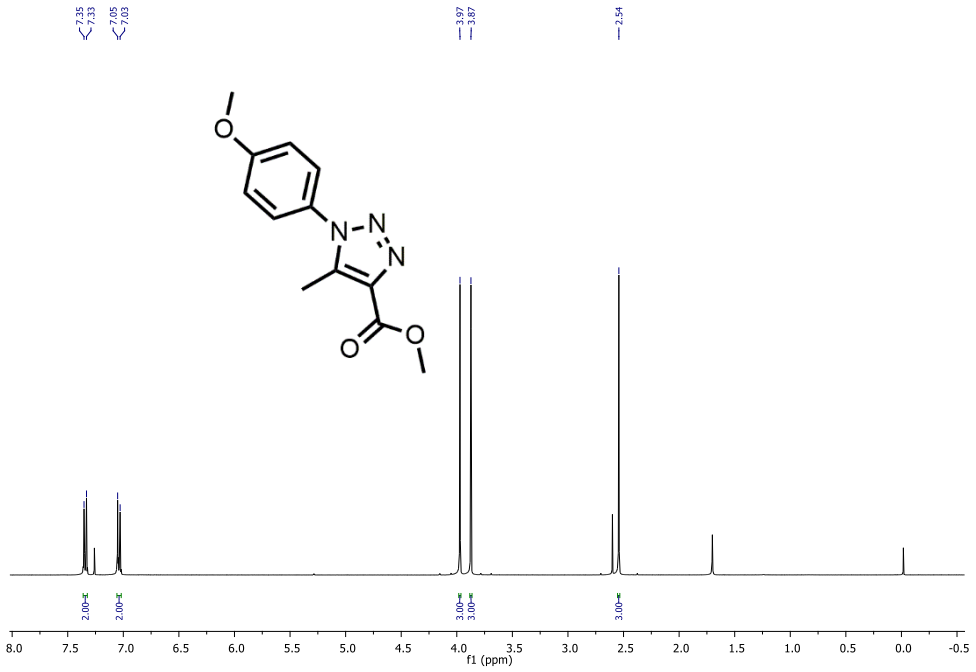

Figure 15: ^{1}H NMR (400 MHz, $CDCl_3$) Spectrum of compound **1f**.

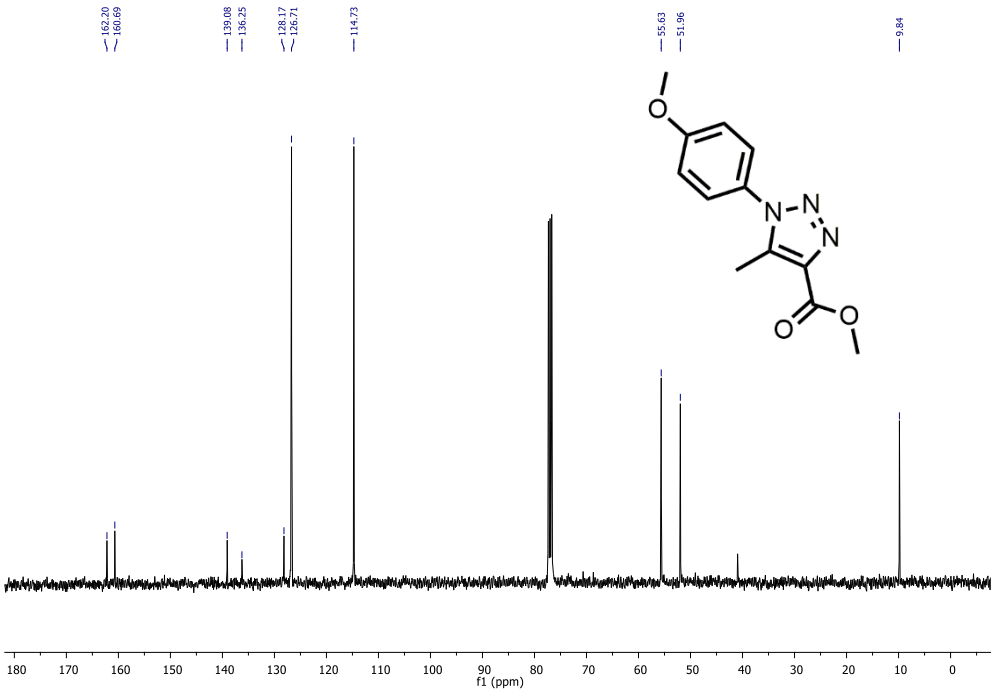

Figure 16: ^{13}C NMR (100 MHz, $CDCl_3$) Spectrum of compound **1f**.

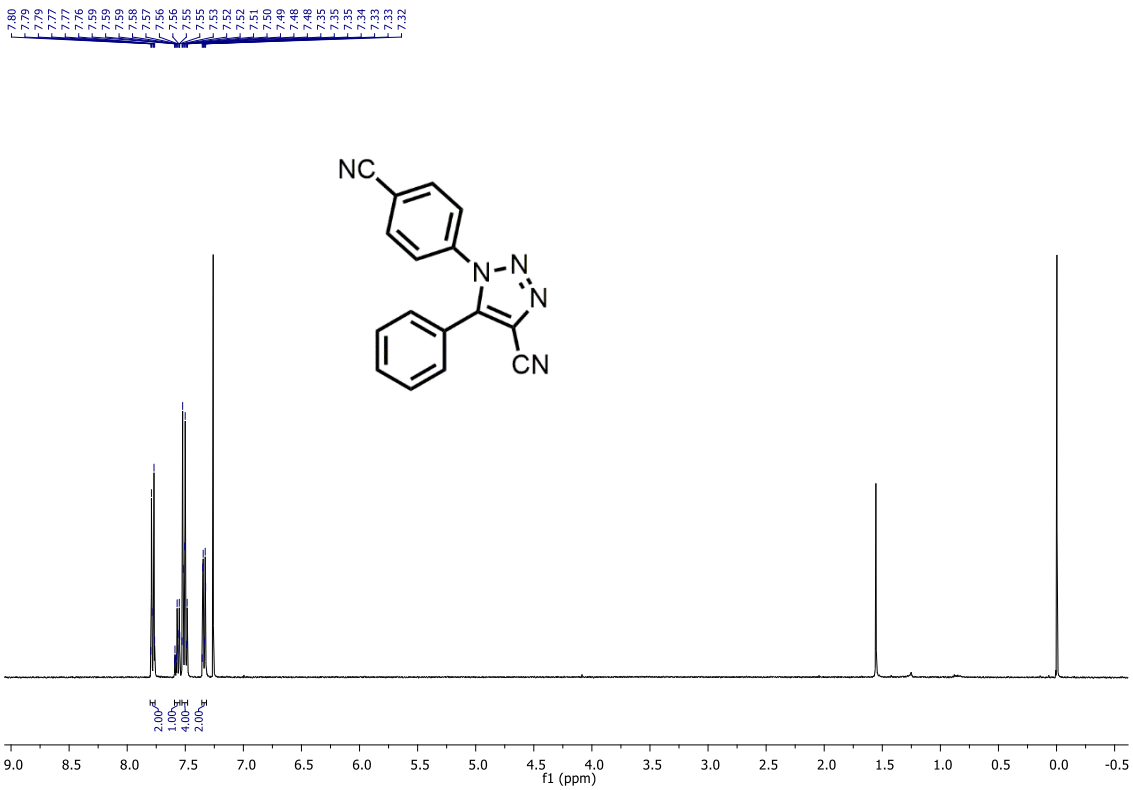

Figure 17: ^{1}H NMR (400 MHz, $CDCl_3$) Spectrum of compound **1g**.

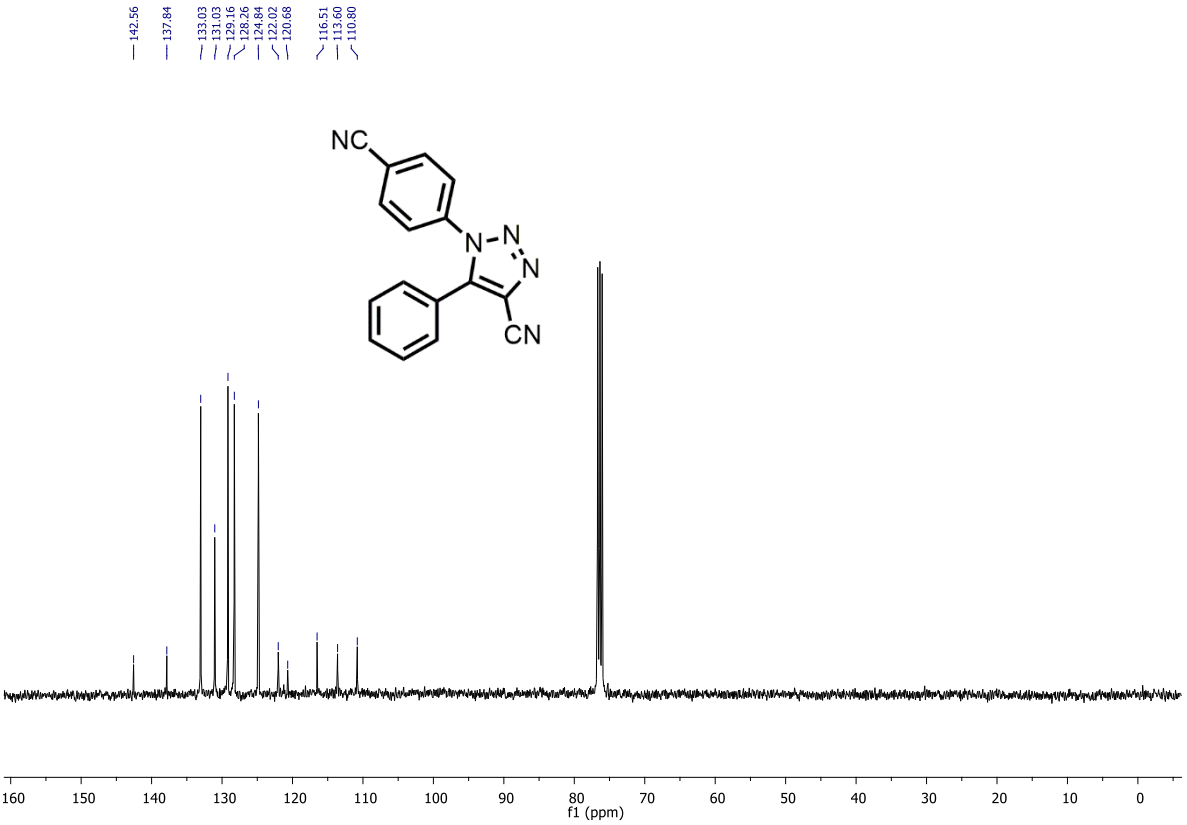

Figure 18: ^{13}C NMR (100 MHz, $CDCl_3$) Spectrum of compound **1g**.

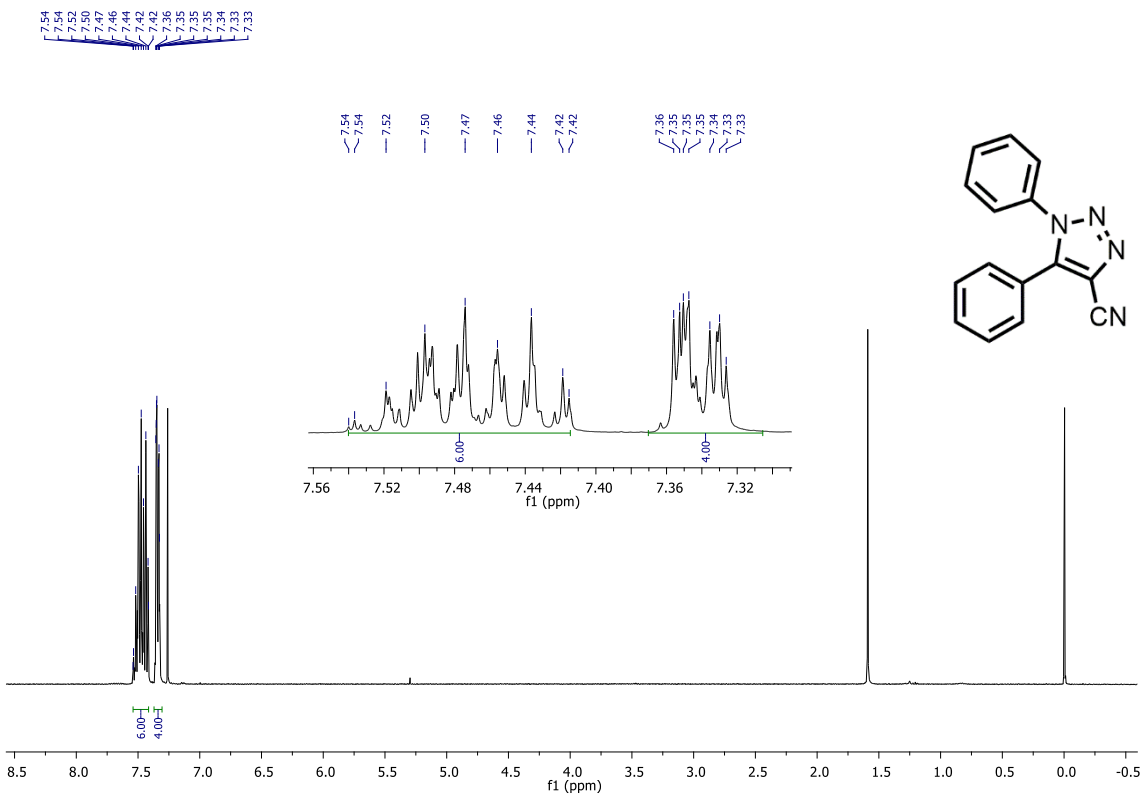

Figure 19: ^{1}H NMR (400 MHz, $CDCl_3$) Spectrum of compound **1h**.

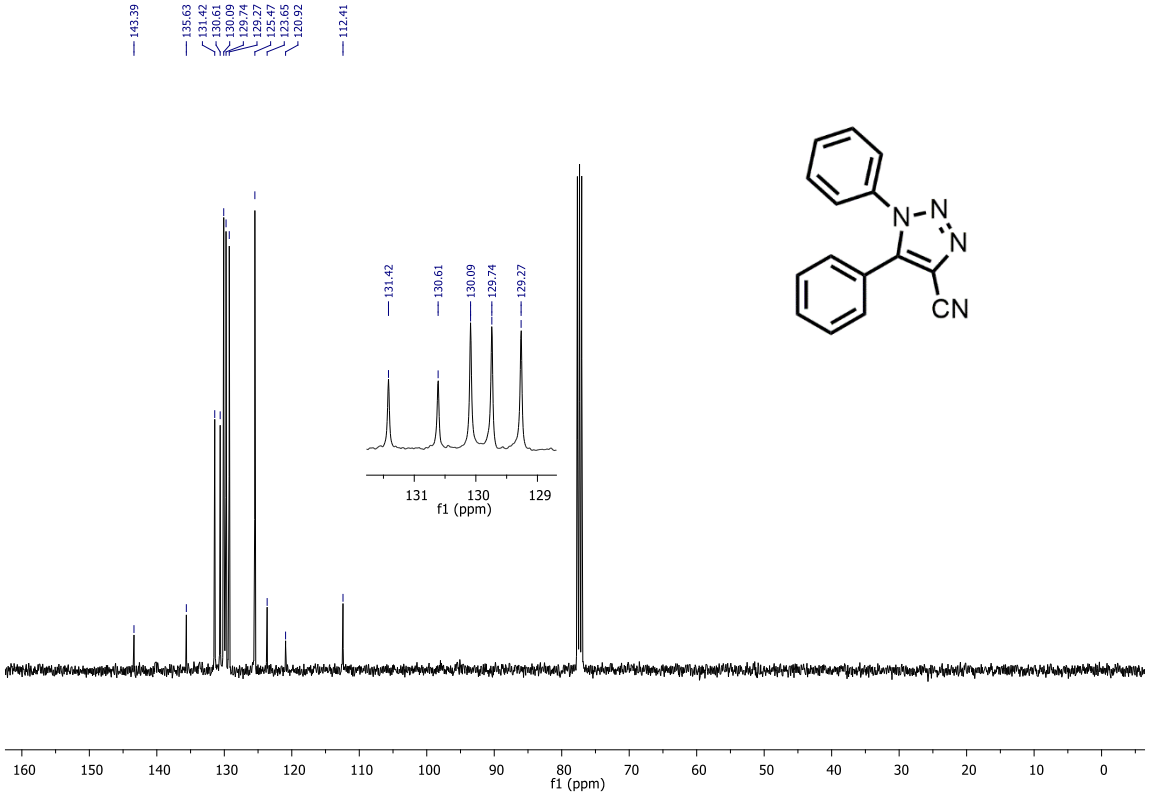

Figure 20: ^{13}C NMR (100 MHz, $CDCl_3$) Spectrum of compound **1h**.

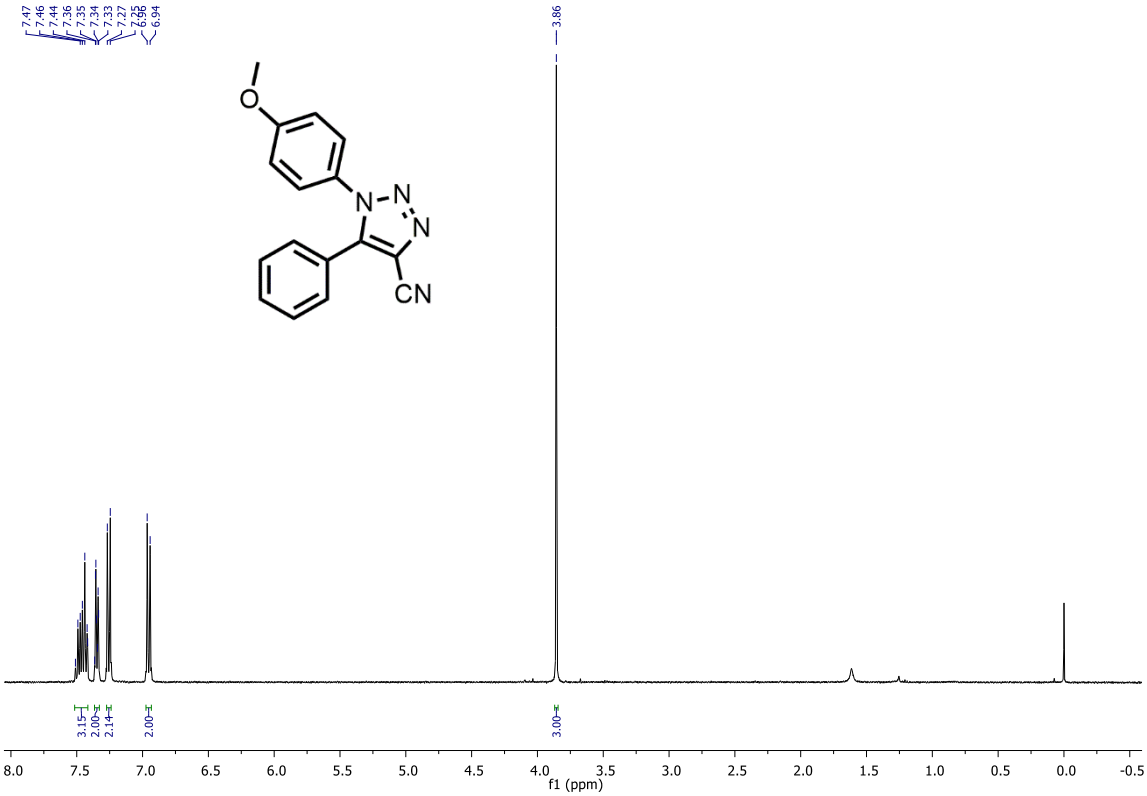

Figure 21: ^{1}H NMR (400 MHz, $CDCl_3$) Spectrum of compound **1i**.

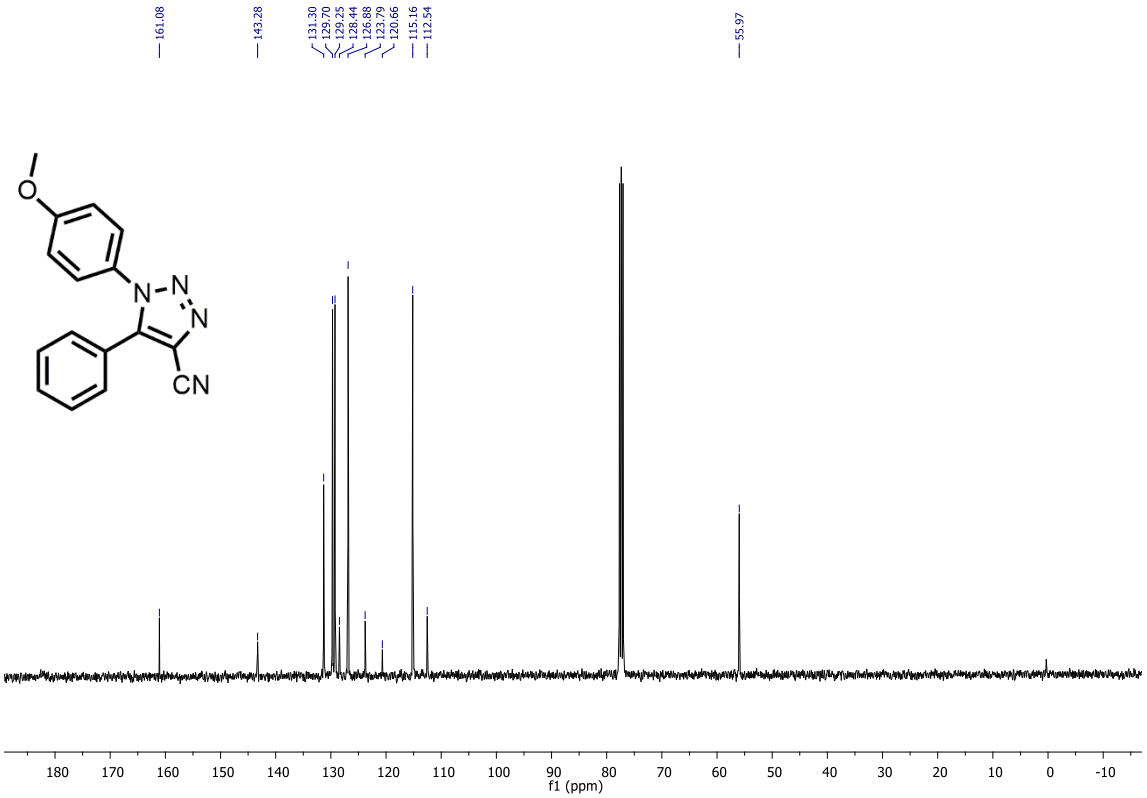

Figure 22: ^{13}C NMR (100 MHz, $CDCl_3$) Spectrum of compound **1i**.

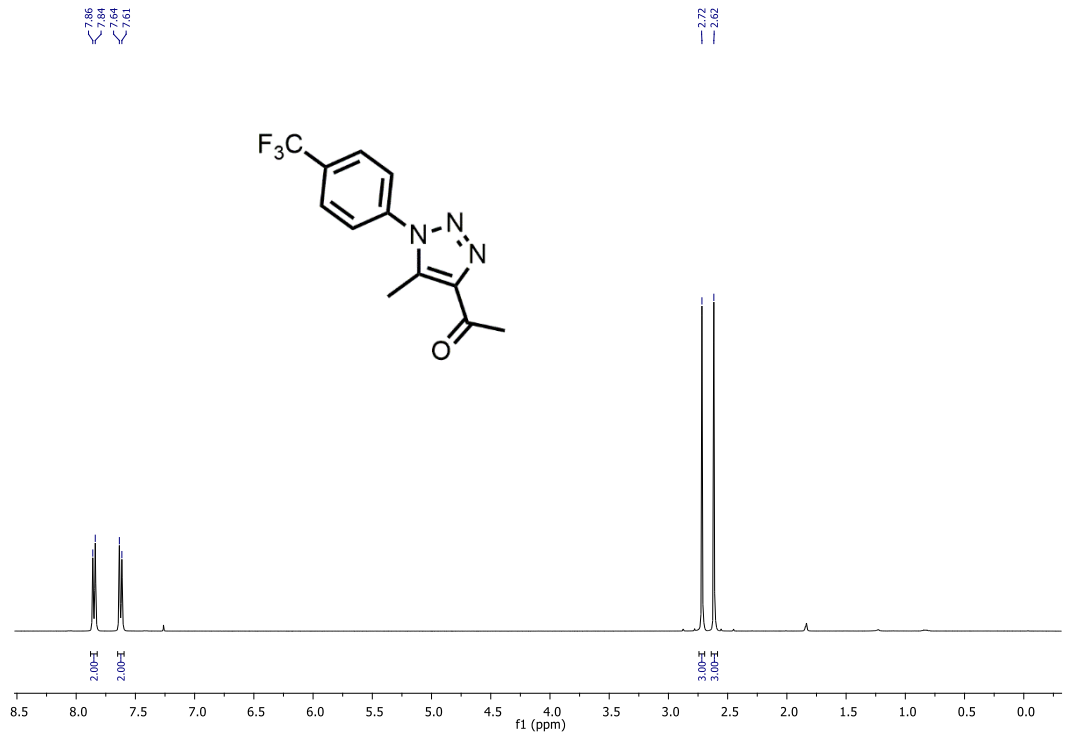

Figure 23: ^{1}H NMR (400 MHz, $CDCl_3$) Spectrum of compound **1k**.

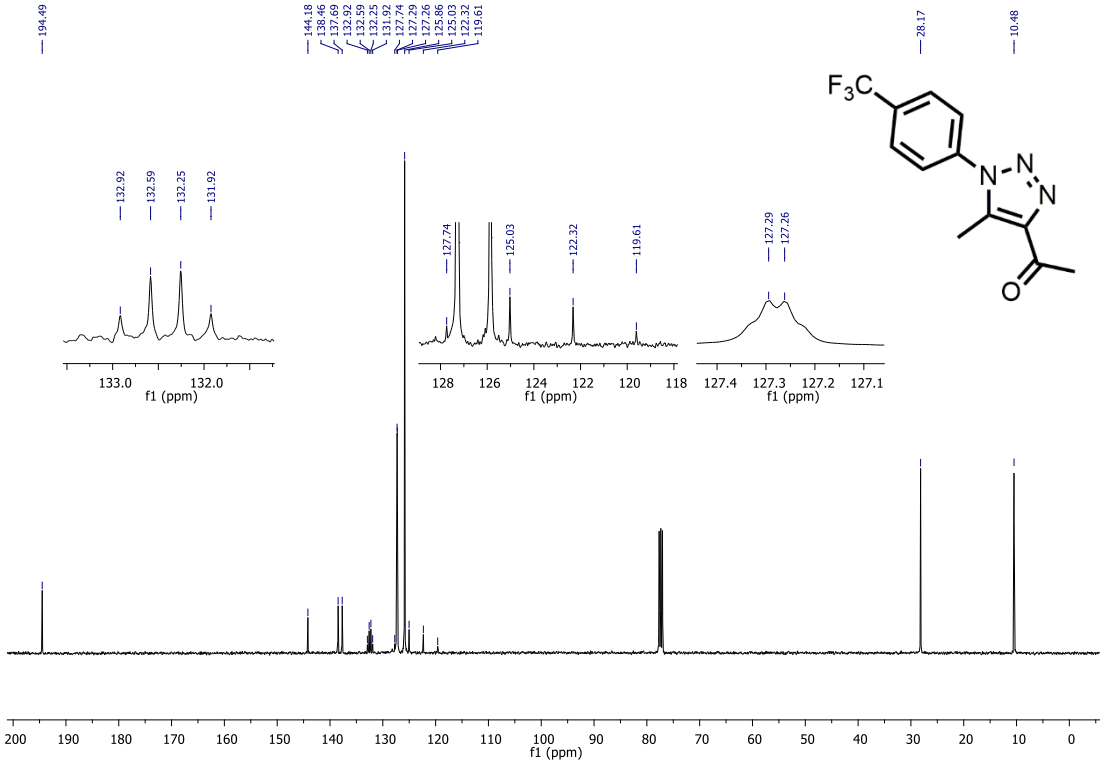

Figure 24: ^{13}C NMR (100 MHz, $CDCl_3$) Spectrum of compound **1k**.

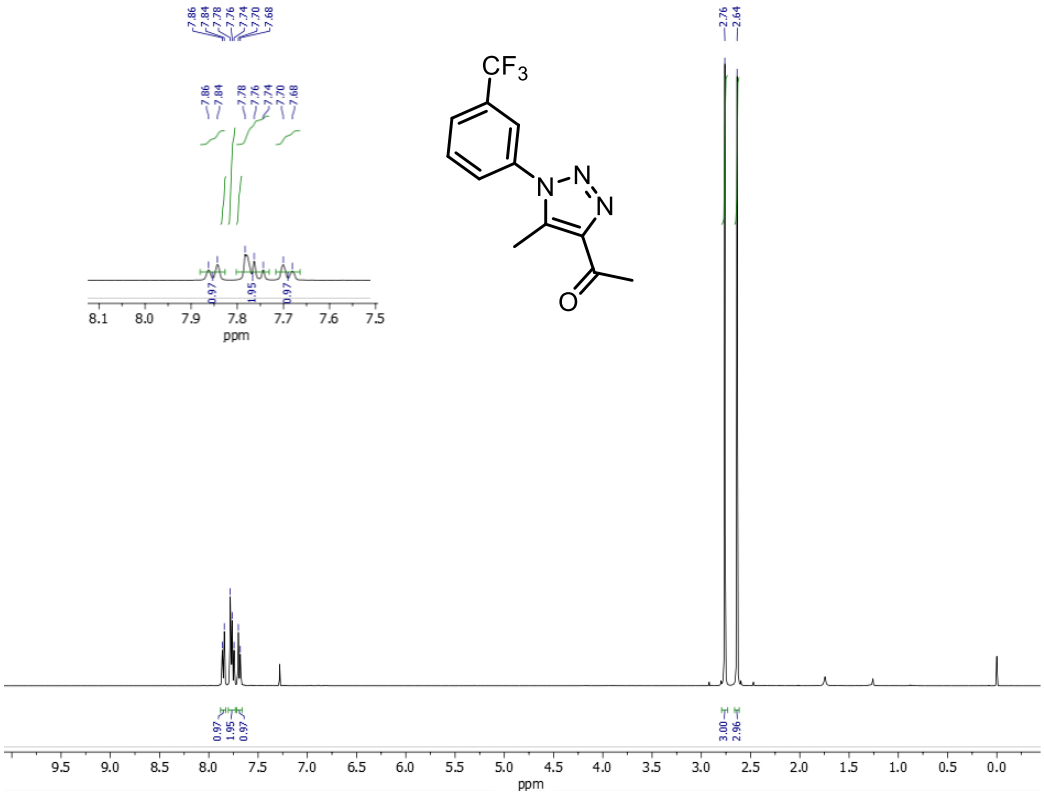

Figure 25: ^{1}H NMR (400 MHz, $CDCl_3$) Spectrum of compound **1l**.

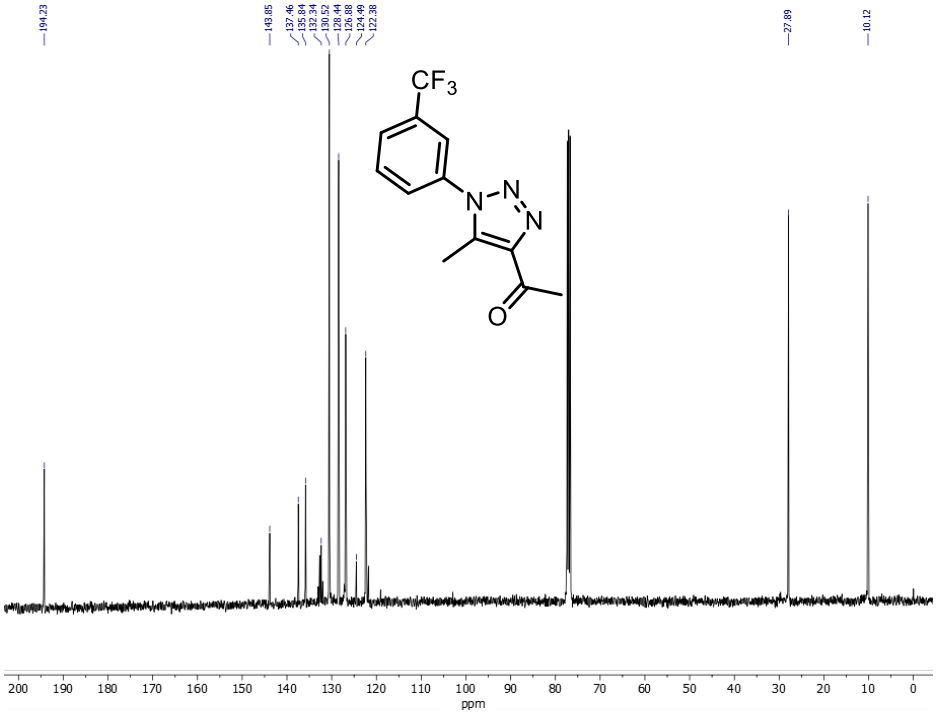

Figure 26: ^{13}C NMR (100 MHz, $CDCl_3$) Spectrum of compound **1l**.

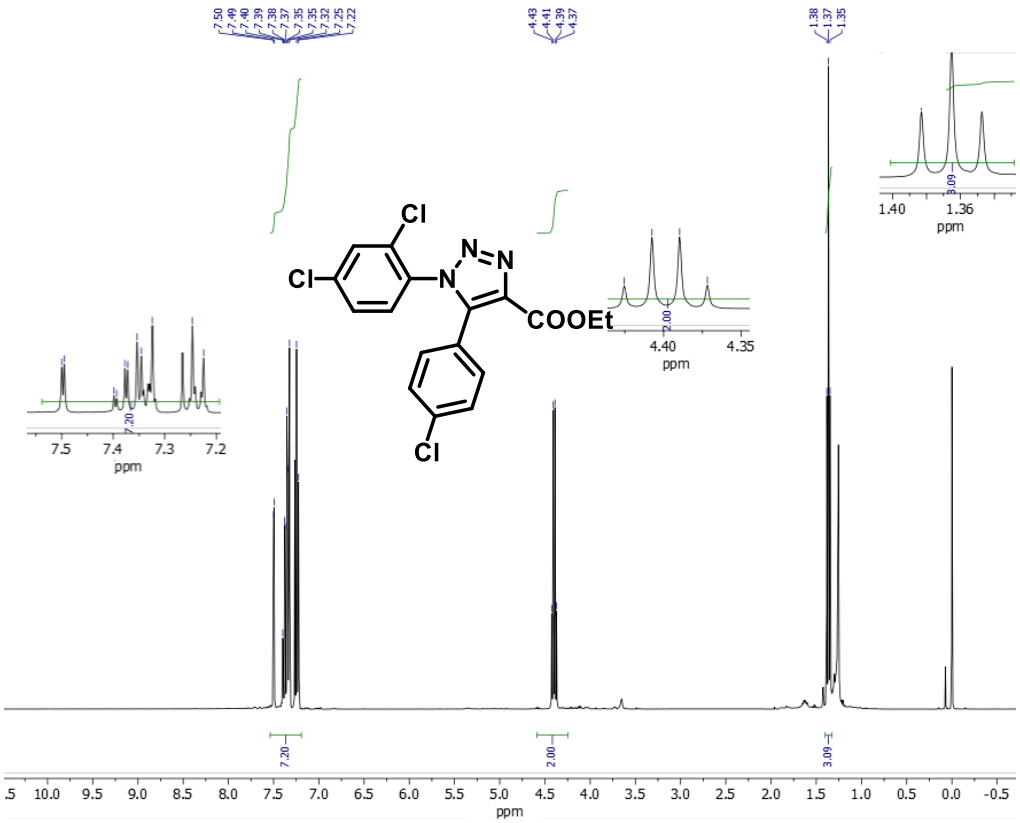

Figure 27: ^{1}H NMR (400 MHz, $CDCl_3$) Spectrum of compound **1p**.

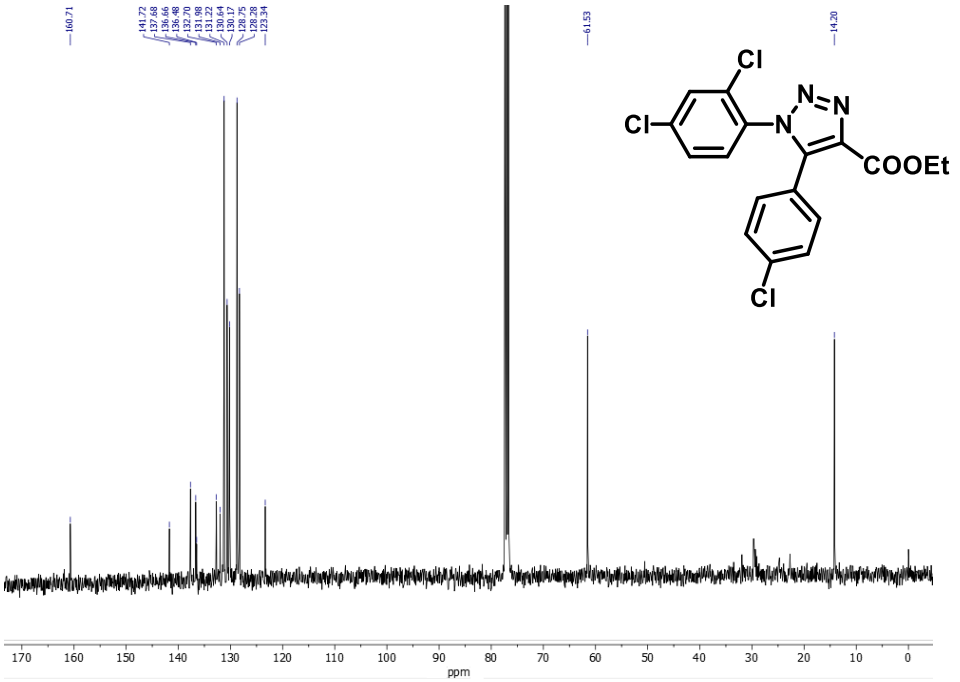

Figure 28: ^{13}C NMR (100 MHz, $CDCl_3$) Spectrum of compound **1p.**

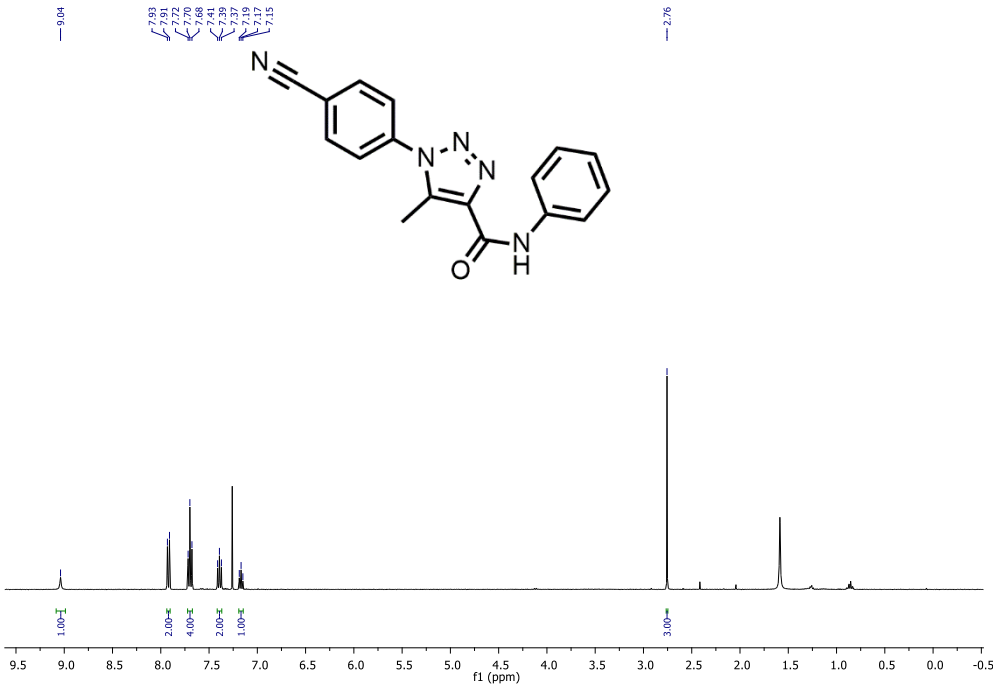

Figure 29: ^{1}H NMR (400 MHz, $CDCl_3$) Spectrum of compound **1n.**

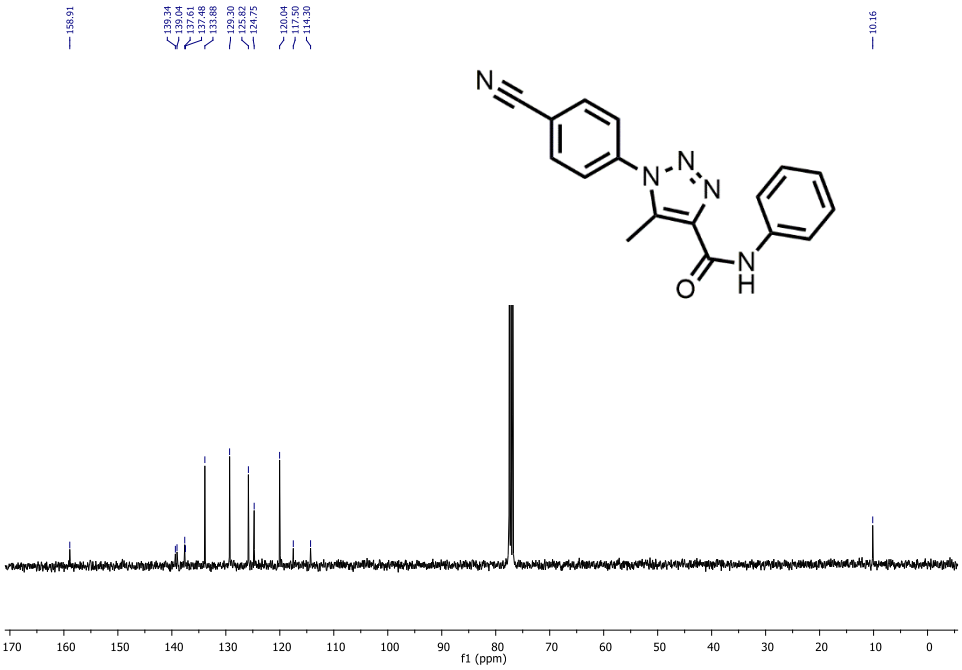

Figure 30: ^{13}C NMR (100 MHz, $CDCl_3$) Spectrum of compound **1n**.

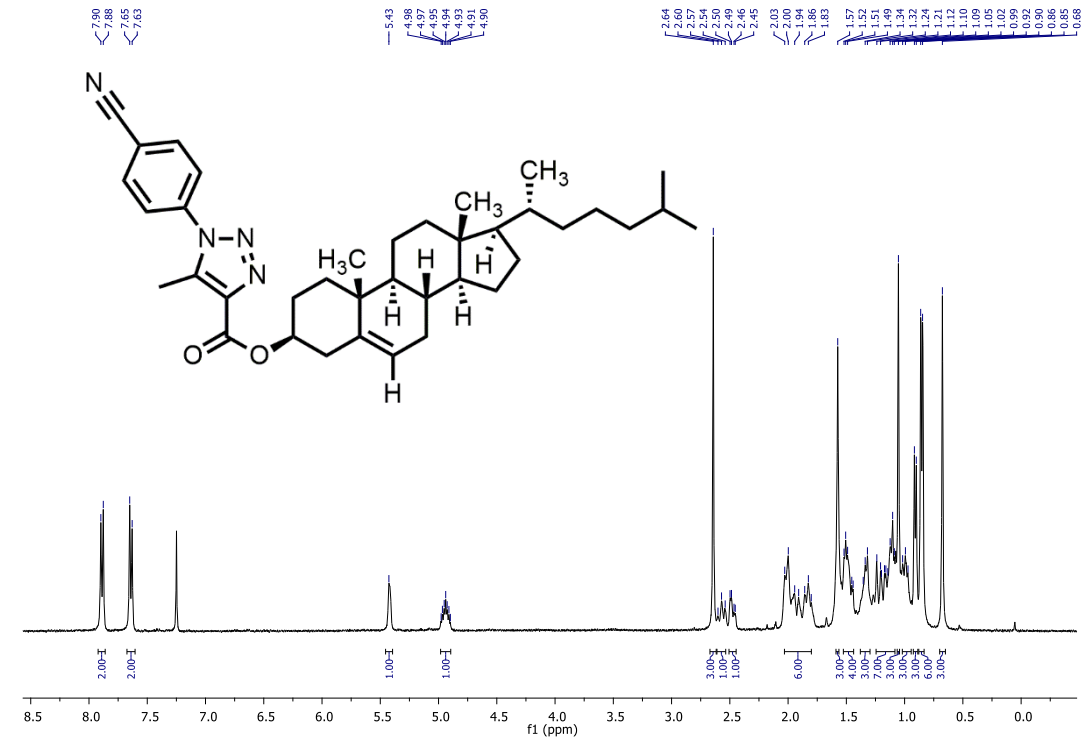

Figure 31: ^{1}H NMR (400 MHz, $CDCl_3$) Spectrum of compound **1q**.

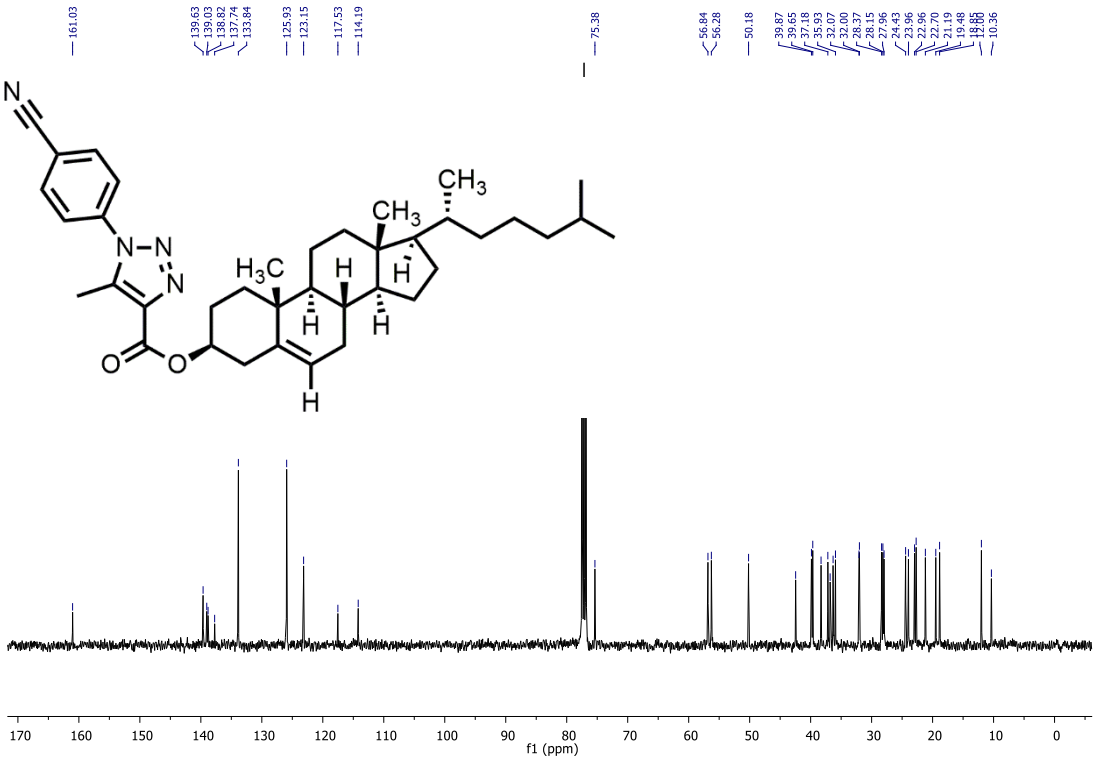

Figure 32: ^{13}C NMR (100 MHz, $CDCl_3$) Spectrum of compound **1q**.

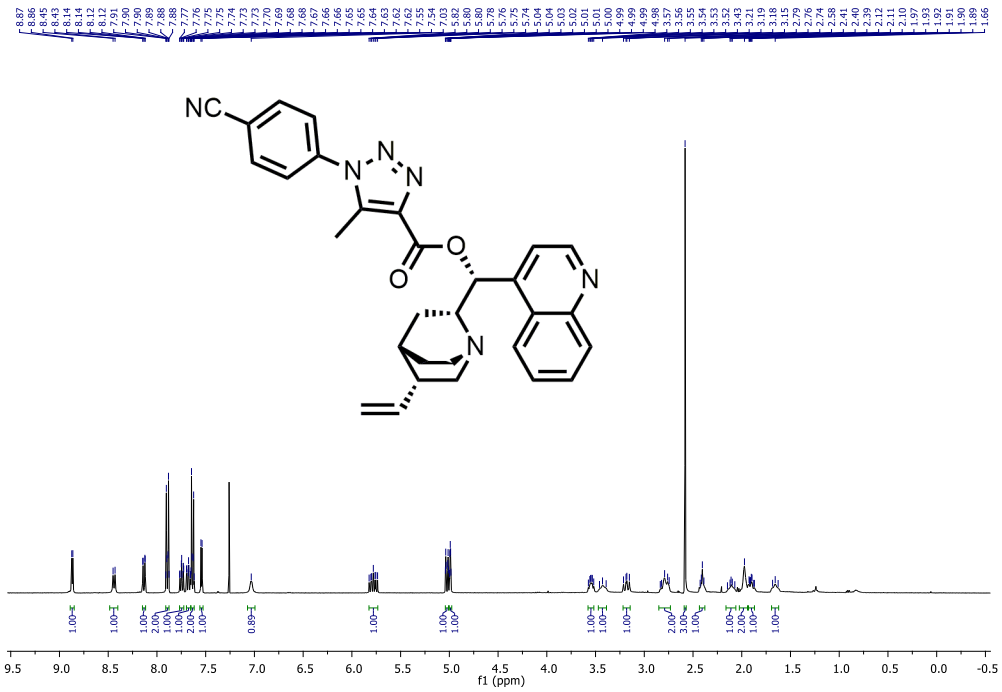

Figure 33: ^{1}H NMR (400 MHz, $CDCl_3$) Spectrum of compound **1r**.

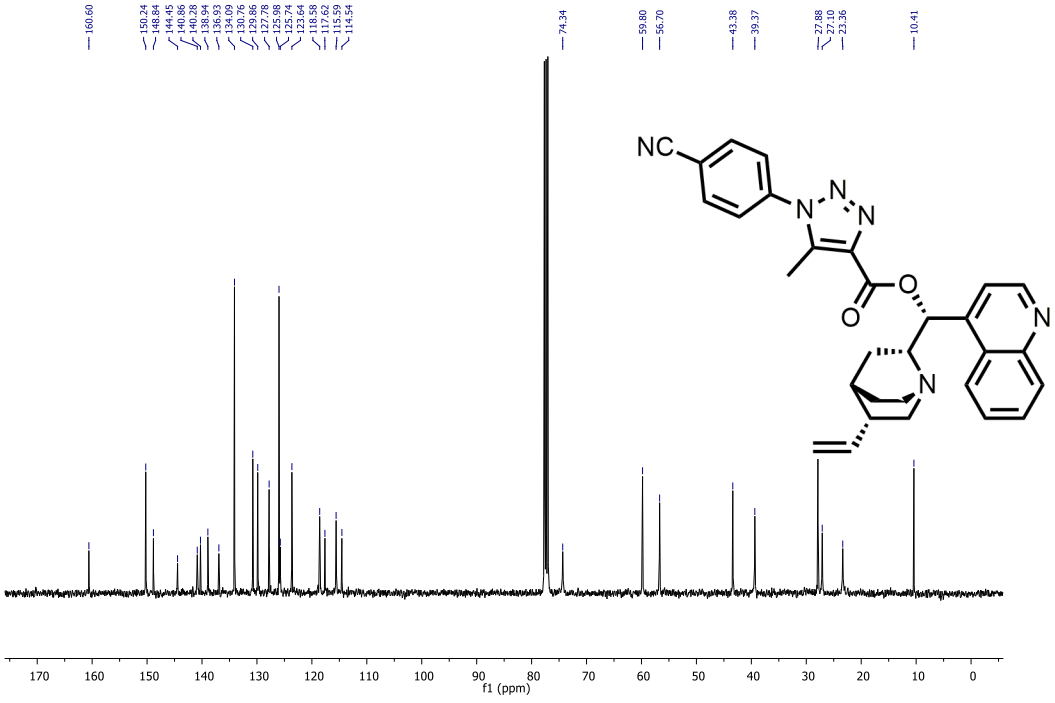

Figure 34: ^{13}C NMR (100 MHz, $CDCl_3$) Spectrum of compound **1r**.

2.5. References

(1) DUA1, R.; DUA, R.; SHRIVASTAVA, S.; SONWANE, S. K.; SRIVASTAVA, S. K. Pharmacological Significance of Synthetic Heterocycles Scaffold: A Review. *Adv. Biol. Res. (Rennes).* **2011**, *5* (3), 120–144.

(2) BONANDI, E.; CHRISTODOULOU, M. S.; FUMAGALLI, G.; PERDICCHIA, D.; RASTELLI, G.; PASSARELLA, D. The 1,2,3-triazole ring as a bioisostere in medicinal chemistry. *Drug Discov. Today* **2017**, *22* (10), 1572–1581. https://doi.org/10.1016/J.DRUDIS.2017.05.014.

(3) DHEER, D.; SINGH, V.; SHANKAR, R. Medicinal attributes of 1,2,3-triazoles: Current developments. *Bioorg. Chem.* **2017**, *71*, 30–54. https://doi.org/10.1016/j.bioorg.2017.01.010.

(4) PETERSON, L. B.; BLAGG, B. S. J. Click chemistry to probe Hsp90: Synthesis and evaluation of a series of triazole-containing novobiocin analogues. *Bioorg. Med. Chem. Lett.* **2010**, *20* (13), 3957–3960. https://doi.org/10.1016/J.BMCL.2010.04.140.

(5) NAHRWOLD, M.; BOGNER, T.; EISSLER, S.; VERMA, S.; SEWALD, N. “Clicktophycin-52”: A Bioactive Cryptophycin-52 Triazole Analogue. *Org. Lett.* **2010**, *12* (5), 1064–1067. https://doi.org/10.1021/ol1000473.

(6) DOIRON, J.; SOULTAN, A. H.; RICHARD, R.; TOURÉ, M. M.; PICOT, N.; RICHARD, R.; ČUPERLOVIĆ-CULF, M.; ROBICHAUD, G. A.; TOUAIBIA, M. Synthesis and structure–activity relationship of 1- and 2-substituted-1,2,3-triazole letrozole-based analogues as aromatase inhibitors. *Eur. J. Med. Chem.* **2011**, *46* (9), 4010–4024. https://doi.org/10.1016/J.EJMECH.2011.05.074.

(7) POKHODYLO, N.; SHYYKA, O.; MATIYCHUK, V. Synthesis of 1,2,3-Triazole Derivatives and Evaluation of their Anticancer Activity. *Sci. Pharm.* **2013**, *81* (3), 663–676. https://doi.org/10.3797/scipharm.1302-04.

(8) PEYTON, L. R.; GALLAGHER, S.; HASHEMZADEH, M. Triazole antifungals: a review. *Drugs Today (Barc).* **2015**, *51* (12), 705–718. https://doi.org/10.1358/dot.2015.51.12.2421058.

(9) GIFFIN, M. J.; HEASLET, H.; BRIK, A.; LIN, Y.-C.; CAUVI, G.; WONG, C.-H.; MCREE, D. E.; ELDER, J. H.; STOUT, C. D.; TORBETT, B. E. A Copper(I)-Catalyzed 1,2,3-Triazole Azide−Alkyne Click Compound Is a Potent Inhibitor of a Multidrug-Resistant HIV-1 Protease Variant. *J. Med. Chem.* **2008**, *51* (20), 6263–6270. https://doi.org/10.1021/jm800149m.

(10) BRIK, A.; ALEXANDRATOS, J.; LIN, Y.-C.; ELDER, J. H.; OLSON, A. J.; WLODAWER, A.; GOODSELL, D. S.; WONG, C.-H. 1,2,3-Triazole as a Peptide Surrogate in the Rapid Synthesis of HIV-1 Protease Inhibitors. *ChemBioChem* **2005**, *6* (7), 1167–1169. https://doi.org/10.1002/cbic.200500101.

(11) BEKTAŞ, H.; KARAALI, N.; ŞAHIN, D.; DEMIRBAŞ, A.; KARAOGLU, Ş. A.; DEMIRBAŞ, N. Synthesis and Antimicrobial Activities of Some New 1,2,4-Triazole Derivatives. *Molecules* **2010**, *15* (4), 2427–2438. https://doi.org/10.3390/molecules15042427.

(12) HUISGEN, R. 1,3-Dipolar Cycloadditions. Past and Future. *Angew. Chemie Int. Ed. English* **1963**, *2* (10), 565–598. https://doi.org/10.1002/ANIE.196305651.

(13) TRON, G. C.; PIRALI, T.; BILLINGTON, R. A.; CANONICO, P. L.; SORBA, G.; GENAZZANI, A. A. Click chemistry reactions in medicinal chemistry: Applications of the 1,3-dipolar cycloaddition between azides and alkynes. *Med. Res. Rev.* **2008**, *28* (2), 278–308. https://doi.org/10.1002/med.20107.

(14) AMBLARD, F.; CHO, J. H.; SCHINAZI, R. F. Cu(I)-Catalyzed Huisgen Azide−Alkyne 1,3-Dipolar Cycloaddition Reaction in Nucleoside, Nucleotide, and Oligonucleotide Chemistry. *Chem. Rev.* **2009**, *109* (9), 4207–4220. https://doi.org/10.1021/cr9001462.

(15) LI ZHANG, XINGUO CHEN, PENG XUE, HERMAN H. Y. SUN, IAN D. WILLIAMS, K. BARRY SHARPLESS, VALERY V. FOKIN, AND; GUOCHEN JIA. Ruthenium-Catalyzed Cycloaddition of Alkynes and Organic Azides. **2005**. https://doi.org/10.1021/JA054114S.

(16) KAMALRAJ, V. R.; SENTHIL, S.; KANNAN, P. One-pot synthesis and the fluorescent behavior of 4-acetyl-5-methyl-1,2,3-triazole regioisomers. *J. Mol. Struct.* **2008**, *892* (1–3), 210–215. https://doi.org/10.1016/J.MOLSTRUC.2008.05.028.

(17) ANDERSON, N. G. Using Continuous Processes to Increase Production. *Org. Process Res. Dev.* **2012**, *16* (5), 852–869. https://doi.org/10.1021/op200347k.

(18) BRIAN P. MASON; KRISTIN E. PRICE; JEREMY L. STEINBACHER; ANDREW R. BOGDAN, AND; MCQUADE, D. T. Greener Approaches to Organic Synthesis Using Microreactor Technology. **2007**. https://doi.org/10.1021/CR050944C.

(19) MEŠČIĆ, A.; ŠALIĆ, A.; GREGORIĆ, T.; ZELIĆ, B.; RAIĆ-MALIĆ, S. Continuous flow-ultrasonic synergy in click reactions for the synthesis of novel 1,2,3-triazolyl appended 4,5-unsaturated l -ascorbic acid derivatives. *RSC Adv.* **2017**, *7* (2), 791–800. https://doi.org/10.1039/C6RA25244C.

(20) ZHANG, H.; DONG, D.-Q.; WANG, Z.-L. Direct Synthesis of N-Unsubstituted 4-Aryl-1,2,3-triazoles Mediated by Amberlyst-15. *Synthesis (Stuttg).* **2015**, *48* (01), 131–135. https://doi.org/10.1055/s-0035-1560488.

(21) LI, D.; LIU, L.; TIAN, Y.; AI, Y.; TANG, Z.; SUN, H.; ZHANG, G. A flow strategy for the rapid, safe and scalable synthesis of N-H 1, 2, 3-triazoles via acetic acid mediated cycloaddition between nitroalkene and NaN 3. *Tetrahedron* **2017**, *73* (27–28), 3959–3965. https://doi.org/10.1016/j.tet.2017.05.065.

(22) BORUKHOVA, S.; NOËL, T.; METTEN, B.; DE VOS, E.; HESSEL, V. From alcohol to 1,2,3-triazole via a multi-step continuous-flow synthesis of a rufinamide precursor. *Green Chem.* **2016**, *18* (18), 4947–4953. https://doi.org/10.1039/C6GC01133K.

(23) GU, J.; FANG, Z.; YANG, Z.; LI, X.; ZHU, N.; WAN, L.; WEI, P.; GUO, K. A two-step continuous flow synthesis of 1,4-disubstituted 1,2,3-triazoles under metal- and azide-free conditions. *RSC Adv.* **2016**, *6* (92), 89073–89079.

https://doi.org/10.1039/C6RA19022G.

(24) Molecular Sieves - Technical Information Bulletin | Sigma-Aldrich https://www.sigmaaldrich.com/chemistry/chemical-synthesis/learning-center/technical-bulletins/al-1430/molecular-sieves.html (accessed Nov 23, 2017).

Chapter 2

Peptoids catalysts grafted on the renewable polymer, polyfurfuryl alcohol, for the applications in heterogeneous enamine catalysis

Abstract: In this chapter the multicomponent assembly of prolyl pseudo-peptide catalysts with the simultaneous incorporation of a polymerizable furan handle is described. This protocol enabled the subsequent polymerization of the organocatalyst with furfuryl alcohol, thus rendering polyfurfuryl alcohol-supported catalysts for applications in heterogeneous enamine catalysis. The utilization of the polymer-supported catalysts either in batch or continuous-flow organocatalytic procedures proved to have moderate catalytic efficacy and enantioselection, but diastereoselectivity was found to be excellent in the asymmetric Michael addition reaction of *n*-butanal and *β*-nitrostyrene.

Keywords: Organocatalysis • Asymmetric Michael Addition • Renewable Polymer

3.1. Introduction

The immobilization of secondary amine-based catalysts onto the organic polymers and silica gel has been emerged as an effective strategy that combines the power of heterogeneous and organocatalysis.[1-3] Asymmetric catalysis using polymer-supported chiral organocatalysts usually provides a much greener prospect for the synthesis of enantiomerically enriched building blocks.[4-6] Importantly, immobilized catalysts not only boosts the recyclability of the catalyst but also allow the implementation of continuous-flow procedures, which usually encompass high reaction yields and generation of less waste; all aspects recognized as compatible with the principles of green chemistry.[1-6] An innovative approach was presented by Gutmann, using fibbers from polyethylene terephthalate and polyamide as support for the heterogeneous catalyst (**Scheme 16**).

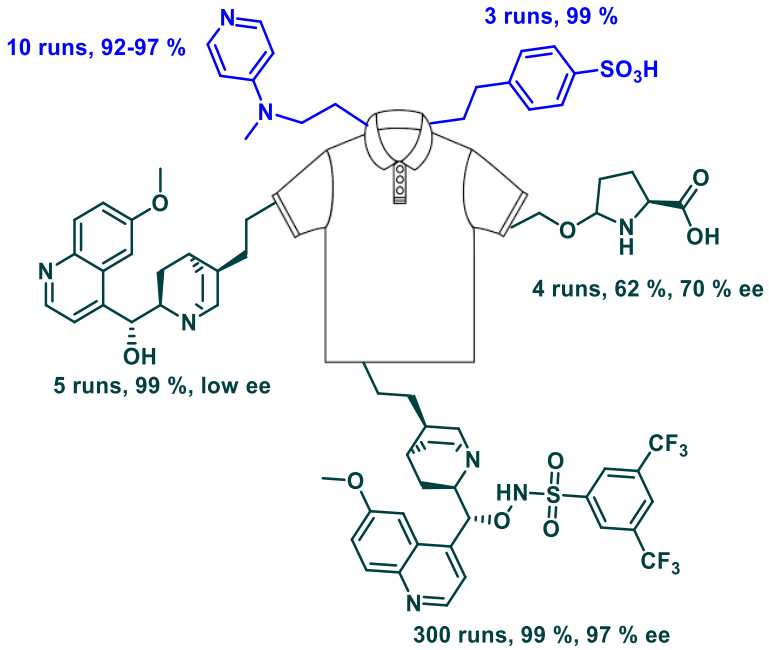

Scheme 16. Textile catalysis - An unconventional approach towards heterogeneous catalysis.

However, almost all the polymers used in the development of supported organocatalysts are made from non-renewable sources and composed of non-biodegradable materials (e.g., polystyrene).[1-3] When the objective is implementing large scale catalytic processes with supported organocatalysts, a

relevant “green” premise is the use of renewable and readily available solid supports.[1-6] Accordingly, we envisioned the utilization of the polymer polyfurfuryl alcohol (pFA) – derived from a renewable resource like sugar cane biomass – for the incorporation of chiral pyrrolidine-based motifs capable to catalyse relevant asymmetric reactions.

The incorporation of an organocatalyst into a polymer support requires either conjugation to the polymer or functionalization with a polymerizable handle that is suitable for subsequent copolymerization with a monomeric counterpart. In this regard, we have previously developed an Ugi reaction-based multicomponent approach suitable for the simultaneous assembly and functionalization of prolyl *pseudo*-peptide catalysts,[7] which has proven great efficacy in asymmetric organocatalytic Michael addition reactions. As an extension of this concept to the field of immobilized organocatalyst, we, next reported the use of the multicomponent approach for the synthesis of silica-grafted peptide catalysts for the application in continuous-flow catalysis.[8] In an endeavour to develop a cheaper and renewable polymer-supported organocatalyst, herein we describe the multicomponent synthesis of furfuryl-containing prolyl *pseudo*-peptide catalysts and their subsequent utilization in the preparation of pFA-supported catalysts amenable for continuous-flow asymmetric enamine catalysis (**Scheme 17**).[9,10]

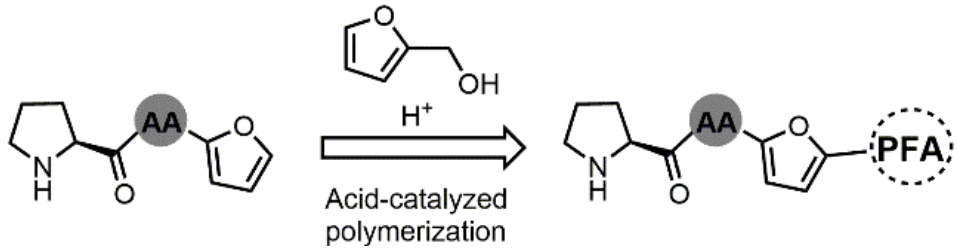

Scheme 17. Schematic synthesis of polyfurfulyl alcohol (pFA) incorporating a prolyl peptide catalyst. AA: Amino acid.

The acid-catalyzed polymerization of furfuryl alcohol renders a dark polymer featuring a complex cross-linked polyunsaturated scaffold derived from polycondensation and Diels-Alder reactions.[11,12] Worldwide, there is a well-stablished industry of furfural production from corncobs and sugarcane pentoses, making the polymers derived from this material among the most versatile and

promising due to their renewable character and easy exploitation of such biomasses.[12,13] As depicted in scheme 17, we envisioned the synthesis of a prolyl dipeptide having a furan ring handle, which could be subsequently incorporated into pFA during the polymerization process.

3.2. Results and discussion

A solution-phase multicomponent procedure – based on the Ugi reaction[16-18] – was employed for the one-pot assembly of prolyl *pseudo*-peptide catalysts bearing the furan functionality. As shown in scheme 17, Boc-L-proline and acetone were employed as acid and oxo-components, respectively, for the Ugi four-component reaction in combination either with furfuryl amine and cyclohexyl isonitrile or with *S*-(α)-methylbenzyl amine and furfuryl isonitrile. We have previously proven the feasibility of this multicomponent approach for the combinatorial synthesis and rapid screening of *pseudo*-peptide catalysts [7] and their silica gel-immobilized variants.[8] In this case, the use of furfuryl derivatives as both the amine and isonitrile component in order to explore whether the position of the polymerizable handle is important for the organocatalytic performance or not. Peptides **1** and **2** were subjected to Boc deprotection by treatment with 20% trifluoroacetic acid (TFA) in CH_2Cl_2 and then to TFA-catalyzed polymerization in the presence of furfuryl alcohol (10 equiv) according to a procedure described to pFA (

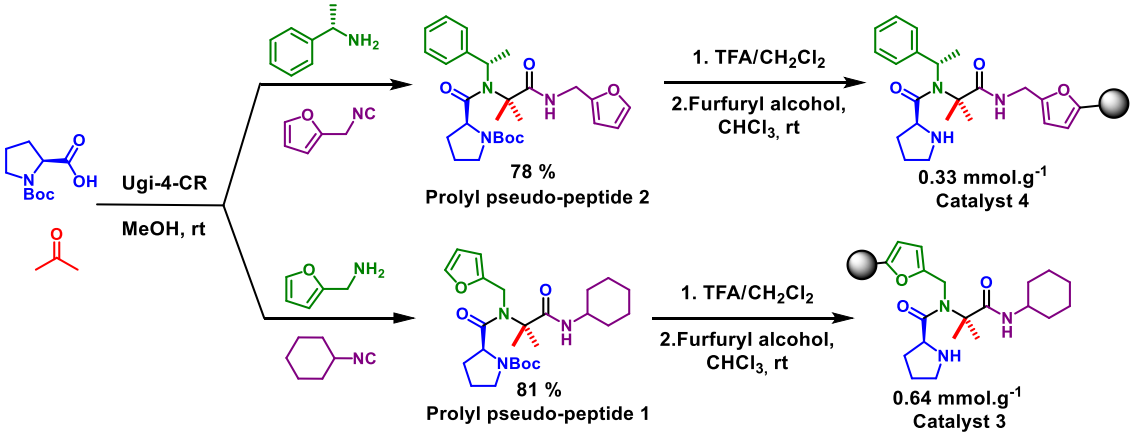

Scheme 18).[16]

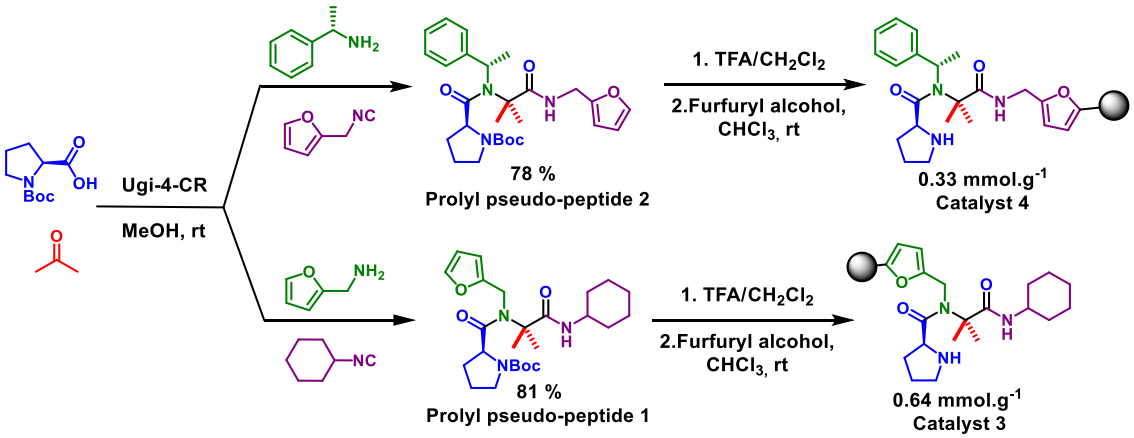

Scheme 18. Ugi-four-component reaction (Ugi-4CR) for the synthesis of prolyl pseudo-peptide catalysts and their subsequent polymerization with furfuryl alcohol to obtain polymeric chiral materials **3** and **4**. TFA = Trifluoroacetic acid. pFA = polyfurfuylalcohol.

The polymerization starts as a green solution that eventually turns brown and then black. The polymer suspension was neutralized by washing with a 1 M NaOH aqueous solution and then precipitated from petroleum ether. The resulting dark solids were ground until the retained material on 45 μm sieve was lower than 10%, thus rendering enough material of pFA-supported prolyl peptide catalysts **3** and **4**.

The microanalysis of the polymers **3** and **4** shows a peptide catalyst loading of 0.64 mmol·g^{-1} and 0.33 mmol·g^{-1}, respectively, calculated from the content of nitrogen by CHNs analysis. The FT-IR spectrum of **3** and **4** were compared with the pFA that clearly showed the incorporation of the peptidic moiety into the polymer matrix (see the Experimental Section). For example, the new bands appearing at 2930 cm^{-1} and 1700 cm^{-1} corresponds to the Csp^3-H and the carbonyl stretching, respectively that were not present in the neat pFA. Similarly, there are other new bands that were not occurred in the case of pFA, such as the amine stretching and the band around 1420 cm^{-1} that also attributed to the aliphatic segments. The thermo-oxidative degradation of polymeric catalysts **3** and **4** were also examined using TGA, and compared it with that of pFA (see the Experimental Section). These analysis showed that both polymers **3** and **4** are stable up to 100 ºC, but as expected, decompose before the neat pFA. Thus, as a main difference is the significant loss of mass observed in **3** and **4** at the range

of 100-300 ºC, wherein the neat pFA is still much stable at that temperature. This first degradation can be attributed to the decomposition of the peptidic skeleton, while at around 300 ºC starts the decomposition of the polymeric lattice matrix as well as that of pFA. This analysis further demonstrates the incorporation of the peptide moieties into the pFA matrix, while proves the good stability of the pFA-supported catalysts under classical working temperatures (i.e., up to 100 ºC).

To assess the catalytic performance of the pFA-supported catalysts, a model system consisting an organocatalytic conjugate addition of *n*-butanal to *trans*-β-nitrostyrene was implemented. During the initial screening, standard reaction conditions that comprising the use of 10 mol % of catalyst, toluene as solvent and room temperature were employed. As shown in Table 1, pFA – used as control – did not afford the Michael product (entry 1) due to the lack of the catalytic pyrrolidine moiety. On the other hand, pFA-supported catalysts **3** and **4** gave moderate to good yields depending on the solvent used. In general, catalyst **3** provided better yield, enantio and diastereoselectivity in the Michael adduct than catalyst **4** in the tested solvents and conditions. As pFA-supported catalyst **3** proved more effective than **4**, a comprehensive screening of solvents was carried out for the asymmetric Michael addition reaction catalysed by the catalyst **3**.

This study showed that, yield can be increased up to 90% by using *i*-propanol (entry 9) while the diastereoselectivity remains constantly high in all the solvents. Unfortunately, the enantioselectivity of the Michael additions remained moderate with both catalysts in all the tested solvents and conditions, only rising upto 84% of ee when catalyst **3** was used in toluene. The better catalytic performance of pFA-supported catalyst **3** compared to **4** may be not only due to the higher catalyst loading in the polymer, but also because of position of the furan ring.

Table 1. Screening of pFA-supported prolyl peptide catalysts and reaction under batch conditions heterogeneous Michael addition.

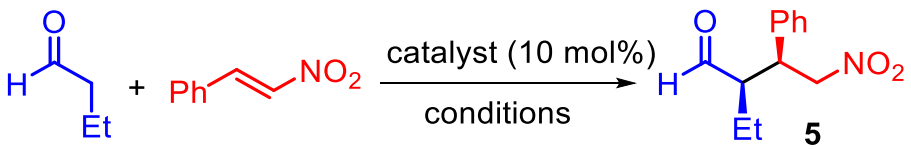

Entry[a]	Catalyst	Solvent	Yield (%)[c]	*dr.* (*syn*/*anti*)[d]	ee (%)[e]
1	pFA	Toluene	-	-	-
2	3	Toluene	58	95:5	84
3	4	Toluene	52	94:6	29
4	3	THF	83	93:7	77
5	4	THF	62	96:4	53
6	3	Acetonitrile	72	94:6	54
7	3	*n*-Hex	54	95:5	56
8[b]	3	*n*-Hex/*i*-PrOH	70	96:4	68
9	3	*i*-PrOH	90	97:3	61
10	3	Ethanol	69	96:4	53
11	3	H_2O	76	96:4	66

a) All reactions were conducted using 3 equivalents of *n*-butanal and 0.25 mmol of *β*-nitrostyrene in 1 mL of solvent. b) 9:1 mixture of *n*-hexane/*i*-propanol. c) Yield of isolated pure product. d) Determined by ^{1}H NMR spectroscopy analysis on the crude product. e) Determined by chiral-stationary phase HPLC analysis on the pure product.

During the implementation of the heterogeneous organocatalytic reaction in batch, some of the polymer features proved to be limiting the efficiency. For example, the polymer powder showed to have low density, thus making difficult for the catalyst recovery by decantation. In addition, gravity filtration was employed but the powder material was mostly remained on the filter paper. To overcome this problem, we turned our attention to implement a continuous-flow organocatalytic system by charging an HPLC column with the pFA-supported catalyst **3**. Thus, catalyst **3** was packed into a stainless-steel column (Ø = 0.21 cm (diameter), l = 15 cm (length), particle size = 45µm). The main features of the resulting packed microreactor were determined by the pycnometry method,[19,20] as reported in Table 2.

Table 2. Main features of the catalytic microreactor.

Loading of **3** (mmol g^{-1})[a]	Amount w_{tot} (mg)[b]	V_0 (µL)[c]	V_G (µL)[d]	V_{bed} (µL)[e]	τ (min)[f]	ε_{tot}[g]

0.639	264	349	519	170	140	0.67

a) Determined by elemental analysis. b) w_{tot} =V_0 δ_0+ w_{ads} + w_{hw} c) V_0= w_1-w_2/ δ_1 - δ_2 d) Geometric Volume V_G=πhr^2*10^3 (h=15cm, r=0.105cm). e) V_{bed} = V_G-V_0 f) residence time calculated at flow rate ϕ =2.5 µL min^{-1}, τ=V_0/ϕ) Total porosity ε_{tot}= V_0/V_G

This method consists of filling the microreactor successively with two distinct solvents (here noted as 1, ethanol and 2, *n*-hexane) and then weighting the filled microreactor accurately. The difference between the masses (*w*) of a filled reactor divided by the differences of solvent densities (δ) permits to calculate the microreactor void volume (V_0) (dead volume). This feature is important because it provides an idea of the volume that is not utilized in the microreactor. The catalysts loading was kept the same as determined by microanalysis, that is previously described for catalyst **3**. Packing amount (w_{tot}) was also determined by pycnometry. Porosity (ε_{tot}) of 0.67 that is an optimal value for this material, was according to the accepted values. One of the most important features of a microreactor for continuous-flow chemistry is the residence time (τ). Residence time is known as the time at which a substrate passes through the microreactor without interacting. In some cases, the residence time is measured by the time needed to pass a determined dye through the reactor. In the present work it was calculated by dividing V_0 by the used flow rate (ϕ) at 2.5 µL/min.

The study of Michael reaction on continuous-flow model started with the optimization of flow rate. Initially, a solution of β-nitrostyrene (1 equivalent, 0.25 M), *n*-butanal (3 equivalents, 0.75 M) was pumped with a syringe-pump at 2.5 µL.min^{-1} (τ = 140 min) (**Figure 35A**). The concentration was chosen by considering the retention profile of *n*-butanal and β-nitrostyrene in the microreactor. After 22 hours, moderate conversion of the β-nitrostyrene in toluene was observed, indicating poor efficiency of the process. The investigation clearly showed that first, the conversion of the starting material is increasing with the passage of time i.e 24 h, and after that, the reactor productivity decreases considerably (**Figure 35.** Continuous-flow catalytic system monitoring the production of a γ-nitroaldehyde **5** with pFA-supported catalyst **3** packed in a microreactor.**Figure 35B**).

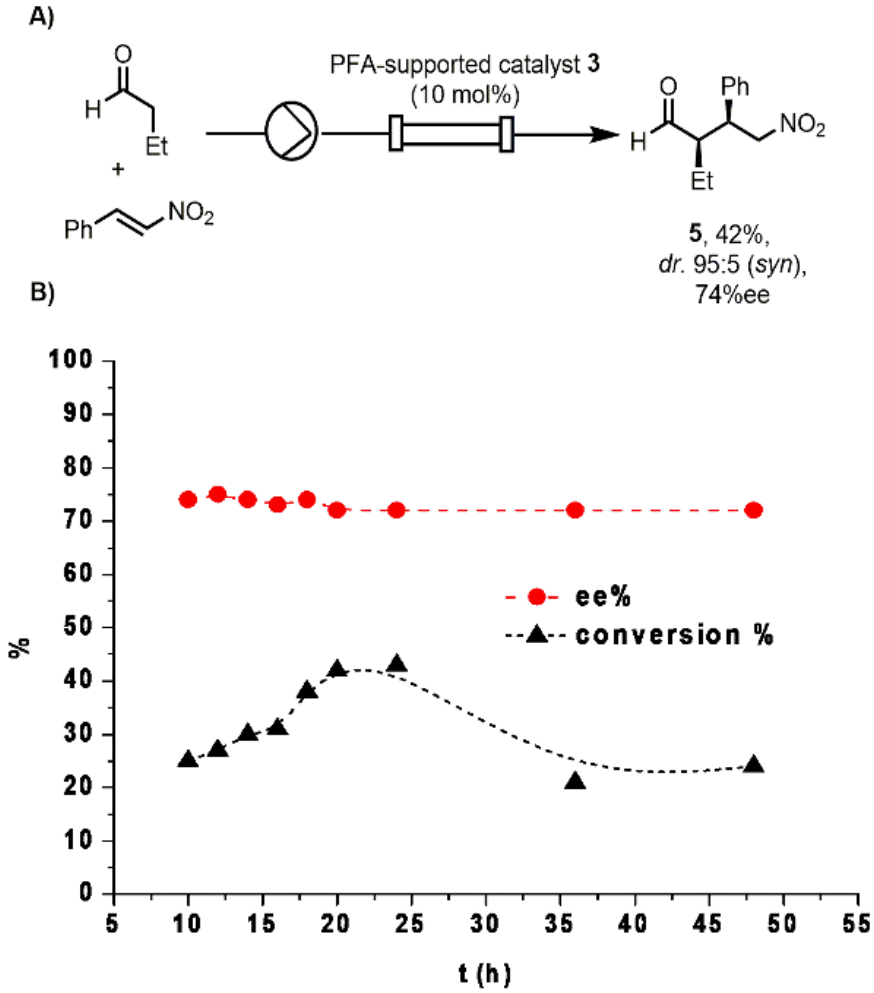

Figure 35. Continuous-flow catalytic system monitoring the production of a γ-nitroaldehyde **5** with pFA-supported catalyst **3** packed in a microreactor.

We hypothesized that the higher residence time of β-nitrostyrene in the reactor may lead to the lower yield or the catalyst may acquire inactivation. Accordingly, all the substrates were injected into the reactor that was coupled to HPLC system where the retention time of each substrate within the reactor was measured by UV detector at a wavelength of 210 nm. A retention time of 70 min for β-nitrostyrene for a flow 0.1 ml/min into the reactor was observed. Then, this preferential occupancy of the packing material by β-nitrostyrene (50 times as residence time calculated) limits the formation of the Michael product and, consequently, lowers the chemical efficiency. Despite the good level of diastereocontrol in Michael addition (dr. 95:5 *syn*/*anti*), a little drop in the enantioselectivity was observed (i.e., 74%ee) as compared to the batch process using the same catalyst. Nonetheless, the enantioselection remains constant all

the time of the whole experiment, as shown in Figure 35B. Finally, the overall yield of isolated Michael adduct **5** was achived as 42% after column chromatography, which is in agreement with the conversion determined during the continuous-flow study.

3.3. Conclusion

In conclusion, we have implemented a multicomponent approach for the one-pot assembly of furfuryl-containing organocatalysts that is suitable for incorporation into a polyfurfuryl polymer. Two polymer supported prolyl peptide catalysts were produced by means of an initial Ugi reaction followed by an acid-catalyzed polymerization. The catalytic polymers were screened in the heterogeneous catalytic Michael addition in batch, proving that catalyst **3** is more effective and provides better stereoselectivity as compare to catalyst 4. A continuous-flow organocataytic system was also implemented with catalyst **3**, enabling the continuous production of a γ-nitroaldehyde in moderate yield and enantioselectivity, but with the excellent diastereoselectivity.

Peptoids catalysts grafted on the renewable polymer polyfurfuryl alcohol for applications in heterogeneous enamine catalysis

3.4. Experimental Section

Materials and reagents used were of the highest commercially available grade and used without further purification. ^{1}H NMR and ^{13}C NMR spectra were recorded at 400 MHz for ^{1}H and 100 MHz for ^{13}C, respectively. Chemical shifts (δ) are reported in parts per million relative to the residual solvent signals, and coupling constants (J) are reported in Hertz. HPLC chromatograms were obtained on an apparatus with a LC-10AT Pump, SPD-10A UV-Vis Detector, SCL-10A System Controller, using a Chiralpak OD-H (4,6 mmØ x 250 mmL, particle size 5 µm). Optical rotations were measured with a Polarimeter at 589 nm, 30°C. Thermogravimetric analysis (TGA) was conducted using a thermogravimetric analyser (TGA, Perkin Elmer) operated in the temperature range of 10–700 ºC under nitrogen gas and a heating rate of 10 °C min^{-1}. The Syringe Pump was a Harvard apparatus Plus 11 model. A high-pressure slurry packer fitted with a Haskel 780-3 pump was used for the analytical column packing. Microanalyses were performed with a CHNS analyser Model EA 1108 from Fisons Instruments.

General procedures

General procedure A

The prolyl pseudo-peptides **1** and **2** were prepared according to the literature procedure from a dissolution of the amine (1.0 mmol), the aldehyde (or ketone) (1.0 mmol), the carboxylic acid (1.0 mmol) and the isocyanide (1.0 mmol) in MeOH (5 mL) was stirred at room temperature for 24 h.

General procedure B

The prolyl pseudo-peptides catalyst was dissolved in 3 mL of CH_2Cl_2 and treated with 1 mL of trifluoroacetic acid at 0 °C. The reaction mixture was allowed to reach to the room temperature, stirred for 4 h and then concentrated to dryness (the excess of TFA was removed by repetitive addition and evaporation of further CH_2Cl_2). The crude product was re-dissolved in 10 mL of $CHCl_3$ for polymerization step. To a suspension of the salt pseudo-peptide catalysts (1.0 mmol, 1 equiv.) and furfuryl alcohol (10 mmol, 10 equiv.) in $CHCl_3$ (5 mL) was added TFA (0.5 mmol, 5 mol%) drop by drop for 10 min, and stirred for 24 h at room temperature. The mixture solution changed the colour from yellow-green to brown or dark during the course of reaction. The neutralization of the polymerizing solution was carried out with a concentrated basic solution i.e1 M NaOH (5 mL) solution requires two washes of 10 min each but at the end of the reaction an emulsion may appear. In order to avoid this problem an excess of 0.1 M NaOH solution was used. Polymers were isolated by precipitation in petroleum ether and dried by using a high vacuum line. The resulting dark solid was ground until the retained on 45 µm-sieve was lower than 10%.

pFA: For comparison, pFA was prepared in a conventional way according to the reported procedure.[14]

General procedure C

The nitro-olefin (0.25 mmol) and the aldehyde (0.75 mmol, 3.0 equiv) were added to a solution of the prolyl pseudo-peptide catalyst (0.025 mmol, 0.01 equiv.) in the solvent of choice (1 mL). The reaction mixture was stirred for 24 h and then concentrated under reduced pressure. The resulting crude product was purified by flash column chromatography on silica gel using n-hexane/EtOAc as eluent. Enantiomeric excess (ee) was determined by chiral HPLC analysis through comparison with the authentic racemic material. Assignment of the stereoisomers was performed by comparison with literature data.

For preparation of the racemic standard the same procedure was done, utilizing piperidine (10 mol%) as catalyst.

Prolyl pseudo-peptide 1. According to the general procedure A, furfuylamine (177 µL, 2 mmol), acetone (116 mg, 2 mmol), Boc-(L)-Pro-OH (431 mg, 2 mmol) and cyclohexylisocyanide (249 µL, 2 mmol) were reacted in MeOH (5 mL). Flash column chromatography purification (EtOAc/hexane = 1:1 v/v) afforded the Boc-proline-based peptoid 1 as a colorless oil. A mixture of conformers were observed by NMR (ratio 3:1). Assigned signals belong to the mixture of conformers. Yiled: 81%. R_f = 0.34 (EtOAc/hexane = 1:1 v/v). $[\alpha]_D^{20}$ = - 19.9 (c = 0.0085 $g \cdot cm^{-3}$ in MeOH). ^{1}H NMR (400 MHz, $CDCl_3$, δ) 0,99-1.19 (m, 3H); 1,29-1.39 (m, 2H); 1.43 (s, 3H); 1.45 (s, 9H); 1.48 (s, 3H); 1,58-2.01 (m, 9H); 2.10 (m, 1H); 3.39 (m, 1H); 3.53 (m, 1H); 3.65 (m, 1H); 4.50, 4.52 (2d, 1H, J = 16.0 Hz); 4.60 (m, 1H); 4.77, 5.09 (2d, 1H, J = 18.2 Hz); 5.70, 5.94 (2d, 1H, J = 7.2 Hz, NH) 6.39 (m, 1H); 7.40 (d, 1H, J = 7.8 Hz). ^{13}C NMR (100 MHz, $CDCl_3$, δ) 23.1, 24.2, 24.4, 24.9, 25.1, 25.5, 28.6, 30.2, 32.7, 32.8, 41.5, 47.2, 48.4, 56.9, 63.3, 79.5, 107.3, 110.8, 141.9, 152.2, 154.7, 173.7, 174.1.

Prolyl pseudo-peptide 2. (S)-(-)-alpha-Methylbenzylamine (257 µL, 2 mmol), acetone (147 µL, 2 mmol), Boc-(L)-Pro-OH (431 mg, 2 mmol) and furfurylisocyanide (216 µL, 2 mmol) were reacted in MeOH (5 mL) according to the general procedure A. Flash column chromatography purification (EtOAc/hexane = 1:1 v/v) afforded the proline-based peptoid 2 as a colorless oil. Yiled: 78%. R_f = 0.30 (EtOAc/hexane = 1:1 v/v). $[\alpha]_D^{23}$ = - 6.26 (c = 0.0047 $g \cdot cm^{-3}$ in MeOH). ^{1}H NMR (400 MHz, $CDCl_3$, δ) 1.40 (s, 9H); 1.41-1.75 (m, 9H); 1.94 (m, 3H); 3.26-3.37 (m, 2H); 4.08-4.11 (m, 2H); 4.59-4.65 (m, 1H); 6.23-6.29 (m, 2H); 7.26-7.40 (m, 4H); 7.53 (m, 2H). ^{13}C NMR (100 MHz, $CDCl_3$, δ) 19.2, 24.2, 24.4, 26.7, 28.9, 37.2, 47.7, 51.9, 59.3, 64.8, 79.5, 106.4, 110.4, 127.4, 128.9, 141.3, 142.8, 152.9, 154.8, 175.4, 175.5.

pFA-supported catalyst 3. Compound 1 (476mg, 1 mmol, 1.0 equiv.), furfuryl alcohol (860 µL, 10mmol, 10.0 equiv.) and TFA (38 µL, 0.5 mmol) were reacted in $CHCl_3$ (5 mL) according to the general procedure B. After precipitation in

petroleum ether, afford the **3** as a black amorphous solid. IR (KBr, cm^{-1}): 3500, 2930, 1720, 1420, 1320, 1100, 1038, 767. Microanalysis: N (2.68%), C (58.29%), H (5.12%), S (0%). Loading = 0.64 mmol·g^{-1}.

pFA-supported catalyst 4. Compound 2 (545 mg, 1 mmol, 1.0 equiv.), furfuryl alcohol (860 µL, 10mmol, 10.0 equiv.) and TFA (38 µL, 0.5 mmol) were reacted in $CHCl_3$ (5 mL) according to the general procedure B. After precipitation in petroleum ether, afford **4** as a black amorphous solid. IR (KBr, cm^{-1}): 3500, 2930, 1720, 1420, 1320, 1100, 1038, 767. Microanalysis: N (1.36%), C (50.52%), H (3.77%), S (0%). Loading = 0.33 mmol·g^{-1}**.**

pFA. Furfuryl alcohol (860 µL, 10 mmol) and TFA (38 µL, 0.5 mmol) were reacted in $CHCl_3$ (5 mL) according to the general procedure B. After precipitation in petroleum ether, afford the pFA as a black amorphous solid. IR (KBr, cm^{-1}): 3500, 2930, 1720, 1420, 1320, 1100, 1038, 767. Microanalysis: N (0 %), C (56.14%), H (4.10%), S (0%). Loading = 0 mmol·g^{-1} (mmol of catalyst per gram of polymer determined based on the content of nitrogen).

(2*R*,3*S*)-2-Ethyl-4-nitro-3-phenylbutanal (5). Prepared by reaction of *n*-butanal with trans-*β*-nitrostyrene according to the general procedure C. The compound was purified by flash column chromatography (EtOAc/hexane = 1:9 v/v). The spectroscopic data are in agreement with the published data.[15] The enantiomeric excess was determined by chiral-stationary phase HPLC (Chiralpak OD-H, hexane/*i*-PrOH 99:1 v/v, 25°C) at 1.00 ml/min, UV detection at 210 nm: t_R: (syn, major) = 28.4 min, (syn, minor) = 20.9 min. R_f = 0.26 (EtOAc/hexane = 2:8 v/v). $[\alpha]_D^{23}$ = +25.21 (c 0.0046 g·cm^{-3} in MeOH). **^{1}H NMR** (400 MHz, $CDCl_3$, δ) 9.72, 9.49 (2d, *J* = 2.6 Hz, 1H; CHO), 7.36- 7.29 (m, 3H; Ph), 7.19- 7.17 (m, 2H; Ph), 4.72 (dd, *J* = 5.0 Hz, 12.7 Hz, 1H; CH_2NO_2), 4.63 (dd, *J* = 9.6 Hz, 12.7 Hz, 1H, CH_2NO_2), 3.79 (td, *J* = 5.0 Hz, 9.8 Hz, 1H; CHPh), 2.71- 2.65 (m, 1H; CHCHO), 1.54- 1.47 (m, 2H; CH_2CH_3), 0.83 (t, *J* = 0.83 Hz, 3H, CH_3). **^{13}C NMR** (100 MHz, $CDCl_3$, δ) 203.2, 136.8, 129.1, 128.1, 128.0, 78.5, 55.0, 42.7, 20.4, 10.7.

2.3 Preparation of microreactor column.

pFA-supported catalyst **3** (500 mg, excess, suspended in 25 mL of ethanol) was packed into a stainless-steel HPLC column (Ø = 2.1 mm, l = 150 mm, particle size = 10 mm). The packing was performed under constant pressure (2500 psi) using ethanol (250 mL) as the solvent by using an air-driven liquid pump.

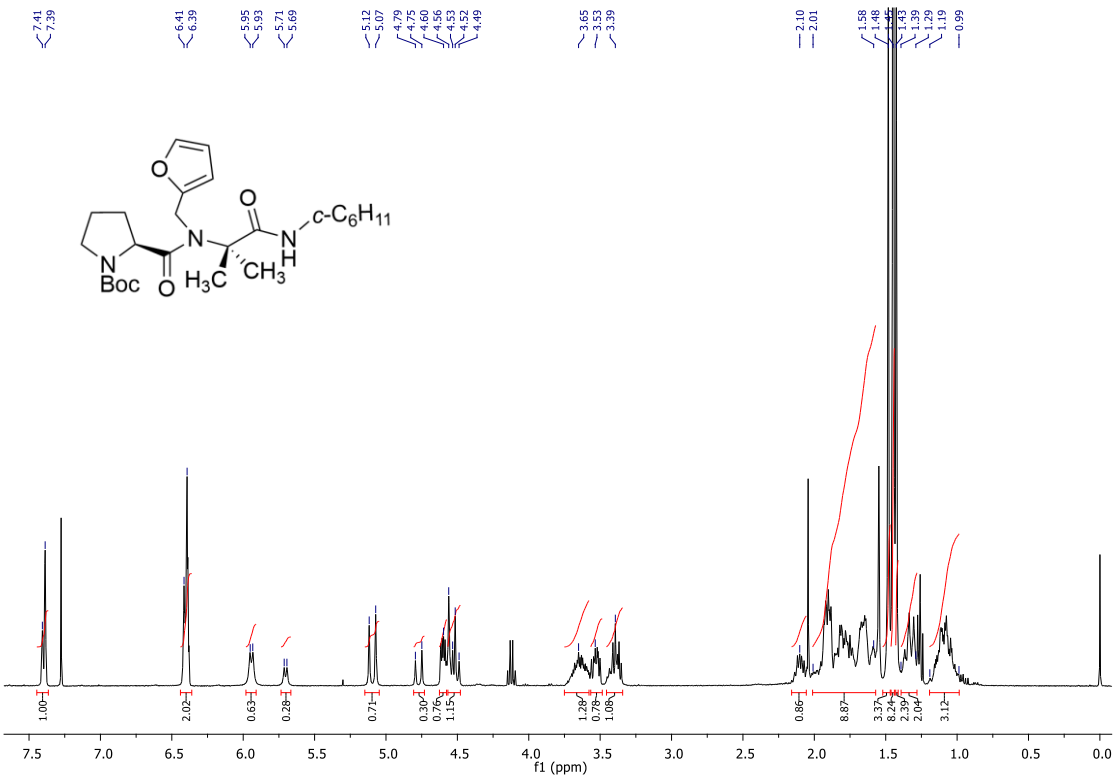

FIGURE 36: 400 MHz ^{1}H NMR spectrum in $CDCl_3$ of **1**.

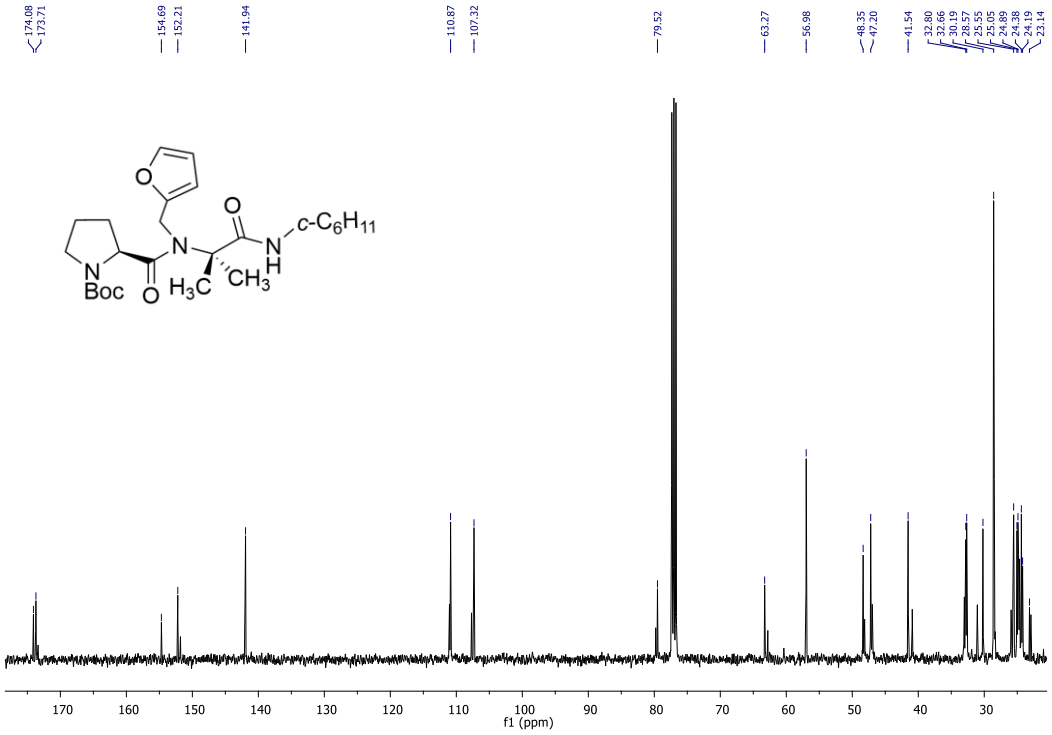

FIGURE 37: 100 MHz ^{13}C NMR spectrum in $CDCl_3$ of **1**.

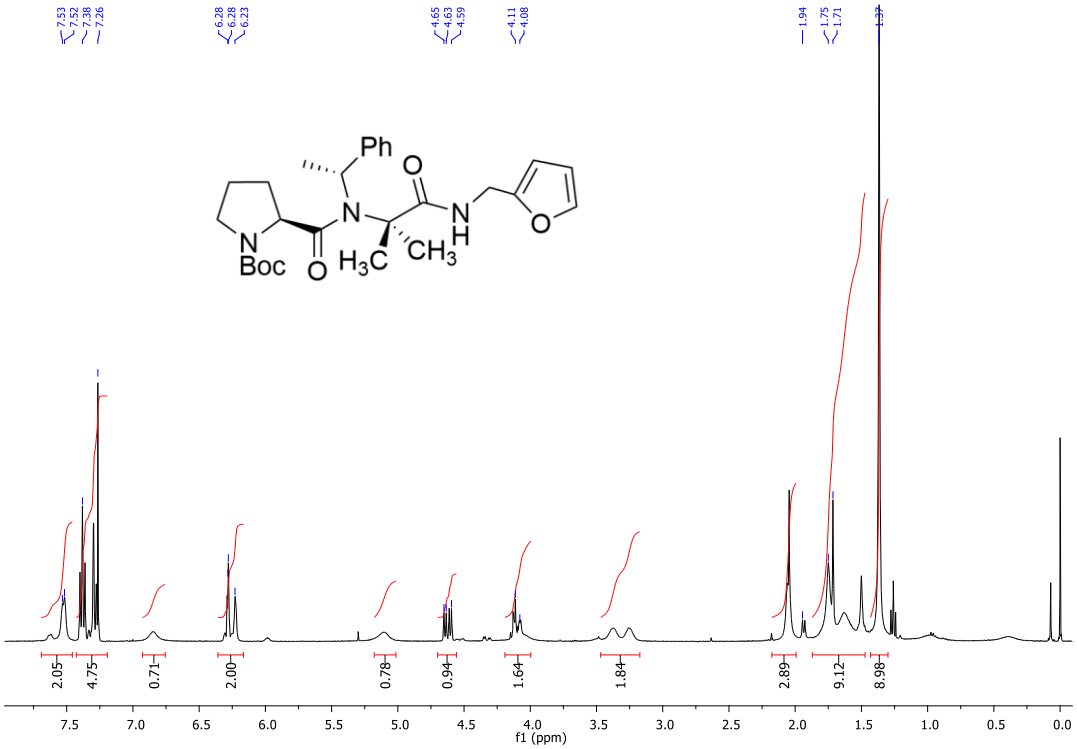

FIGURE 38: 400 MHz ^{1}H NMR spectrum in $CDCl_3$ of **2**.

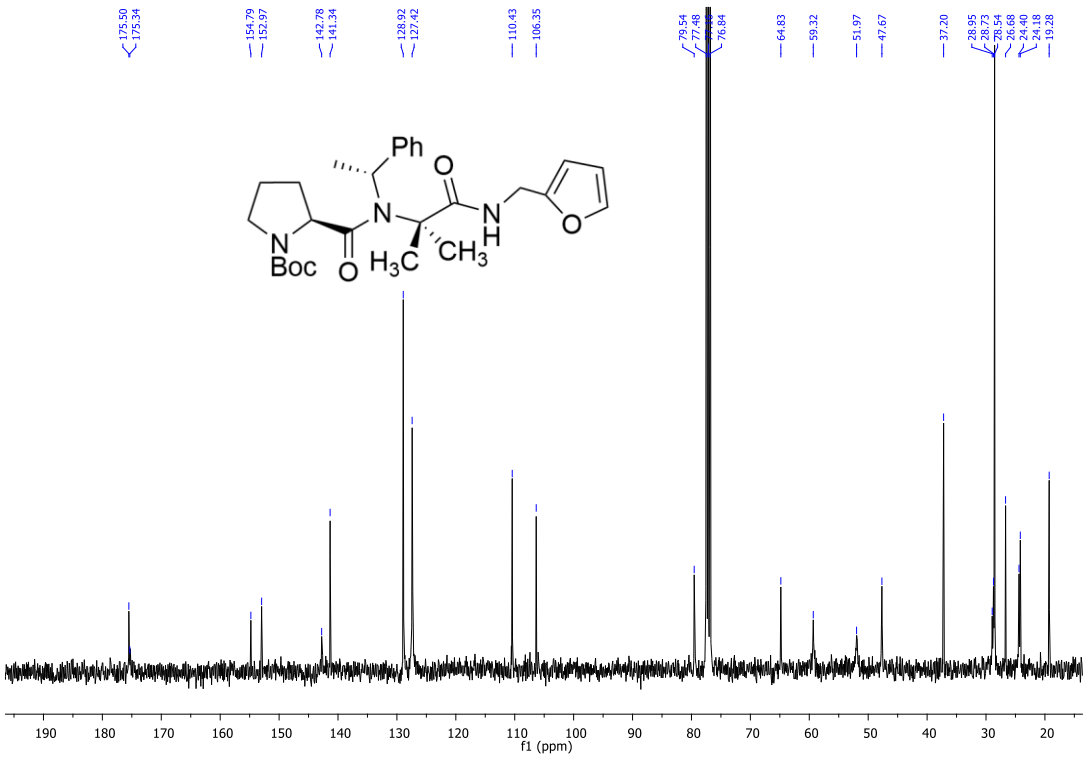

FIGURE 39: 100 MHz ^{13}C NMR spectrum in $CDCl_3$ of **2**.

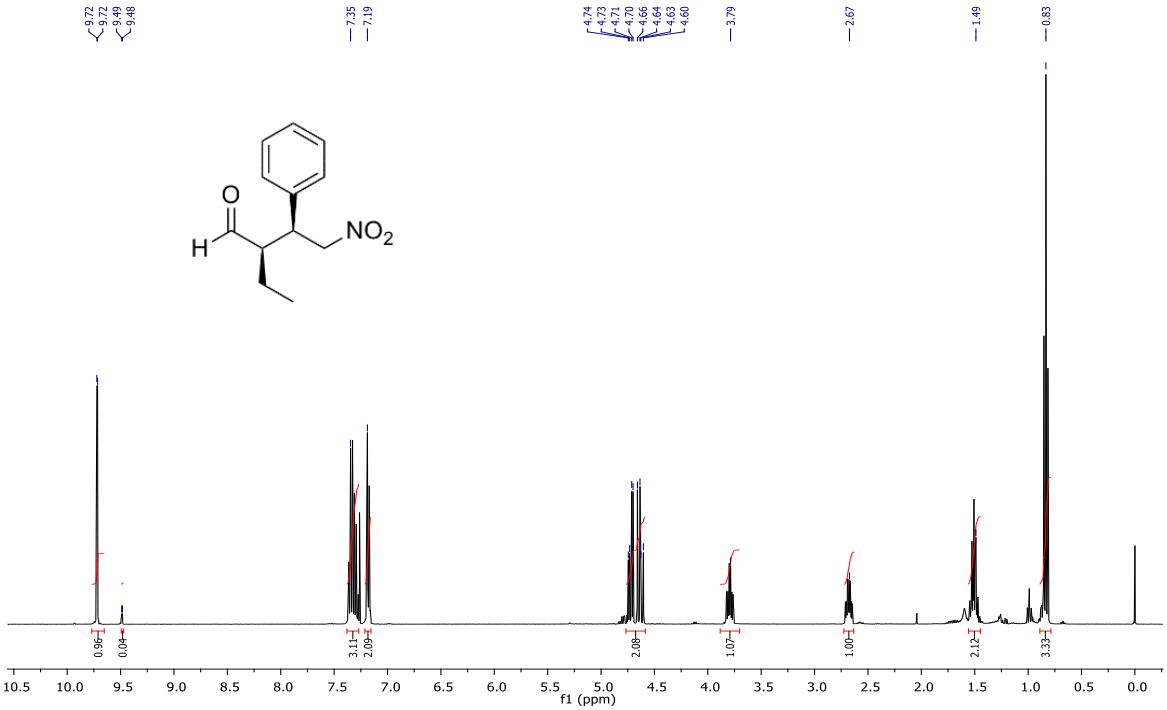

FIGURE 40: 400 MHz ^{1}H NMR spectrum in $CDCl_3$ of (2*R*,3*S*)-2-Ethyl-4-nitro-3-phenylbutanal (**5**).

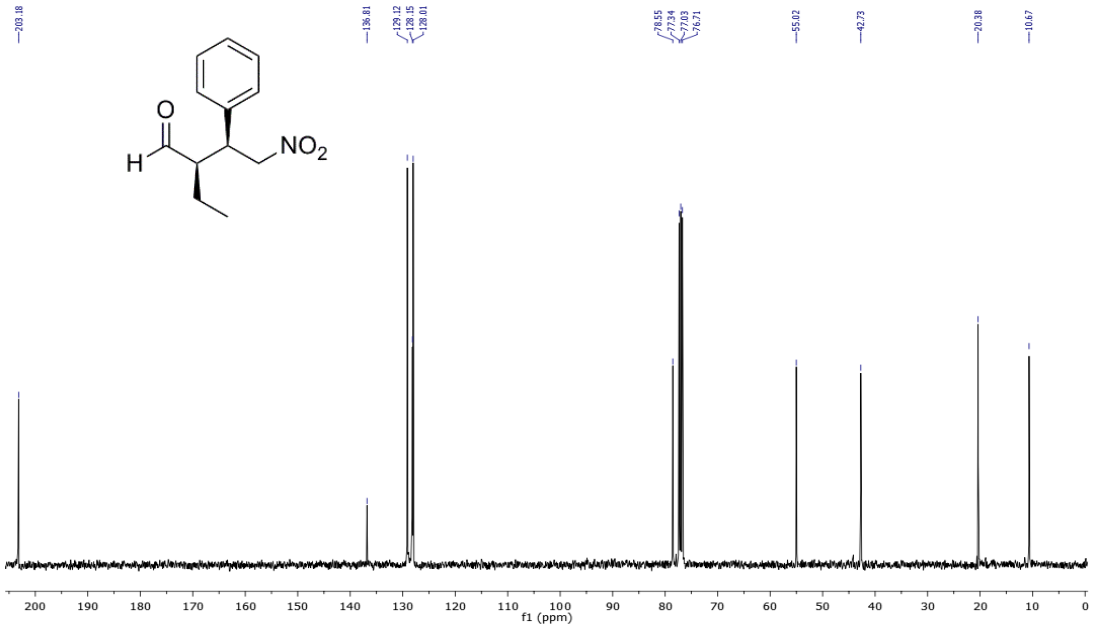

FIGURE 41: 100 MHz ^{13}C NMR spectrum in $CDCl_3$ of (2*R*,3*S*)-2-Ethyl-4-nitro-3-phenylbutanal (**5**).

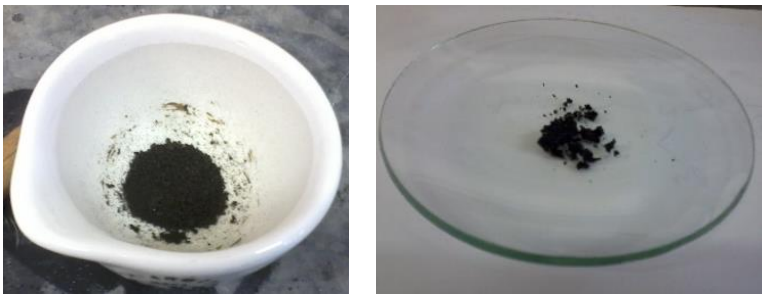

FIGURE 42: Photograph of pFA-supported catalysts material.

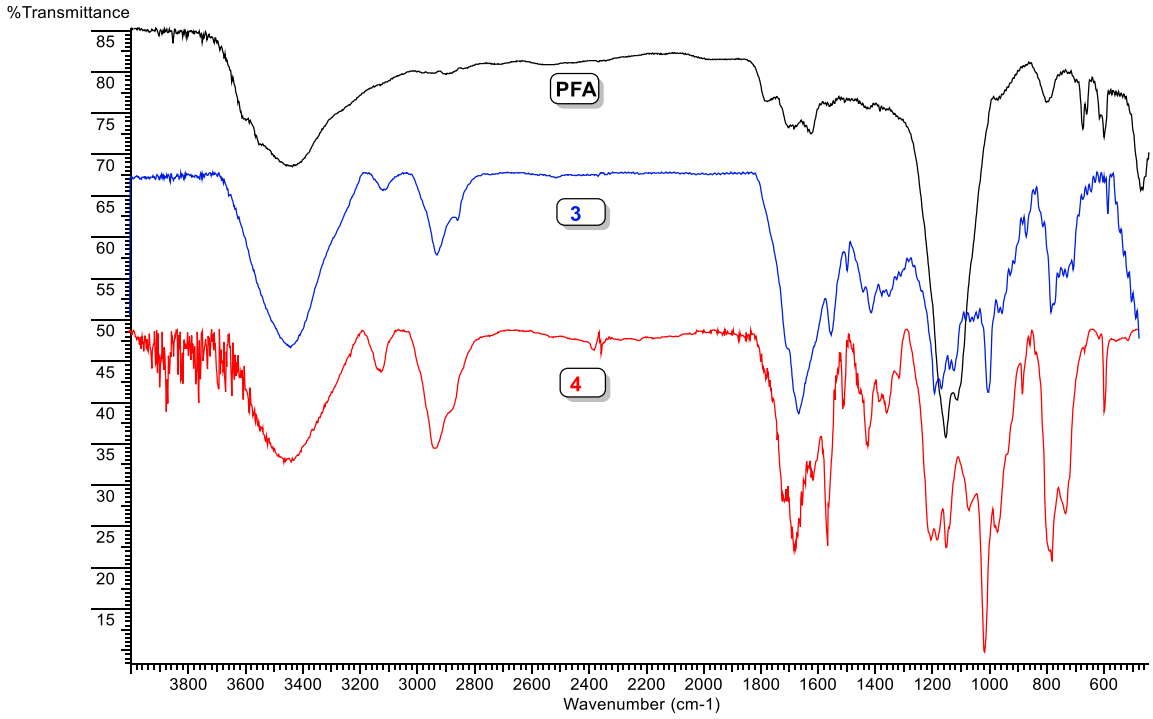

FIGURE 43: FT-IR spectrum of polymers **pFA** (black), **3** (blue) and **4** (red) in the range of 4000–600 cm^{-1}.

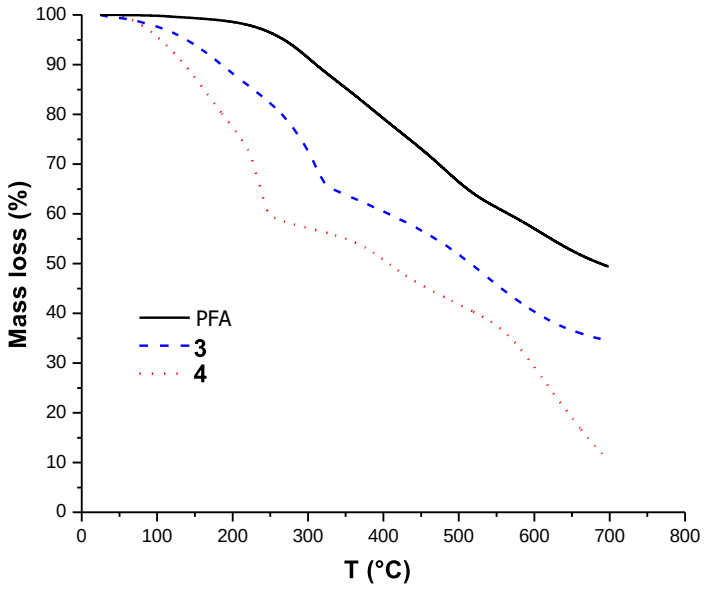

FIGURE 44: Variation of mass vs. temperature measured by TGA for the **pFA**, **3** and **4** conducted under oxidative atmosphere at 10 ºC min^{-1}.

Chiral HPLC results and spectrum

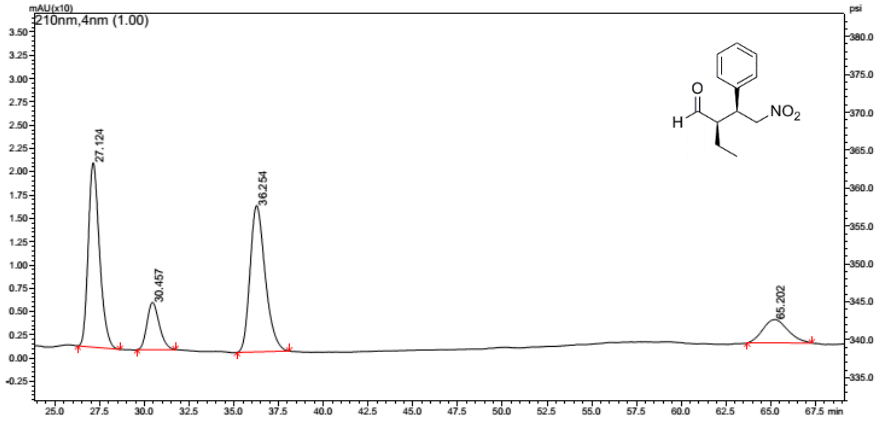

PeakTable

PDA Ch1 210nm 4nm

Peak#	Ret. Time	Area	Height	Area %	Height %
1	27.124	867445	19800	37.957	45.951
2	30.457	242098	5070	10.593	11.767
3	36.254	931040	15712	40.739	36.463
4	65.202	244769	2508	10.710	5.819
Total		2285353	43090	100.000	100.000

FIGURE 45: Chiral HPLC of racemic 2-ethyl-4-nitro-3-phenylbutanal. Chiralpak OD-H (*n*-hexane/i-PrOH 91:9), 25°C at 0.9 ml/min, UV detection at 210 nm.

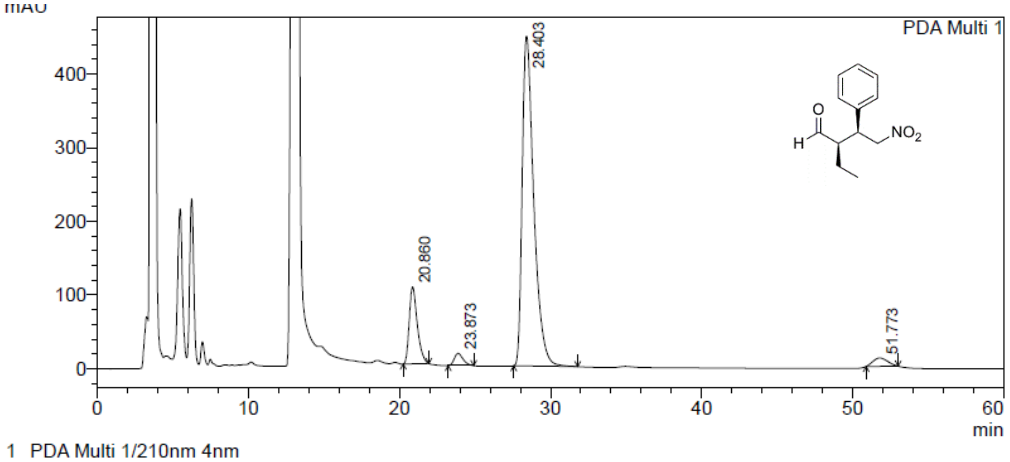

1 PDA Multi 1/210nm 4nm

PeakTable

PDA Ch1 210nm 4nm

Peak#	Ret. Time	Area	Height	Area %	Height %
1	20.860	3875196	104361	13.278	17.997
2	23.873	674856	16601	2.312	2.863
3	28.403	23865884	447601	81.774	77.189
4	51.773	769271	11317	2.636	1.952
Total		29185207	579880	100.000	100.000

FIGURE 46: Chiral HPLC of the crude asymmetric 2-ethyl-4-nitro-3-phenylbutanal (**5**) obtained by batch reaction with pFA-supported catalyst **3**. Chiralpak OD-H (*n*-hexane/*i*-PrOH 90:10), 25°C) at 1.0 ml/min, UV detection at 210 nm of the crude reaction.

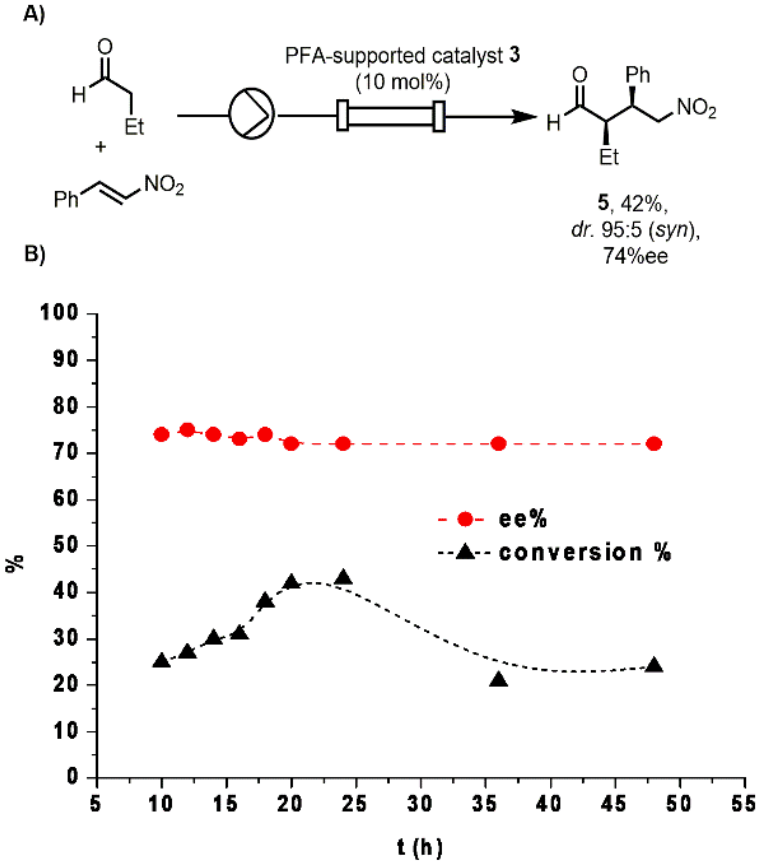

Figure 35. Continuous-flow catalytic system monitoring the production of a γ-nitroaldehyde **5** with pFA-supported catalyst **3** packed in a microreactor.

Table 1: Results of continuous flow of Michael addition between *n*-butanal and *β*-nitrostyrene using the microreactor filled with pFA-supported catalyst **3**.

Entry [a]	Flow rate ϕ(µL min^{-1})	Running time (h)	Residence time τ(min)[b]	Conversion [c]	*dr.* (*syn:anti*) [e]	ee% [f]
1	2.5	0-10	-	-	-	-
2	2.5	10-12	140	25	95:5	74
3	2.5	12-14	140	27	95:5	75
4	2.5	14-16	140	30	95:5	74
5	2.5	16-18	140	31	95:5	73
6	2.5	18-20	140	38	95:5	74
7[d]	2.5	20-22	140	42	95:5	72
8	1	24-36	349	43	94:6	72
9	1	36-48	349	21	94:6	72
10	1	48-72	349	24	94:6	72

a) Reactions conditions: HPLC column (0.21cm i.d. x 15cm, containing 0.639 mmol of catalyst 1a); *β*-nitrostyrene (2.5 mmol, 1 equiv., 0.25M), *n*-butanal (3 equiv., 0.75M) in *n*-hexane/ *i*-PrOH (90:10) mixture. b) Residence time calculated as void volume/rate flow ($\tau = V_0/\phi$). c) Conversion determined by ^{1}H NMR spectroscopic analysis. d) Productivities are measured in mmol.product h^{-1} $mmol_{catalyst}^{-1}$. e) *dr.* determined by ^{1}H NMR spectroscopic analysis. f) Determined by chiral-stationary phase HPLC analysis.

Entry	HPLCs of Table 1.
2	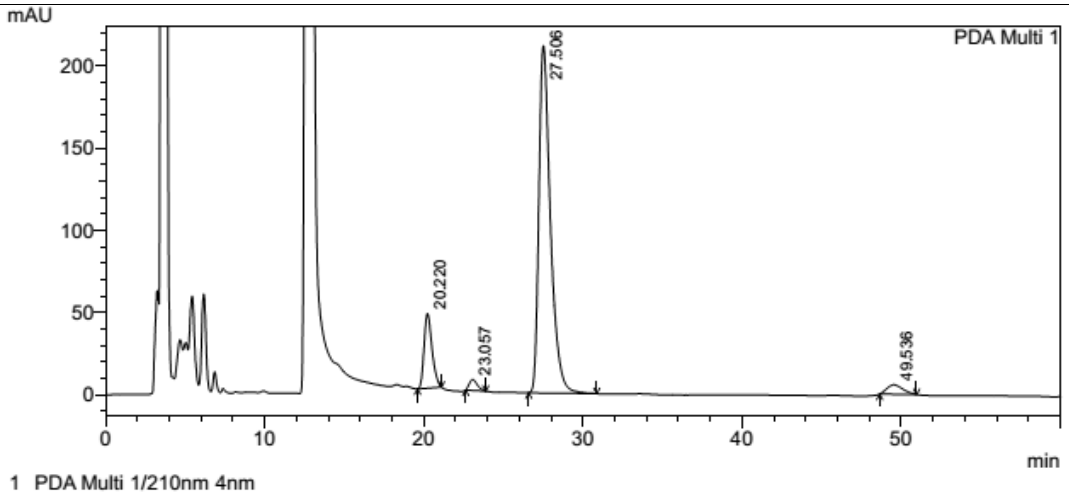

PeakTable

PDA Ch1 210nm 4nm

Peak#	Ret. Time	Area	Height	Area %	Height %
1	20.220	1587854	45517	12.317	16.913
2	23.057	229856	6527	1.783	2.425
3	27.506	10678706	211414	82.837	78.558
4	49.536	394748	5660	3.062	2.103
Total		12891163	269118	100.000	100.000

3

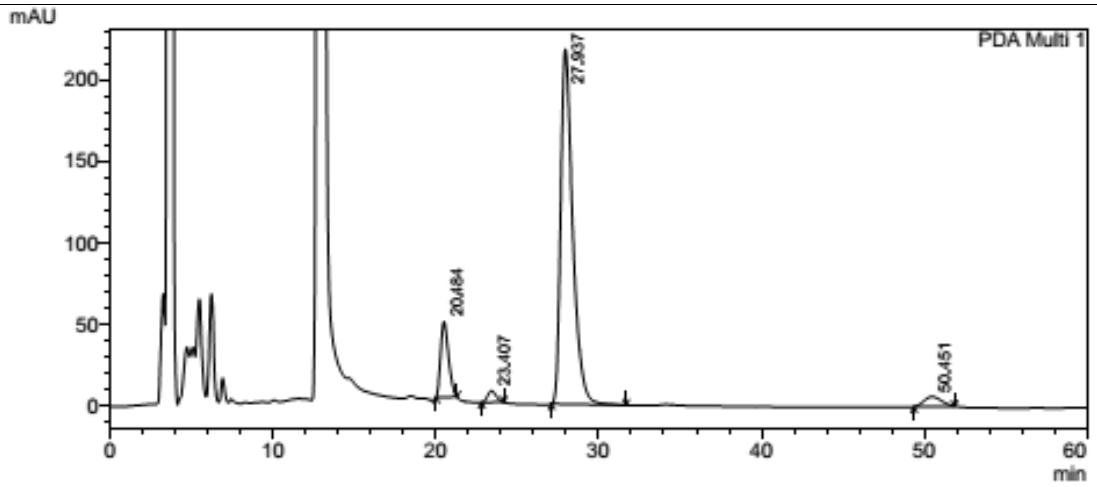

1 PDA Multi 1/210nm 4nm

PeakTable

PDA Ch1 210nm 4nm

Peak#	Ret. Time	Area	Height	Area %	Height %
1	20.484	1557976	46209	11.639	16.702
2	23.407	260434	7046	1.946	2.547
3	27.937	11116474	217305	83.047	78.543
4	50.451	450875	6108	3.368	2.208
Total		13385758	276669	100.000	100.000

4

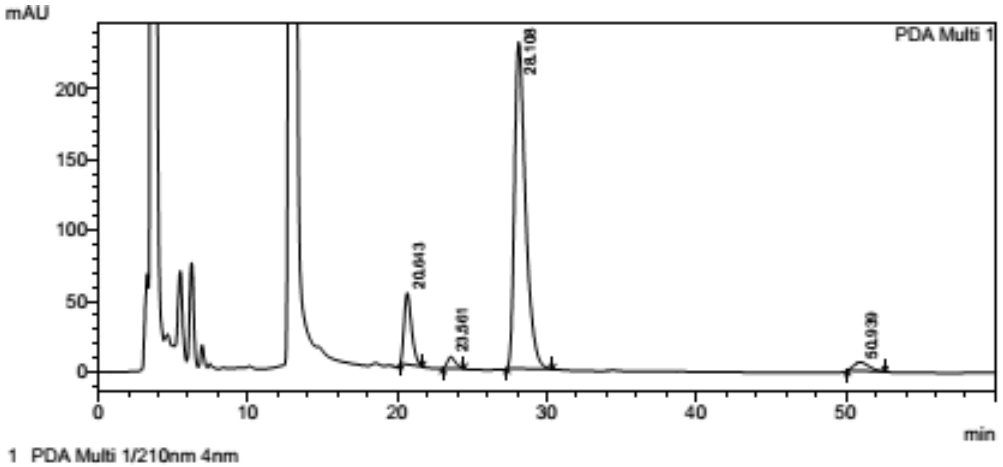

1 PDA Multi 1/210nm 4nm

PeakTable

PDA Ch1 210nm 4nm

Peak#	Ret. Time	Area	Height	Area %	Height %
1	20.643	1759063	50465	12.300	17.081
2	23.561	304022	7992	2.126	2.705
3	28.108	11808725	230951	82.570	78.168
4	50.939	429640	6046	3.004	2.046
Total		14301450	295454	100.000	100.000

5

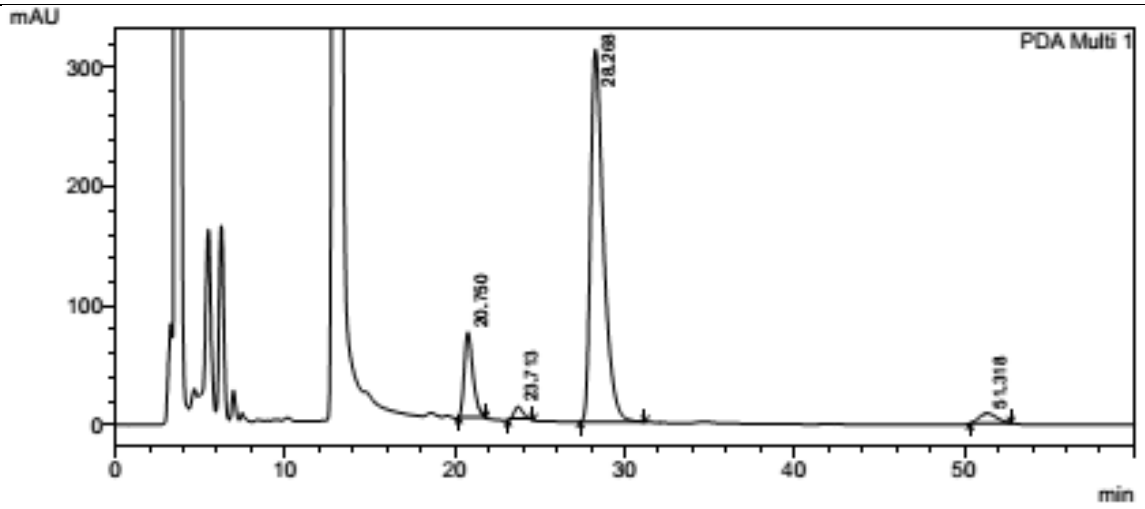

1 PDA Multi 1/210nm 4nm

PeakTable

PDA Ch1 210nm 4nm

Peak#	Ret. Time	Area	Height	Area %	Height %
1	20.750	2558251	71344	12.801	17.688
2	23.713	430531	11138	2.154	2.761
3	28.268	16396233	312604	82.044	77.501
4	51.318	599641	8266	3.001	2.049
Total		19984657	403353	100.000	100.000

6

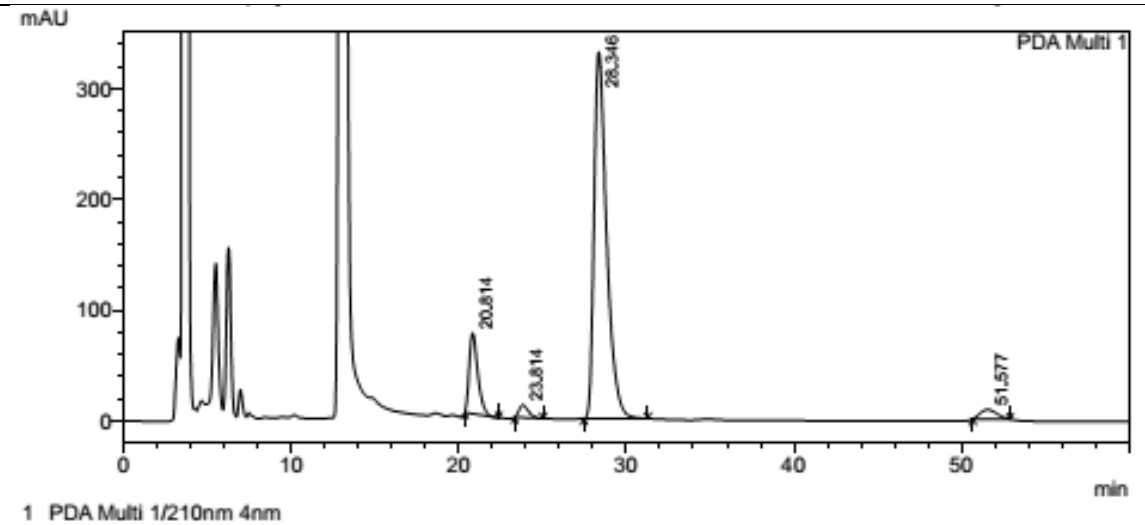

1 PDA Multi 1/210nm 4nm

PeakTable

PDA Ch1 210nm 4nm

Peak#	Ret. Time	Area	Height	Area %	Height %
1	20.814	2609783	72871	12.500	17.194
2	23.814	445781	11406	2.135	2.691
3	28.346	17230466	330988	82.526	78.095
4	51.577	592685	8561	2.839	2.020
Total		20878715	423826	100.000	100.000

7

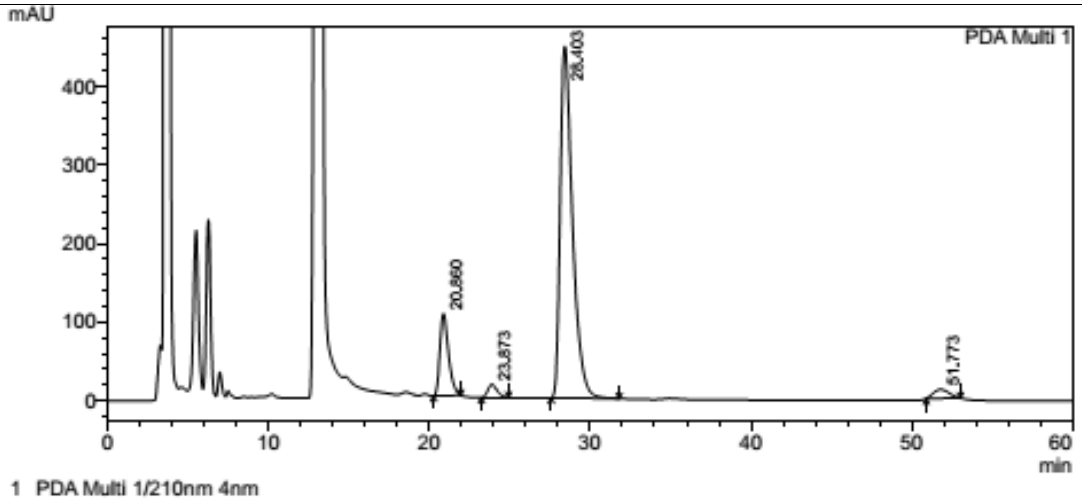

1 PDA Multi 1/210nm 4nm

PeakTable

PDA Ch1 210nm 4nm

Peak#	Ret. Time	Area	Height	Area %	Height %
1	20.860	3875196	104361	13.278	17.997
2	23.873	674856	16601	2.312	2.863
3	28.403	23865884	447601	81.774	77.189
4	51.773	769271	11317	2.636	1.952
Total		29185207	579880	100.000	100.000

8

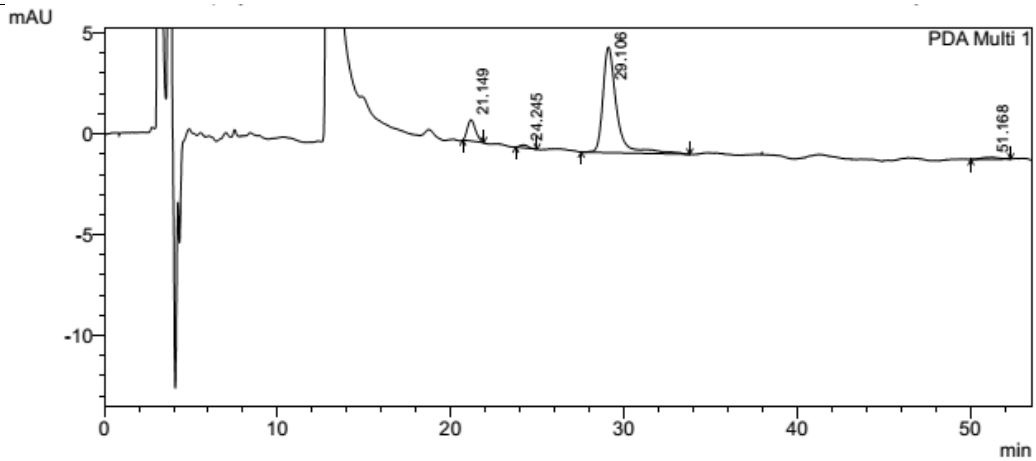

1 PDA Multi 1/210nm 4nm

PeakTable

PDA Ch1 210nm 4nm

Peak#	Ret. Time	Area	Height	Area %	Height %
1	21.149	34196	1054	10.236	16.098
2	24.245	4504	148	1.348	2.267
3	29.106	288448	5240	86.342	80.030
4	51.168	6929	105	2.074	1.606
Total		334078	6547	100.000	100.000

9

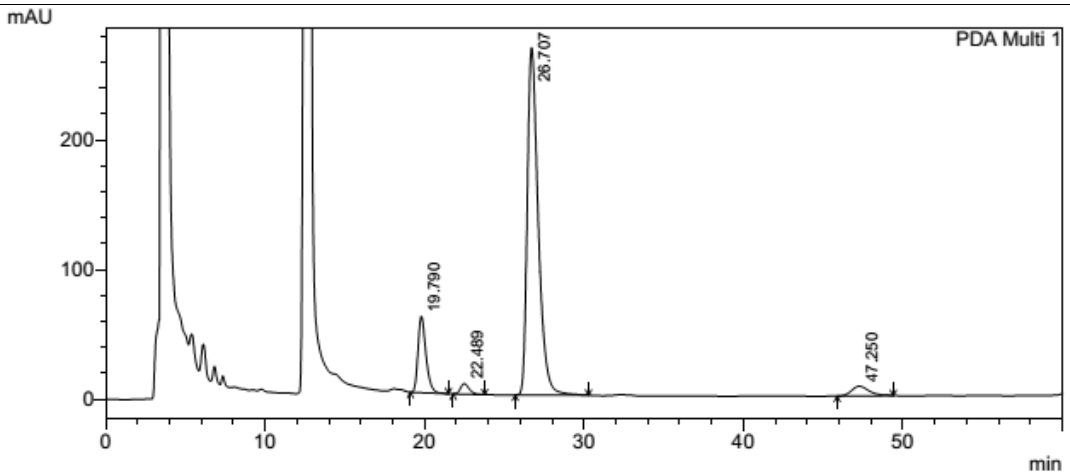

1 PDA Multi 1/210nm 4nm

PeakTable

PDA Ch1 210nm 4nm

Peak#	Ret. Time	Area	Height	Area %	Height %
1	19.790	2045275	58935	13.030	17.215
2	22.489	308886	8179	1.968	2.389
3	26.707	12772745	267759	81.372	78.214
4	47.250	569814	7469	3.630	2.182
Total		15696720	342341	100.000	100.000

10

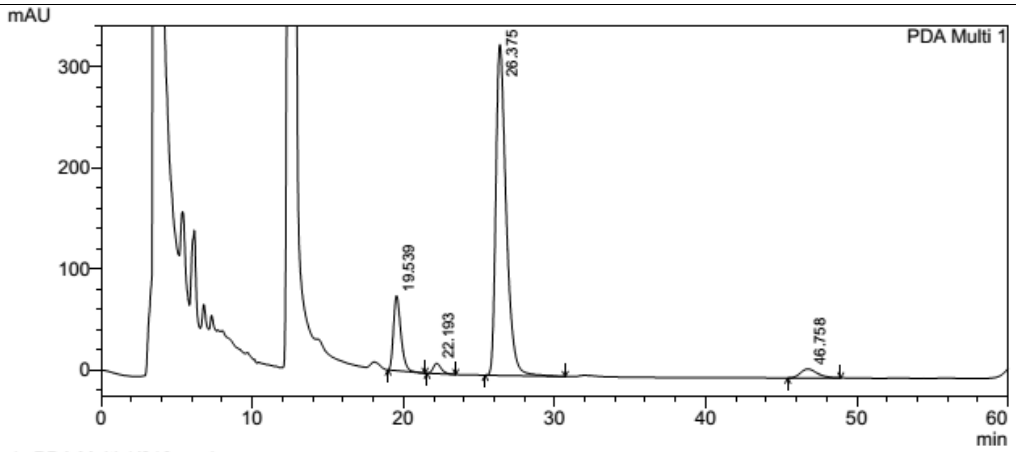

1 PDA Multi 1/210nm 4nm

PeakTable

PDA Ch1 210nm 4nm

Peak#	Ret. Time	Area	Height	Area %	Height %
1	19.539	2514588	73878	13.158	17.609
2	22.193	373640	10131	1.955	2.415
3	26.375	15533770	326639	81.282	77.855
4	46.758	688913	8902	3.605	2.122
Total		19110912	419550	100.000	100.000

FIGURE 47: Different examples of Chiral HPLC of the crude asymmetric 2-ethyl-4-nitro-3-phenylbutanal (**5**) obtained by continuous flow chemistry reaction with pFA-supported catalyst **3** and reported in Table 1. Chiralpak OD-H (*n*-hexane/*i*-PrOH 90:10), 25°C) at 1.0 ml/min, UV detection at 210 nm of the crude reaction.

3.5. References

1. PUGLISIS A, BENAGLIA M, CHIROLI V. Stereoselective organic reactions promoted by immobilized chiral catalysts in continuous flow systems.*Green Chem.* **2013**; *15*: 1790-1813.

2. TSUBOGO T, ISHIWATA T, KOBAYASHI S. Asymmetric carbon-carbon bond formation under continuous-flow conditions with chiral heterogeneous catalysts. *Angew. Chem. Int. Ed.* **2013**; *52*: 6590-6604.

3. KRISTENSEN TE, HANSEN T. Polymer-Supported Chiral Organocatalysts: Synthetic Strategies for the Road Towards Affordable Polymeric Immobilization.*Eur. J. Org. Chem.* **2010**; 3179-3204.

4. MAYER-GALL T, LEE JW, OPWIS K, LIST B, GUTMANN JS. Textile Catalysts—An unconventional approach towards heterogeneous catalysis.*ChemCatChem.* **2016**; *8*: 1428-1436.

5. FROST CG, MUTTON L. Heterogeneous catalytic synthesis using microreactor technology. *Green Chem.* **2010**; *12*: 1687-1703.

6. MAK XY, LAURINO P, SEEBERGER PH. Asymmetric reactions in continuous flow. *Beilstein J. Org. Chem.* **2009**; *5*: No 19. doi: 10.3762/bjoc.5.19.

7. DE LA TORRE AF, RIVERA DG, FERREIRA MAB, CORRÊA AG, PAIXÃO MW. Multicomponent Combinatorial Development and Conformational Analysis of Prolyl Peptide–Peptoid Hybrid Catalysts: Application in the Direct Asymmetric Michael Addition. *J. Org. Chem.* **2013**; *78*: 10221-10232.

8. SCATENA GS, DE LA TORRE AF, CASS QB, RIVERA DG, PAIXÃO MW. Multicomponent Approach to Silica-Grafted Peptide Catalysts: A 3 D Continuous-Flow Organocatalytic System with On-line Monitoring of Conversion and Stereoselectivity. *ChemCatChem* **2014**; *6*: 3208-3214.

9. ARAKAWA Y, WIESNER M, WENNEMERS H. Efficient Recovery and Reuse of an Immobilized Peptidic Organocatalyst. *Adv. Synth. Catal.* **2011**; 353: 1201-1206.

10. ARAKAWA Y, WENNEMERS H. Enamine Catalysis in Flow with an Immobilized Peptidic Catalyst.*ChemSusChem.* **2013**; 6: 242-245.

11. KIM T, ASSARY RS, MARSHALL CL, GOSZTOLA DJ, CURTISS LA, STAIR PC. Acid-Catalyzed Furfuryl Alcohol Polymerization: Characterizations of Molecular Structure and Thermodynamic Properties.*ChemCatChem.* **2011**; *3*: 1451–1458.

12. GANDINI A. Furans as offspring of sugars and polysaccharidesand progenitors of a family of remarkable polymers: a review of recent progress. *Polym. Chem.* **2010**; *1*: 245–251.

13. GANDINI A. Polymers from Renewable Resources: A Challenge for the Future of Macromolecular Materials. *Macromolecules*. **2008**; 41: 9491-9504.

14. PRINCIPE M, MARTÍNEZ R, ORTIZ P, RIEUMONT J. The Polymerization of Furfuryl Alcohol with p-toluenesulfonic Acid: PhotocrossLinkeable Feature of the Polymer´´. *Polímeros: Ciência e Tecnologia*. **2000**; *10*: 8-14.

15. BETANCORT JM, BARBAS CF. Catalytic Direct Asymmetric Michael Reactions: Taming Naked Aldehyde Donors. *Org. Lett.* **2001**; *3*(23): 3737-3740.

16. UGI I, MEYR R, FETZER U. STEINBRÜCKER, C. Versuche mit Isonitrilen. *Angew. Chem.* **1959***; 71,* 386.

17. ZHU J, WANG Q, WANG MX. Multicomponent Reactions in Organic Synthesis; Eds.; Wiley-VCH: Weinheim; **2015**. p 73.

18. ZHU J, BIENAYMÉ H. Multicomponent Reactions; Eds.; WILEY-VCH: Weinheim; **2015**. p 6-24.

19. BORTOLINI O, CAVAZZINI A, GIOVANNINI PP, GRECO R, MARCHETTI N, MASSI A, PASTI L. A Combined Kinetic and Thermodynamic Approach for the Interpretation of Continuous-Flow Heterogeneous Catalytic Processes. *Chem Eur J*. **2013**; *19:* 7802-7808.

20. MCCORMICK RM, KARGER B.L. Distribution phenomena of mobile-phase components and determination of dead volume in reversed-phase liquid chromatography. *Anal. Chem.* **1980**; *52* (14): 2249–2257.

Chapter 3

Continuous-Flow Photochemistry in a Practical Metal- and Additive-Free Synthesis of Indoles and Indolines

Abstract: The combination of near-visible-light (UVA I) and tris(trimethylsilyl)silane under the continuous-flow regime, affords a fast-intramolecular reductive cyclization protocol for the synthesis of functionalized indoles and indolines. Under the optimized reaction conditions, a series of nitrogen-based heterocycles were delivered rapidly in good yields (up to 95%).

Keywords: Photocatalysis • Indoles • Indolines • Flow Chemistry • TTMSS

4.1. Introduction

Extensive researches have been undertaken in order to find new biologically active compounds. In this context, nitrogen-based heterocycles are the prime chemical architecture since they are present in the majority of small molecules with the potential biological activity. The class of tryptophan-based compounds (i.e. indoles an indolines) are among the most important classes, with wide range of applications: antifungal, antimicrobial, plant growth regulator, anti-HIV, anticonvulsant anti-inflammatory and analgesic (Figure 48).[1]

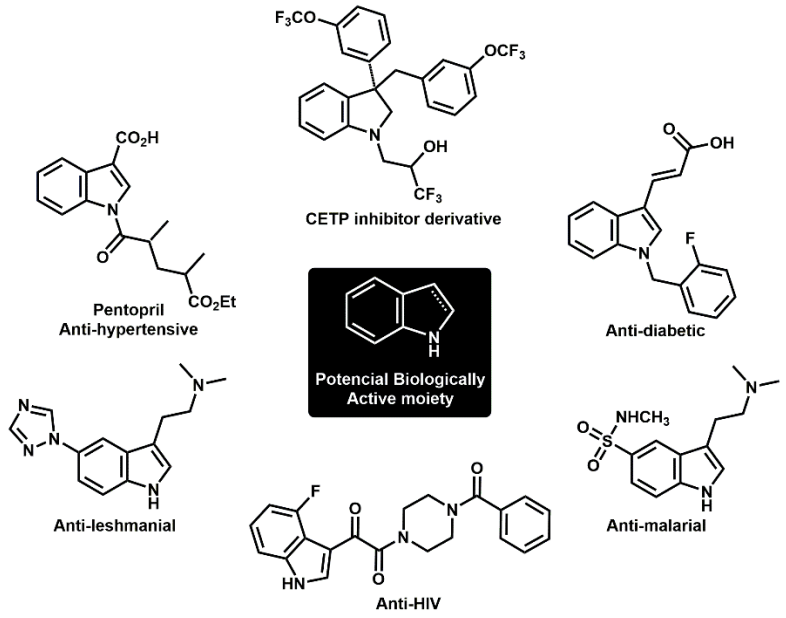

Figure 48. Selected examples of biologically active indoles and indolines.

Those compounds can be obtained from natural sources [2] or synthetic methods.[3] The latter approach is of great importance to study the relationship between chemical structure and the biological activity and also to obtain the unpreceded compounds as well. That can be faced as primordial motivation to the constant development of the traditional synthetic strategies. Consequently, synthetic organic chemists have a long-stating interest in general methods for the synthesis of indoles and indolines.[4–8]

Traditional methodologies generally involve the use of hazardous chemicals (i.e. AIBN, Bu_3SnH) in a non-ecofriendly way (**Scheme 19A**)[9]. Additionally, the important methods for the synthesis of indoles and indolines also include the application of photoredox catalysis (**Scheme 19B**). In both cases metals play a key role in the reaction. Therefore, the design of new greener and straightforward synthetic approaches are highly desirable. In this context Jørgensen and co-workers have described the application of TTMSS (Tris(trimethylsilyl)silane) under visible light irradiation to promote the reduction of aryl and alkyl halides (I and Br). [10]

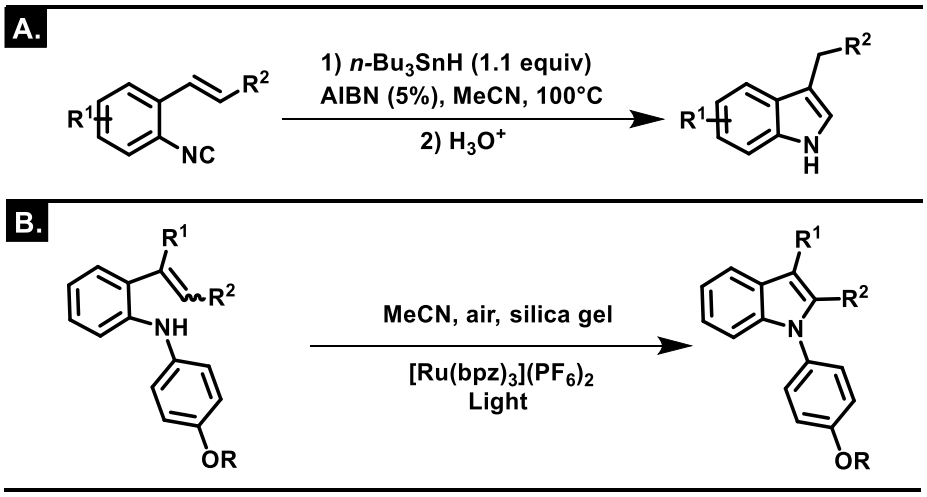

Scheme 19. Traditional methodologies for the indole synthesis.

Recently, our group has reported a visible-light-promoted intramolecular reductive cyclization protocol for the synthesis of indoles and oxindoles.[11] Furthermore, similar strategy could also be implemented to the synthesis of functionalized indolines and 2,3-dihydrobenzofurans. In both cases visible light (white or blue) was used. With the aim to reduce reactive time, UVA irradiation was employed, however, the results under batch conditions were merely satisfactory. [12]

The use of photocatalysis in organic reactions has developed greatly in the last few years.[13] Photochemical methodologies are of great interest because they are economically and environmentally attractive. Furthermore, they are an energy-efficient process with enhanced selectivity potential, a narrow energy

distribution could be achieved with the use of flow chemistry (**Scheme 20**).

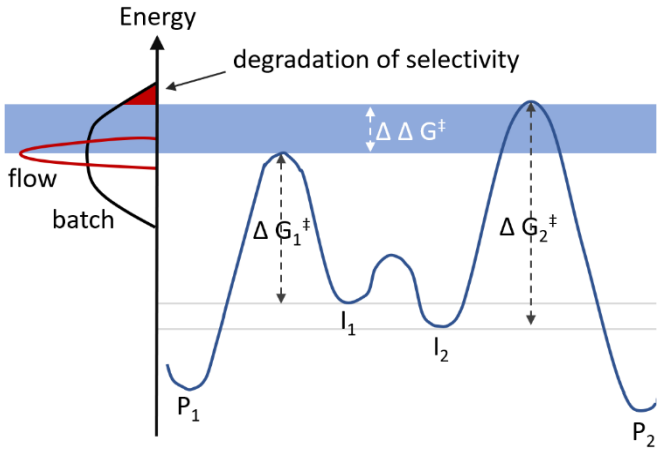

Scheme 20. Continuous Flow and batch comparison. Flow have a narrow distribution energy. Better control on degradation and formation of side products.

However, the use of light in a batch reaction conditions could present some drawbacks, such as difficulties in the upscaling, selectivity and reproducibility, mainly due to the rapidly loss of intensity of light along the reactor path and the formed product continues to expose in solution and to reactive intermediates under light incidence, which may cause degradation as well as reducing the selectivity (**Scheme 21**).

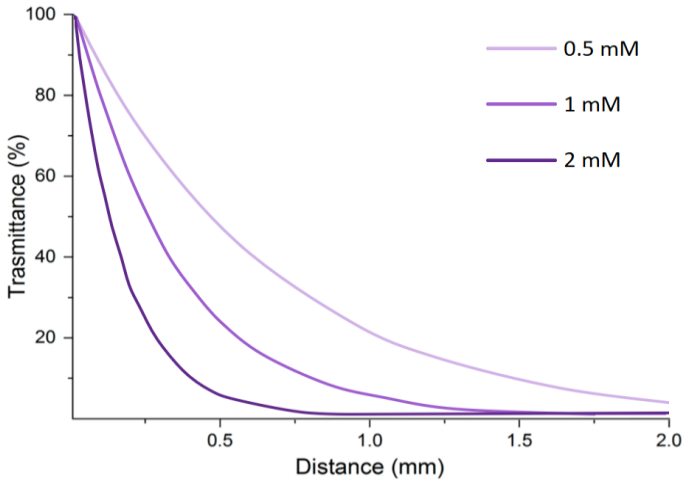

Scheme 21. Transmission of light as a function of distance in a photocatalytic reaction using $Ru(bpy)_3Cl_2$ utilizing the Bouguer−Lambert−Beer correlation.

On the other hand, the use of flow reactors assists to overcome some limitation of the photochemical reactions under batch conditions. Transparent

microreactors (i.e. chip, column, tubular) allows efficient energy transmission through the reaction, with low loss of the intensity, due to the micrometric diameter of reactor.[14,15] Besides, adjusting the flow rate and monitoring the outcome of reaction permits precisely determination of the starting material consumption, avoiding the product degradation. Those characteristics may turn the protocol to more predictable and easier to be tuned. Therefore, the flow chemistry should always be considered as an important ally to the photochemistry (**Scheme 22**).

Scheme 22. Transparent flow reactors: chip, column (middle), tubular (right).

There is a constant evolution in the methodologies for the synthesis of N-based heterocycles. Larock et al. described a metal catalyzed synthesis of indoles from the terminal alkynes and the respective 2-protected-iodoamine. Several nitrogen protection groups, e.g. tosyl, acetyl, methyl as well as unprotected amines were evaluated and good to excellent yields were achieved in case of the synthesis of these desired products.[16] More recently, the synthesis of 3-substituted indolines using a single step Nickel/photoredox catalysis, iodoacetanilides, and alkenes was described by Jamison and co-workers. The mechanism of this C–N bond-forming reaction was investigated where the theoretical and experimental results suggested the formation of a Ni(III) specie(s?) which prompt undergoes reductive elimination in order to generate the new bond and consequently producing a Ni(I) complex, which is further reduced to Ni(0). Reinforcing the importance of single electron transfer photoredox catalysis in a multi-oxidation state metals catalysis. The 3-substituted indolines were obtained with a high regioselectivity for styrenyl and aliphatic derived olefins, with yields up 97 %. [17]

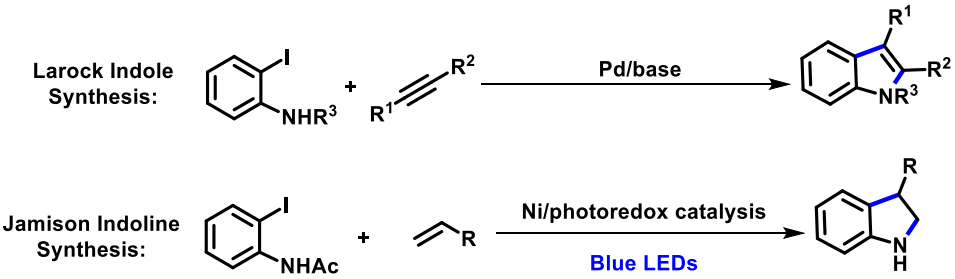

Scheme 23. Metal catalyzed synthesis of indoles and indolines.

Alternatively, highly functionalized indoles could be produced from the corresponding indoline. One example is the synthesis of elbasvir precursor, used for the treatment of chronic hepatitis C (potent NS5A antagonist). A photoredox protocol is applied in order to avoid epimerization of the hemiaminal stereocenter where $Ir[(dF(CF_3)ppy)_2(dtbbpy)]PF_6$ is being used as photocatalyst that resulted an excellent enantiomeric excess 99.8% and with 85% of the isolated yield of the desired compound.[18] The conversion of the indole ring into the indoline counterpart is not a trivial operation, thus the implementation of an applicable methodology to produce both of these cores is of extremal relevance (**Scheme 24**).

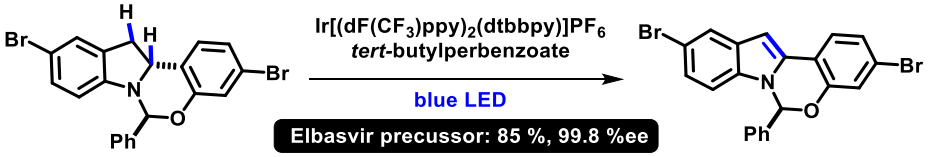

Scheme 24. Photoredox synthesis of the elbasvir precursor.

Collins et al. used a combined continuous flow and photochemistry approach for the synthesis of indole and polycyclic heterocycles. Two different wavelengths 254 nm (UV) and 394 nm (purple LEDs) were tested. From this study, the azide decomposition could be observed when the reaction was carried out using the UV irradiation. On the other hand, although taking a longer reaction time, the latter one provides higher yields. These results represent a sustainable route to the synthesis of heterocycles with improved functional group tolerance, in good to excellent yields, up to 95 %. Also, a gram scale synthesis of the reaction was done successfully(**Scheme 25**).[19]

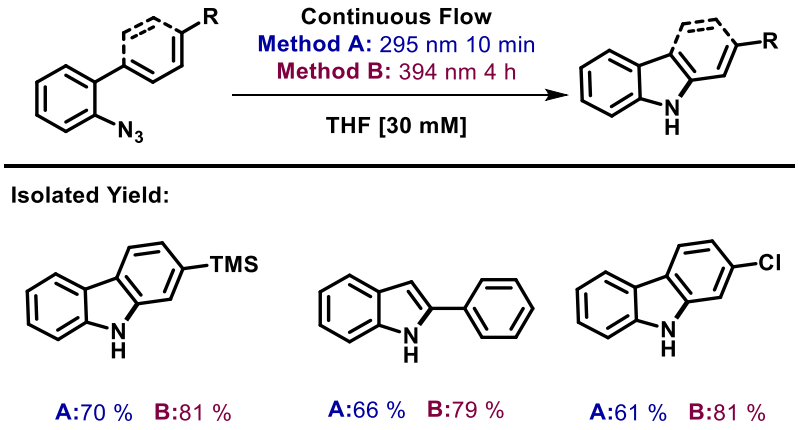

Scheme 25. Combined continuous flow and photochemistry approach for the synthesis of indole and polycyclic heterocycles.

Rueping et al. reported the synthesis of highly functionalized indoles by an oxidative photoredox palladium-catalyzed C-H arylation using visible light source (11 W CFL). According to the authors, only a small amount of the oxidative specie, molecular oxygen, is formed and is readily consumed, so side reactions could be avoided which proves that this methodology is suitable for the oxidative sensitive substrates. Transition metal-catalyzed reactions usually demands strong stoichiometric oxidants. Mild reaction conditions were successfully applied and good yields i.e 65 to 95% were achived (**Scheme 26**).[20]

.

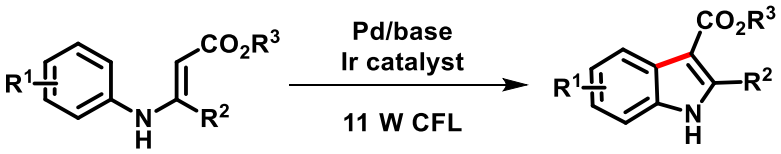

Scheme 26. Oxidative photoredox palladium-catalyzed C-H arylation.

In 2017, C. J. Li and co-workers developed an interesting protocol for the synthesis of iodo-indolines under mild reaction conditions using aryl bromide and inexpensive sodium iodide. The photo-induced carbo-iodination was performed under the ultraviolet radiation, 254 nm. The reaction pathway probably proceeds via a pseudo halogen transfer in a 5-exo cyclization. Important building blocks

can be obtained through this methodology in good to excellent yields, up to 99% (**Scheme 27**).[21]

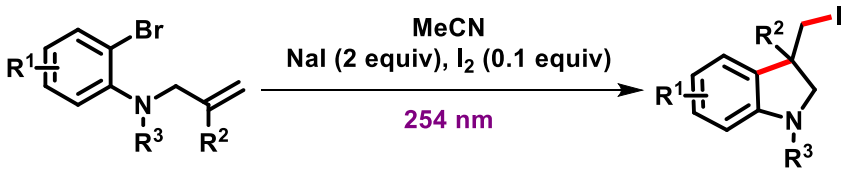

Scheme 27. Synthesis of iodo-indolines under very mild conditions.

4.2. Results and Discussion

In order to improve reaction time, energy transfer and reaction selectivity, herein we report a metal free (TTMSS based) synthesis of indoles and indolines, via reductive intramolecular cyclization, using near-visible-light (UVA I) under continuous flow conditions (**Scheme 28**).

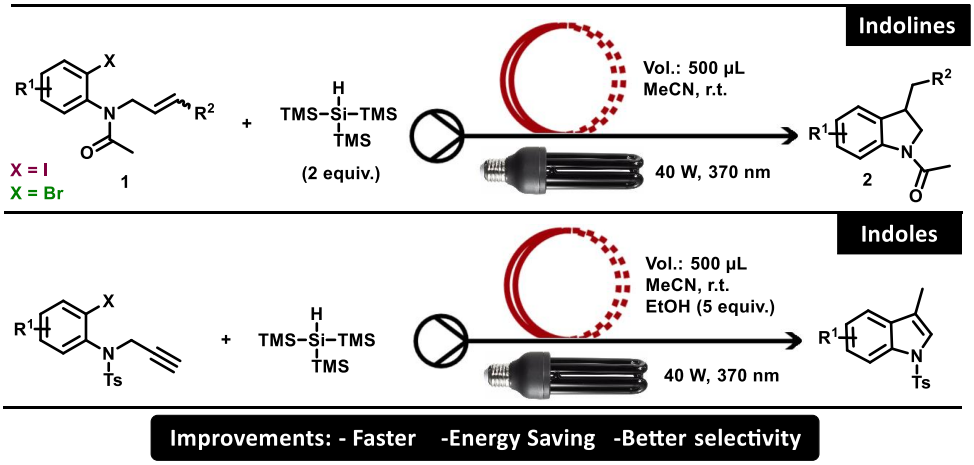

Scheme 28. General scheme for the synthesis of indolines and indole derivatives.

We started our investigation using black light (near-visible-light, UVA I), that have maximum emission of 370 nm. The isolated starting material, the TTMSS and a mixture of both, absorbs modestly in this region but is sufficient to form an intermediary/promoter for which the maximum absorbance wavelength is similar to the incident radiation. This intermediate acts as a promoter and is the driving force of reaction (**Figure 49**).

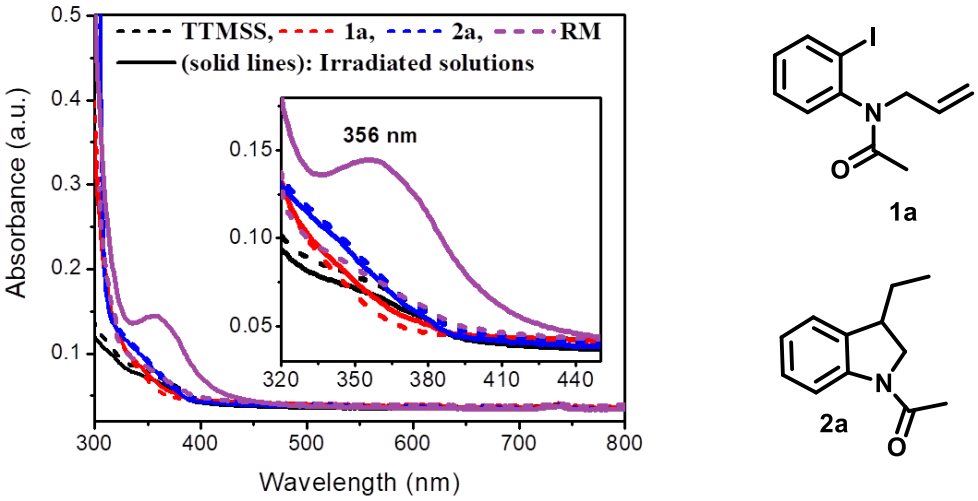

Figure 49. Absorbance spectrum for TTMSS solutions (0.02 M); **1a** (0.01 M) SM; **2a** (0.01 M) and the reaction mixture of TTMSS (0.02 M) + **1a** (0.01 M) Reaction Media: RM. SM: starting material. *Irradiated with blue LED. Irradiation with Black light cause saturation of the detector, once the absorption band formed is of high intensity, above the detection limit.

To find the best reaction condition, we evaluated the relation of concentration and reaction time. 0.2 M, 0.1M and 0.05 M concentrations of the substrate **1a** were used and the TTMSS was kept fixed as 2 equivalents. From this study, we observed that the lowest concentration resulted in lower reaction time. Higher concentrations, above 0.05 M, results in a non-homogeneous reaction due to the limited solubility of the TTMSS and its fast decrease of intensity of light owing the absorption of the starting materials.

After the optimal condition established, we then turned our attention to the study of the scope and limitation of the continuous-flow photochemical approach. To this end, the application of different starting materials to the intramolecular cyclization photo-promoted synthesis of indoline has been investigated. In this study, acetonitrile was used as solvent due to its low cutoff wavelength, which is important for further scaling up purposes (**Scheme 29**).

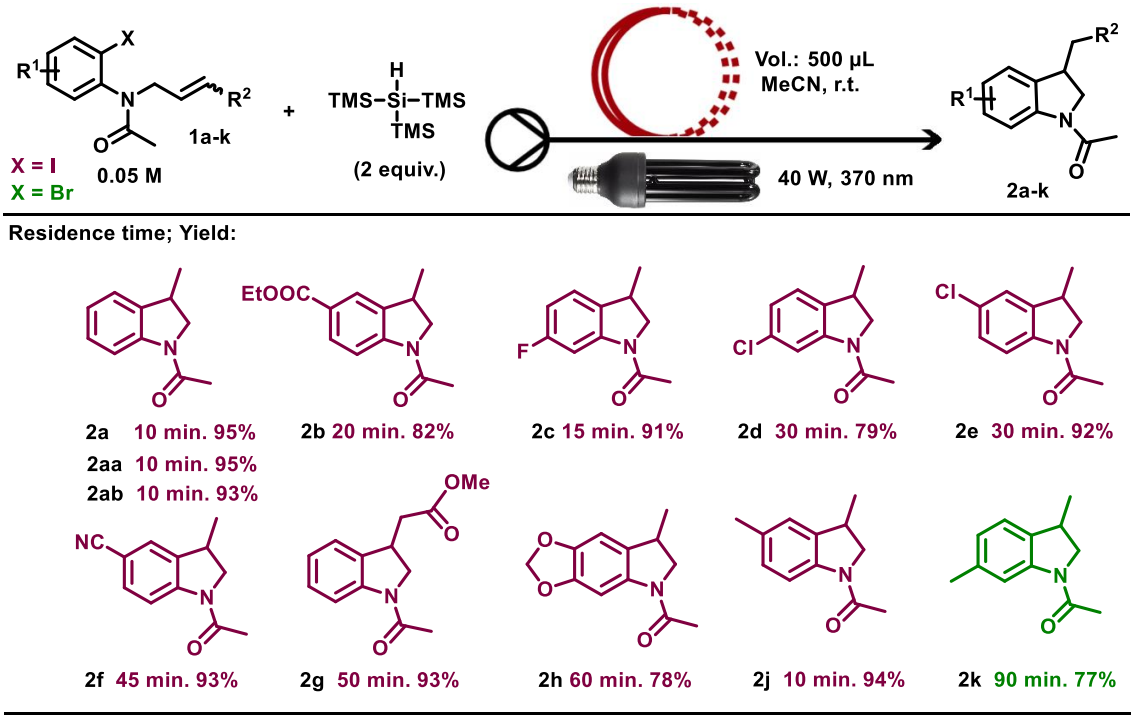

Scheme 29. Substrate scope for the visible-light-mediated indoline synthesis. Reaction conditions: 2 equiv of TTMSS and starting material 0.05 M in MeCN, irradiation with Black light bulb 40 W. Yields of isolated products.

To our delight, the reaction appeared to be very efficient for a broad range of aryl substituted substrates bearing both electron donating groups (EDG) and electron withdrawing groups (EWG) though for the latter case the reaction time was slightly higher.

The reaction scope was further investigated aiming the possible increase in the structural complexity by further transformation. For example, (a) the halogens present on the aryl moiety could be used in a catalyzed cross coupling functionalization,[22,23] (b) the methyl group could be oxidized,[24] (c) nitrile could be reduced and hydrolyzed, [25,26] ester could be hydrolyzed, [27] thus generating a wide range of compounds with distinct properties.

Substrates with halogen substituted aromatic ring e.g. 6-F, 6-Cl, 5-Cl, (**2c**, **2d**, **2e**) underwent efficiently in the current reaction strategy, affording the corresponding product in good yields i.e 91, 79, and 92 % respectively. Also, the

methyl aryl substituted **1j**, rapidly reacted and excellent yield of 94 % in 10 minutes was achived.

The protocol was compatible with substrates having an ethyl ester and cyano substituted aromatic ring, thus rendering products **2b** and **2f** in 85 and 93 % of isolated yields, but with large difference in reaction time 20 and 45 minutes, respectively. The reaction was much slower i.e took 60 minutes when the *N*-allyl-2-iodophenyl-acetamide (**2h**) contains methylenedioxy moiety, was employed although a good yield of 78% was observed. This could indicate electronic change in UV-Vis spectrum of the starting material, resulting in different absorbances and reactivity.

N-allyl-2-bromophenyl-acetamide derivative were also effective under these reaction conditions, providing product **2k**, albeit in moderate yield and longer reactional time, 90 minutes.

A b-monosubstituted olefin bearing a methyl ester, **1g**, which is suitable for further functionalization, was also observed to be compatible with these reaction conditions. producing the desired product in excellent yield of 93%.

Finally, the limitation of our protocol could be observed when 5-nitro substituted was used as reaction partner. In this case, degradation of the starting material, formation of many undesired products and highly fluorescent solution was observed. Thus, suggesting that the wavelength and energy range are not appropriated in this particular case.

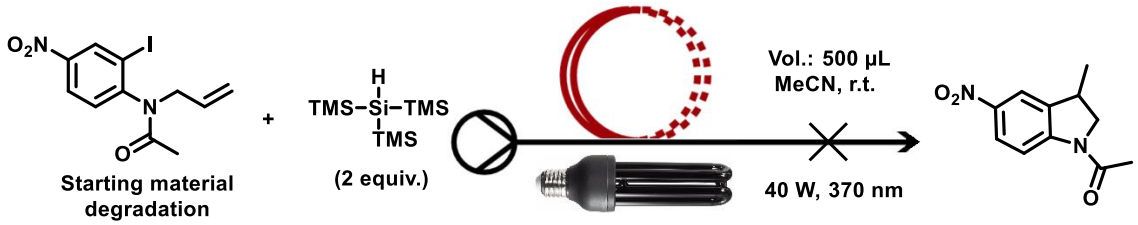

Scheme 30. 5-nitro substituted reaction: degradation of starting material and formation of undesired products.

In order to check the scalability of the reaction setup, a collection of comparative experiments has been performed: i) numbering-up, using (or employing) four identical reactors simultaneously in the same lamp. ii) scale-up,

increasing the reactor length four times. The residence time (RT), calculated by the ratio of the total reactor volume to the total flow rate, was fixed at 10 minutes using substrate **1a** for the reaction. The final yield of the numbering-up was identical to the single reactor, 95% **2aa**. Up to 1.14 mmol of the respective indoline was produced in a total time of 8h, resulting in the production of 3.42 mmol/day. It could be interpreted as an interesting approach because, for each reactor number increase, the productivity raised up to 0.855 mmol/day without changes in the reaction parameters. For the scale-up experiment a slight decrease in the yield was observed, 93 %, **2ab** (**Scheme 29**).

In light of these excellent result, we then applied our continuous-flow photochemical protocol towards the synthesis of indoles, using substituted 2-halobenzenesulfonamides **3a-f** containing terminal alkynes as starting materials. For the synthesis of indole scaffold, the amount of TTMSS was reduced to 1 equivalent and ethanol was used as proton source (5 equivalents).

We believe that it plays a fundamental role in the termination stage, so that TTMSS can be used in a reduced quantity. In addition, the protective group, tosyl, exerts an effect on the reaction. Under the aforementioned conditions, excellent yields were achieved for the synthesis of indoles **4a-f**. The precise control of residence time was imperative to obtain high yields, for all described cases no side products were observed (

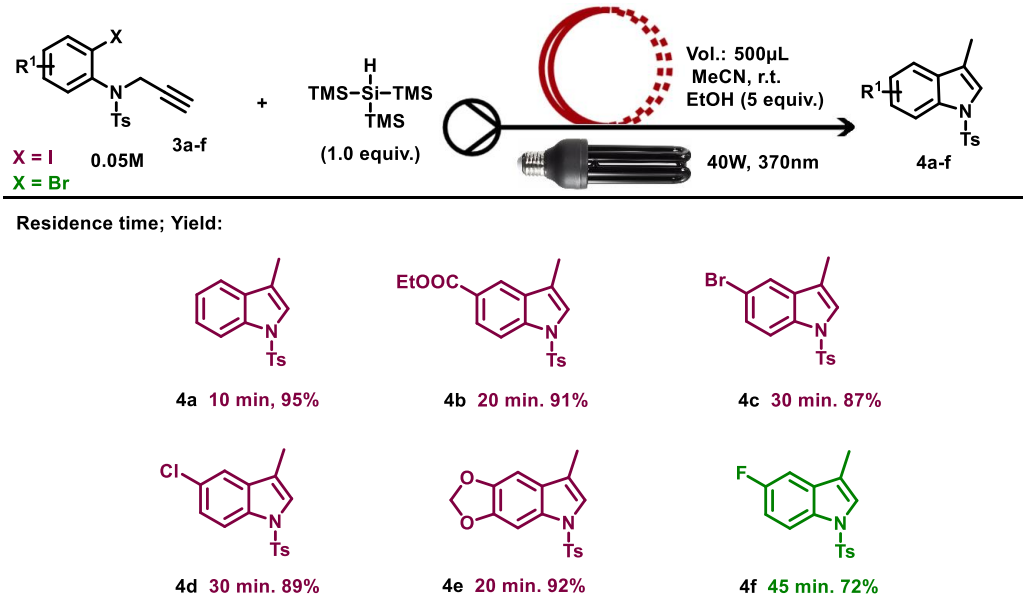

Scheme 31).

Scheme 31. Substrate scope for the visible-light-mediated indole synthesis. Reaction conditions: 1 equiv of TTMSS, 5 equiv of EtOH, and starting material 0.05M in MeCN, irradiation with Black light bulb 4 0W. Yields of isolated products.

The developed protocol was used for the synthesis of the indole core containing important moieties. The reaction of halogen substituted aromatic ring with chloro and bromo afford products **4c** and **4d**, in 30 minutes with 87 and 89 %of the isolated yields respectively. While the one substrate bearing the fluoro moiety, showed that the reaction can be conducted with aryl-bromide instead of aryl-iodide as a radical precursor, led the product **4f** in good yield 72 %, although the reaction time was slightly longer, 45 minutes. Furthermore, the feasibility of the demonstrated cyclization was observed to be compatible with electron withdrawing groups, ester, and electron donating, ether groups, attached to the aromatic ring with good yield 91%, 92% (**4b** and **4e**, respectively). While the reaction time varied for each substituent, no great effect on the yield was observed from the compounds derivated from aryl iodines, evidencing the robustness of the method.

4.3. Conclusion

We developed a simple and highly efficient, energetically and time saving methodology for the synthesis of indoles and indolines via intramolecular cyclization under continuous flow conditions. A metal free protocol that combined to near visible-light (UVA I - black light) irradiation and the use of TTMSS as a carbon-radical promoter was reported. Flow conditions help to decrease reaction time and increase selectivity. The use of continuous flow with microreactors allows highly effective transmission of energy to the reaction stream, decreasing the reaction time. Furthermore, the formation of undesired compounds can be controlled by adjusting the flow rate to minimize the exposure of the desired product to light that interns increasing selectivity of reaction.

Continuous-Flow Photochemistry in a Practical Metal- and Additive-Free Synthesis of Indoles and Indolines

4.4. Experimental Section

Materials and reagents used were of the highest commercially available grade and were used without further purification. Flash column chromatography was carried out using silica gel 60 (230-400 mesh) and analytical thin layer chromatography (TLC) was performed using Merck silica gel 60 F_{254} plates. Compounds were visualized by UV and $KMnO_4$. A near-visible-light, UVA I, 370 nm, 40 W was used. The Syringe Pump used was a Harvard Apparatus, Pump 11 Elite. Analysis were performed using GC-MS (Shimadzu GC-2010 Plus coupled to a Mass Spectrometer; Shimadzu GCMS-QP 2010 Ultra) with an auto sampler unit (AOC-20i, Shimadzu) where the pure isolated products were used as external standard.

Photochemical Reactor setup: Two different setups were tested: Using the tubular reactor externally or internally of the lamp. The internal setup consists in a PFA tubing that is wrapped around a glass tube and placed at the center of the lamp. It shows better results, due to the proximity with lamp, decreasing intensity loss of light. These configurations were used for all of the described reaction. The system was kept at room temperature by air cooling. A PFA Tubing Natural 1/16" OD x .030" ID x 110 cm was used as the reactor. The Total volume was calculated as 500 µL. **Residence Time (RT)** was calculated by the ratio of the total reactor volume to the total flow rate.

$$RT\ (\mathrm{min}) = reactor\ volume\ (\mu L) / \ total\ flow\ rate\ (\mu l/\mathrm{min})$$

General Procedure for the near-visible-light-mediated indoline synthesis. Using the Internal Photochemical Reactor Setup - Reaction conditions: A solution

of *N*-allyl-*N*-(2-halophenyl) acetamides (0.5 mmol, 0.05 M) and TTMSS (1.0 mmol, 2 equiv) in acetonitrile (10 mL) was reacted under black light irradiation (370 nm, 40 W) in a PFA tubular reactor (total volume: 500 µL). The residence time was adjusted and a conversion of >95 %. was achieved. The solution was concentrated under vacuum. The crude mixture was purified by flash chromatography (hexane/EtOAc) to afford the corresponding indoline.

Scheme 32. Internal Photochemical Reactor Setup

Scheme 33. Syringes “labmade”

Preparation of *N*-allyl-*N*-(2-halophenyl) acetamides

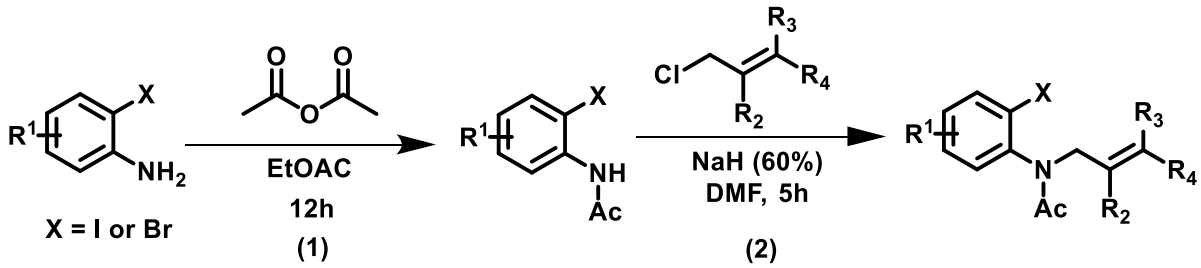

Scheme 34 . Preparation of *N*-allyl-*N*-(2-halophenyl) acetamides

1. In a round bottom flask containing a solution of 2-iodoaniline (2.0 mmol, 438 mg) in 8 mL of EtOAc was added acetic anhydride (4.0 mmol, 408 mg) and the reaction mixture was stirred at room temperature overnight. The solvent was removed under reduced pressure and the crude solid was recrystallized from a mixture of hexane and ethyl acetate to provide the *N*-(2- iodophenyl) acetamide as a white solid.

2. In a round bottom flask containing a solution of *N*-(2-iodophenyl) acetamide (1.0 mmol, 261 mg) in DMF (3.0 mL) was added slowly NaH (60% in mineral oil, 1.5 mmol, 60 mg) at 0 °C under nitrogen atmosphere. After vigorous evolution of hydrogen gas, the reaction mixture was treated with allyl bromide (1.5 mmol, 182 mg) and warmed to room temperature. After stirring for 5 h, the reaction mixture was quenched by careful addition of H_2O (20 mL) and extracted with DCM (50 mL). The organic layers were washed with water (4 x 20 mL) and brine (20 mL), dried over Na_2SO_4, filtered and concentrated under reduced pressure. The crude mixture was purified by flash chromatography (hexane/EtOAc) to afford the *N*-allyl-*N*-(2- iodophenyl) acetamide.

Preparation of the *N*-tosyl-protected aniline

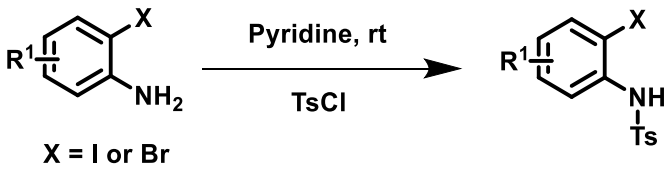

Scheme 35. Preparation of the *N*-tosyl-protected aniline

Synthesis of N-tosyl-protected aniline. In a rounded bottom flask containing a solution of 2-iodoaniline (4.50 mmol, 1 equiv) in pyridine (10 mL) was added *p*-toluenesulfonyl chloride (4.70 mmol, 1.05 equiv). The reaction mixture was stirred at r.t for 1.5 h then quenched with water (10 mL). The solution was extracted with CH_2Cl_2 (3 time) and the combined organic extracts were washed with a 10% aqueous $CuSO_4$ (2 time), dried over anhydrous Na_2SO_4, filtered and concentrated under vacuum. The crude mixture was purified by flash chromatography (hexane/EtOAc) to afford the corresponding tosyl-protected aniline.

Preparation of the *N*-tosyl-propargyl aniline

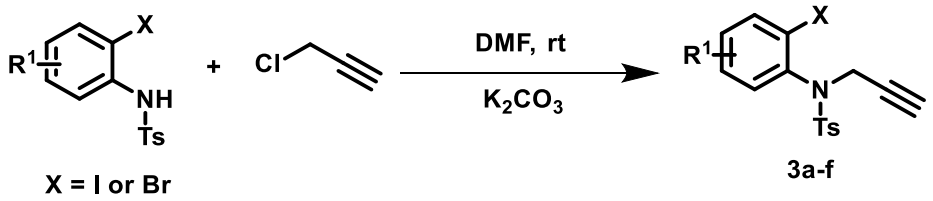

Scheme 36. Preparation of the *N*-tosyl-propargyl aniline

Synthesis of *N*-tosyl-propargyl aniline. In a rounded bottom flask containing a solution of N-tosyl protected 2-iodoaniline (1.0 mmol, 1 equiv) in DMF (5 mL) were added K_2CO_3 (3.0 mmol, 3 equiv) and propargyl chloride (2.0 mmol, 2 equiv). After the total consumption of the aniline, 3h, at room temperature the reaction was quenched with water (5 mL). The aqueous layer was extracted with ether (3 x 10mL) and the combined organic phases were dried over anhydrous Na_2SO_4, filtered and concentrated. The crude mixture was purified by flash chromatography (hexane/EtOAc) to afford *N*-tosyl-propargyl aniline.

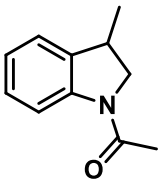

1-(3-methylindolin-1-yl)ethan-1-one (2a): The title compound was synthesized according to the general procedure in 95 % isolated yield as a white solid. **^{1}H NMR** (400 MHz, $CDCl_3$) δ 8.19 (d, *J* = 8.1 Hz, 1H), 7.24 – 7.09 (m, 3H), 7.04 (td, *J* = 7.4, 0.9 Hz, 1H), 4.21 (t, *J* = 9.6 Hz, 1H), 3.57 (dd, *J* = 9.9, 6.7 Hz, 1H), 3.53 – 3.44 (m, 1H), 2.22 (s, 3H), 1.36 (d, *J* = 6.8 Hz, 3H). **^{13}C NMR** (100 MHz, $CDCl_3$) δ 168.6, 142.3, 136.2, 127.7, 123.7, 123.3, 116.8, 56.9, 34.7, 24.2, 20.2.

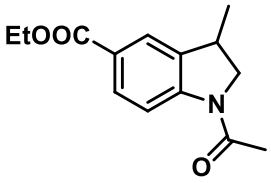

ethyl 1-acetyl-3-methylindoline-5-carboxylate (2b): The title compound was synthesized according to the general procedure in 82 % isolated yield as a white solid. **^{1}H NMR** (400 MHz, $CDCl_3$) δ 8.20 (d, *J* = 8.5 Hz, 1H), 7.93 (dd, *J* = 8.5, 1.5 Hz, 1H), 7.83 (s, 1H), 4.40 – 4.32 (m, 2H), 4.27 (t, *J* = 9.8 Hz, 1H), 3.64 (dd, *J* = 10.0, 6.8 Hz, 1H), 3.58 – 3.47 (m, 1H), 2.24 (s, 3H), 1.42 – 1.35 (m, 6H). **^{13}C NMR** (100 MHz, $CDCl_3$) δ 169.2, 166.3, 146.2, 136.4, 130.2, 125.7, 124.8, 116.1, 60.8, 57.3, 34.4, 24.2, 20.2, 14.3.

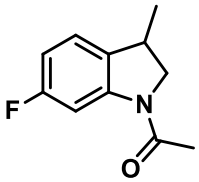

1-(6-fluoro-3-metilindolin-1-il)ethan-1-ona (2c): The title compound was synthesized according to the general procedure in 91 % isolated yield as a white solid. **^{1}H NMR** (400 MHz, $CDCl_3$) δ 8.07 (dd, *J* = 8.7, 4.9 Hz, 1H), 6.84 – 6.75 (m, 2H), 4.16 (t, *J* = 9.8 Hz, 1H), 3.53 (dd, *J* = 10.1, 6.8 Hz, 1H), 3.47 – 3.36 (m, 1H), 2.14 (s, 3H), 1.28 (d, *J* = 6.9 Hz, 3H). **^{13}C NMR** (100 MHz, $CDCl_3$) δ 168.3, 159.4 (d, *J* = 241.8 Hz), 138.5, 138.3, 117.7 (d, *J* = 7.9 Hz), 113.9 (d, *J* = 22.6 Hz), 110.6 (d, *J* = 23.9 Hz), 57.1, 34.7, 23.9, 20.0.

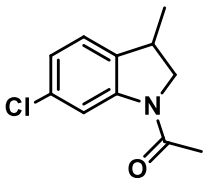

1-(6-cloro-3-metilindolin-1-il)etan-1-ona (2d): The title compound was synthesized according to the general procedure in 79 % isolated yield as a white solid. **^{1}H NMR** (400 MHz, $CDCl_3$) δ 8.21 (d, *J* = 1.7 Hz, 1H), 7.05 (d, *J* = 8.0 Hz, 1H), 6.99 (dd, *J* = 8.0, 1.9 Hz, 1H), 4.22 (t, *J* = 9.8 Hz, 1H), 3.59 (dd, *J* = 10.1, 6.7 Hz, 1H), 3.51 –

3.41 (m, 1H), 2.21 (s, 3H), 1.34 (d, *J* = 6.9 Hz, 3H). **^{13}C NMR** (100 MHz, $CDCl_3$) δ 168.8, 143.3, 134.8, 133.2, 124.0, 123.6, 117.1, 57.3, 34.3, 24.1, 20.2.

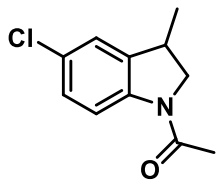

1-(5-chloro-3-methylindolin-1-yl)ethan-1-one (2e): The title compound was synthesized according to the general procedure in 92 % isolated yield as a white solid. **^{1}H NMR** (400 MHz, $CDCl_3$) δ 8.11 (d, *J* = 8.6 Hz, 1H), δ 7.15 (ddd, *J* = 8.6, 2.2, 0.7 Hz, 1H), 7.10 (s, 1H), 4.21 (t, *J* = 9.8 Hz, 1H), 3.58 (dd, *J* = 10.1, 6.8 Hz, 1H), 3.47 (m, 1H), 2.20 (s, 3H), 1.34 (d, *J* = 6.9 Hz, 3H). **^{13}C NMR** (100 MHz, $CDCl_3$) δ 168.6, 141.0, 138.2, 128.5, 127.6, 123.6, 117.7, 57.0, 34.6, 24.1, 20.1.

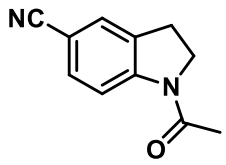

1-acetylindoline-5-carbonitrile (2f): The title compound was synthesized according to the general procedure in 93 % isolated yield as a white solid. **^{1}H NMR** (400 MHz, $CDCl_3$) δ 8.26 (d, *J* = 8.5 Hz, 1H), 7.51 (ddd, *J* = 8.4, 1.7, 0.6 Hz, 1H), 7.41 (s, 1H), 4.29 (t, *J* = 18.8, 8.8 Hz, 1H), 3.66 (dd, *J* = 10.2, 6.7 Hz, 1H), 3.54 (m, 1H), 2.25 (s, 3H), 1.38 (d, *J* = 6.9 Hz, 3H). **^{13}C NMR** (100 MHz, $CDCl_3$) δ 169.4, 146.1, 137.3, 132.9, 127.1, 119.3, 117.1, 106.5, 57.0, 34.4, 24.3, 20.2.

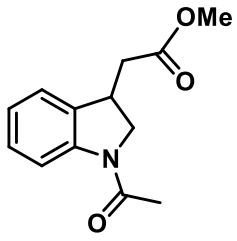

methyl 2-(1-acetylindolin-3-yl)acetate (2g): A The title compound was synthesized according to the general procedure in 93 % isolated yield as a transparent oil. **^{1}H NMR** (400 MHz, $CDCl_3$) δ 8.13 (d, *J* = 8.1 Hz, 1H), 7.14 (t, *J* = 11.5, 1H), 7.07 (d, *J* = 7.5 Hz, 1H), 6.95 (td, *J* = 7.5, 1.0 Hz, 1H), 4.24 (dd, *J* = 10.3, 9.3 Hz, 1H), 3.80 – 3.71 (m, 1H), 3.66 (s, 3H), 2.77 (dd, *J* = 16.6, 4.4 Hz, 1H), 2.49 (dd, *J* = 16.6, 96 10.0 Hz, 1H), 2.15 (s, 3H). **^{13}C NMR** (100 MHz, $CDCl_3$) δ 172.2, 168.8, 142.6, 133.0, 128.4, 123.8, 123.6, 117.1, 55.1, 51.9, 39.6, 36.5, 24.2.

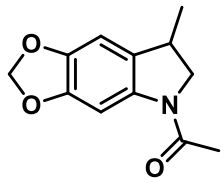

1-(7-methyl-6,7-dihydro-5H-[1,3]dioxolo[4,5-f]indol-5-yl)ethan-1-one (2h): The title compound was synthesized according to the general procedure in 78 % isolated yield as a white solid. **^{1}H NMR** (400 MHz, $CDCl_3$) δ 7.84 (s, 1H), 6.61 (s, 1H), 5.92 (q, *J* = 1.4 Hz, 2H), 4.20 (t, *J* = 10.1 Hz, 1H), 3.56 (dd, *J* = 10.2, 6.6 Hz, 1H), 3.43 – 3.34 (m, 1H), 2.19 (s, 3H), 1.30 (d, *J* = 6.8 Hz, 3H). **^{13}C NMR** (100 MHz, $CDCl_3$) δ 168.0, 146.7, 143.9, 136.6, 129.0, 103.8, 101.3, 99.8, 57.5, 34.6, 24.0, 20.5

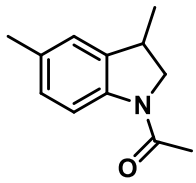

1-(3,5-dimethylindolin-1-yl)ethan-1-one (2j): The title compound was synthesized according to the general procedure in 94 % isolated yield as a white solid. **^{1}H NMR** (400 MHz, $CDCl_3$) δ 8.06 (d, *J* = 8.2 Hz, 1H), 7.00 (d, *J* = 6.6 Hz, 1H), 6.96 (s, 1H), 4.18 (t, *J* = 9.7 Hz, 1H), 3.55 (dd, *J* = 10.0, 6.7 Hz, 1H), 3.45 (m, 1H), 2.31 (s, 3H), 2.20 (s, 3H), 1.34 (d, *J* = 6.8 Hz, 3H). **^{13}C NMR** (100 MHz, $CDCl_3$) δ 168.2, 140.1, 136.4, 133.3, 128.1, 124.0, 116.6, 57.1, 34.7, 24.1, 21.0, 20.2.

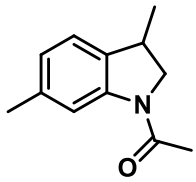

1-(3,6-dimethylindolin-1-yl)ethan-1-one (2k): The title compound was synthesized according to the general procedure in 94 % isolated yield as a white solid. **^{1}H NMR** (400 MHz, $CDCl_3$) δ 8.05 (s, 1H), 7.03 (d, *J* = 7.6 Hz, 1H), 6.85 (dd, *J* = 7.6, 0.7 Hz, 1H), 4.19 (t, *J* = 9.7 Hz, 1H), 3.56 (dd, *J* = 10.0, 6.7 Hz, 1H), 3.45 (m, 1H), 2.34 (s, 3H), 2.21 (s, 3H), 1.33 (d, *J* = 6.8 Hz, 3H). **^{13}C NMR** (100 MHz, $CDCl_3$) δ 168.6, 142.5, 137.7, 133.5, 124.4, 123.0, 117.6, 57.3, 34.4, 24.2, 21.6, 20.4.

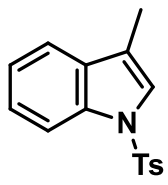

3-methyl-1-tosyl-1H-indole (4a): The title compound was synthesized according to the general procedure in 95 % isolated yield as a white solid. **^{1}H NMR** (400 MHz, $CDCl_3$) δ 7.8 (d, *J* = 8.3 Hz, 1H), 7.6 (d, *J* = 8.4 Hz, 2H), 7.3 (d, *J* = 7.3 Hz, 1H), 7.2 – 7.1 (m, 2H), 7.12 (d, *J* = 6.8 Hz, 1H), 7.1 (d, *J* = 8.0 Hz, 2H), 2.2 (s, 3H), 2.1 (s, 3H).

^{13}C NMR (100 MHz, $CDCl_3$) δ 144.6, 135.4, 135.3, 131.8, 129.8, 126.8, 124.6, 123.1, 122.9, 119.3, 118.6, 113.7, 21.53, 9.7.

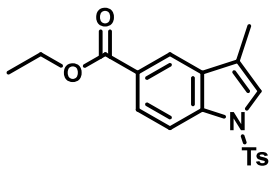

Ethyl 3-methyl-1-tosyl-1H-indole-5-carboxylate (4b): The title compound was synthesized according to the general procedure in 91 % isolated yield as an off-white solid (m.p: 115-117 °C). **^{1}H NMR** (400 MHz, $CDCl_3$) δ 8.1 (t, *J* = 1.2 Hz, 1H), 8.0 – 7.9 (m, 2H), 7.7 – 7.6 (m, 2H), 7.3 (d, *J* = 1.3 Hz, 1H), 7.1 (d, *J* = 8.0 Hz, 2H), 4.3 (q, *J* = 7.1 Hz, 2H), 2.3 (s, 3H), 2.2 (d, *J* = 1.3 Hz, 3H), 1.3 (t, *J* = 7.1 Hz, 3H). **^{13}C NMR** (100 MHz, $CDCl_3$) δ 166.8, 145.1, 137.7, 135.2, 131.6, 129.9, 126.7, 125.8, 125.4, 124.2, 121.7, 119.0, 113.3, 60.9, 21.6, 14.4, 9.6.

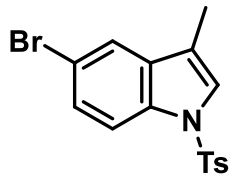

5-bromo-3-methyl-1-tosyl-1*H*-indole (4c): The title compound was synthesized according to the general procedure in 87 % isolated yield as an oil. **^{1}H NMR** (400 MHz, $CDCl_3$) δ 7.7 (d, *J* = 8.8 Hz, 1H), 7.6 (d, *J* = 8.4 Hz, 2H), 7.4 (d, *J* = 1.9 Hz, 1H), 7.3 (dd, *J* = 8.8, 1.9 Hz, 1H), 7.2 (d, *J* = 1.2 Hz, 1H), 7.1 (d, *J* = 8.6 Hz, 2H), 2.2 (s, 3H), 2.1 (d, *J* = 1.3 Hz, 3H). **^{13}C NMR** (100 MHz, $CDCl_3$) δ 144.9, 135.1, 133.9, 133.6, 129.9, 127.4, 126.7, 124.3, 122.3, 117.9, 116.6, 115.1, 21.6, 9.6.

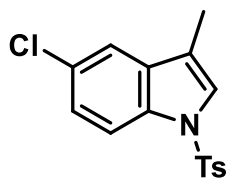

5-chloro-3-methyl-1-tosyl-1*H*-indole (4d): The title compound was synthesized according to the general procedure in 89 % isolated yield as a white solid (m.p: 111-113 °C). **^{1}H NMR** (400 MHz, $CDCl_3$) δ 7.9 (d, *J* = 8.8 Hz, 1H), 7.7 (d, *J* = 8.3 Hz, 2H), 7.4 (d, *J* = 1.6 Hz, 1H), 7.3 (dd, *J* = 20.6, 2.2 Hz, 2H), 7.2 (d, *J* = 8.0 Hz, 2H), 2.3 (s, 3H), 2.2 (d, *J* = 1.2 Hz, 3H). **^{13}C NMR** (100 MHz, $CDCl_3$)

δ 144.9, 135.1, 133.6, 133.1, 129.9, 128.9, 126.7, 124.8, 124.4, 119.2, 118.1, 114.7, 21.6, 9.6.

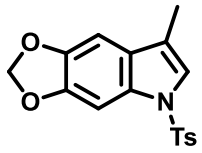

7-methyl-5-tosyl-5*H*-[1,3]dioxolo[4,5-f]indole (4e): The title compound was synthesized according to the general procedure in 92 % isolated yield as a white solid.**^{1}H NMR** (400 MHz, $CDCl_3$) δ 7.7 (d, *J* = 8.4 Hz, 2H), 7.5 (s, 1H), 7.2 (dd, *J* = 10.0, 4.9 Hz, 3H), 6.8 (s, 1H), 5.9 (s, 2H), 2.3 (s, 3H), 2.2 (d, *J* = 1.2 Hz, 3H). **^{13}C NMR** (100 MHz, $CDCl_3$) δ 146.4, 144.9, 144.6, 135.3, 130.0, 129.8, 126.7, 126.1, 122.08, 118.8, 101.3, 98.3, 95.5, 21.6, 9.8.

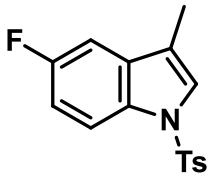

5-fluoro-3-methyl-1-tosyl-1*H*-indole (4f): The title compound was synthesized according to the general procedure in 72 % isolated yield as a white solid (m.p: 98-100 °C). **^{1}H NMR** (400 MHz, $CDCl_3$) δ 7.7 (dd, *J* = 8.7, 4.1 Hz, 1H), 7.6 – 7.5 (m, 2H), 7.2 (d, *J* = 1.2 Hz, 1H), 7.0 (dd, *J* = 8.7, 0.7 Hz, 2H), 6.9 – 6.8 (m, 1H), 6.8 (td, *J* = 8.8, 2.4 Hz, 1H), 2.2 (s, 3H), 2.0 (s, 3H). **^{13}C NMR** (101 MHz, $CDCl_3$) δ 144.8, 135.2, 129.8, 126.7, 124.8, 118.5, 114.8, 114.7, 112.6, 112.3, 105.2, 104.9,

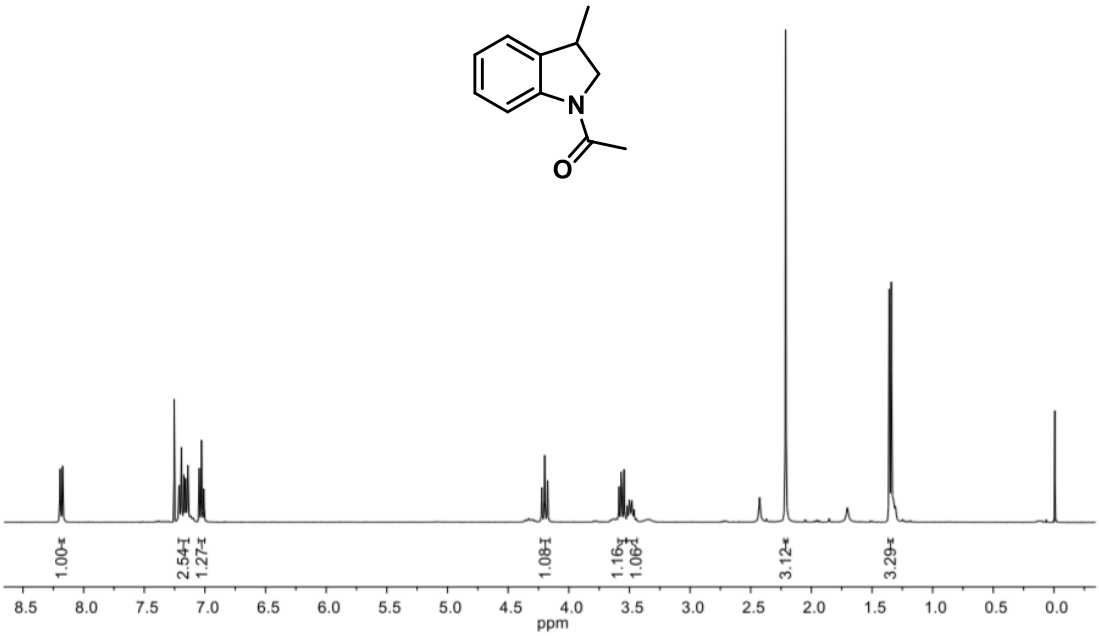

Figure 50: ^{1}H NMR (400 MHz, $CDCl_3$) Spectrum of compound **2a**.

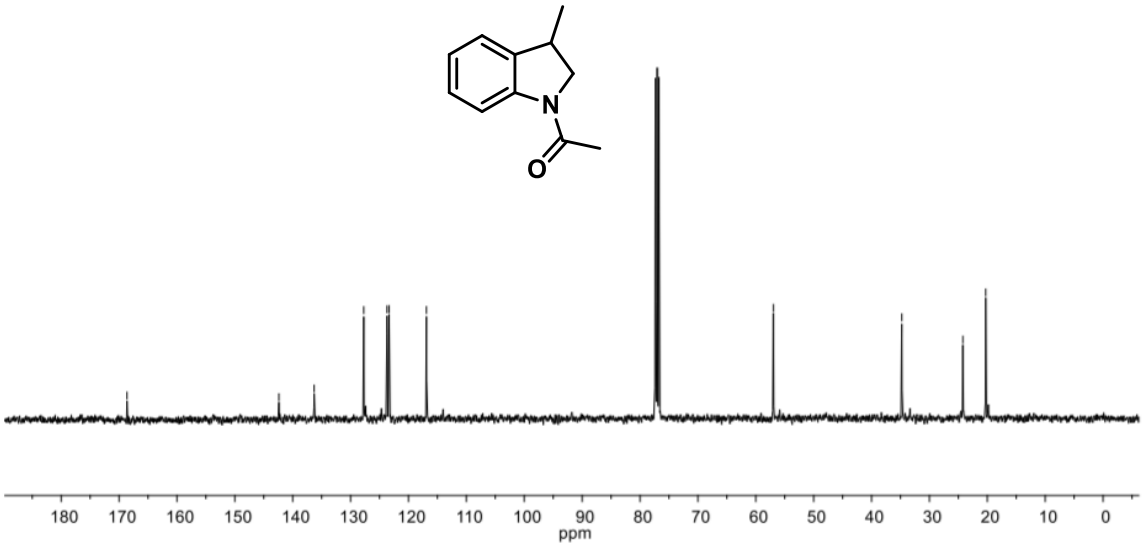

Figure 51: ^{13}C NMR (100 MHz, $CDCl_3$) Spectrum of compound **2a**.

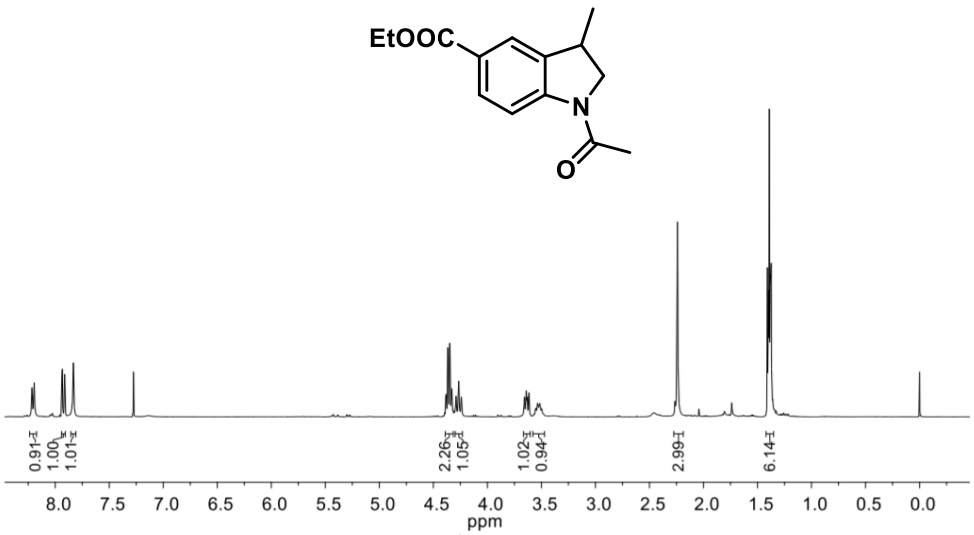

Figure 52: ^{1}H NMR (400 MHz, $CDCl_3$) Spectrum of compound **2b**.

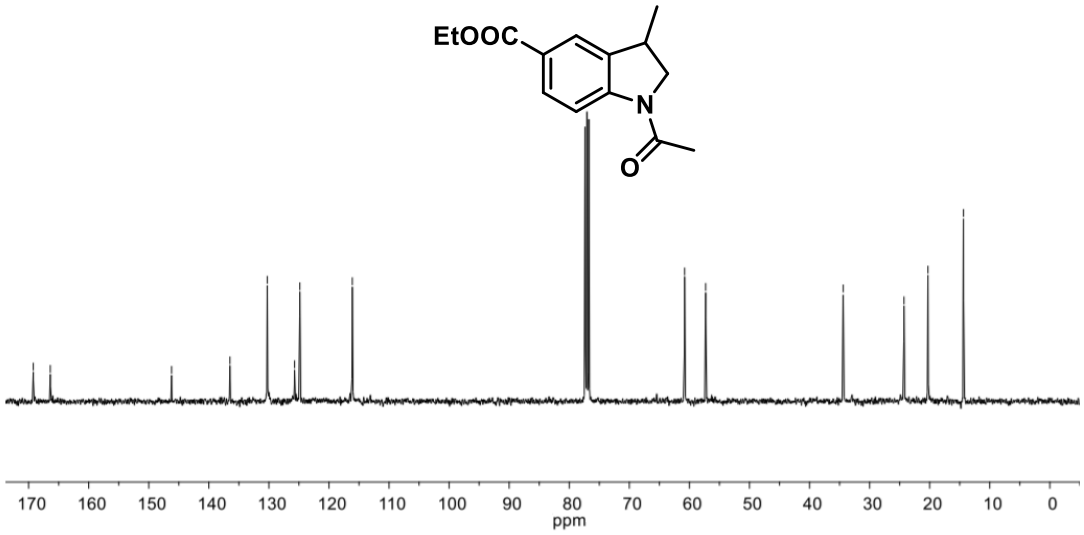

Figure 53: ^{13}C NMR (100 MHz, $CDCl_3$) Spectrum of compound **2b**.

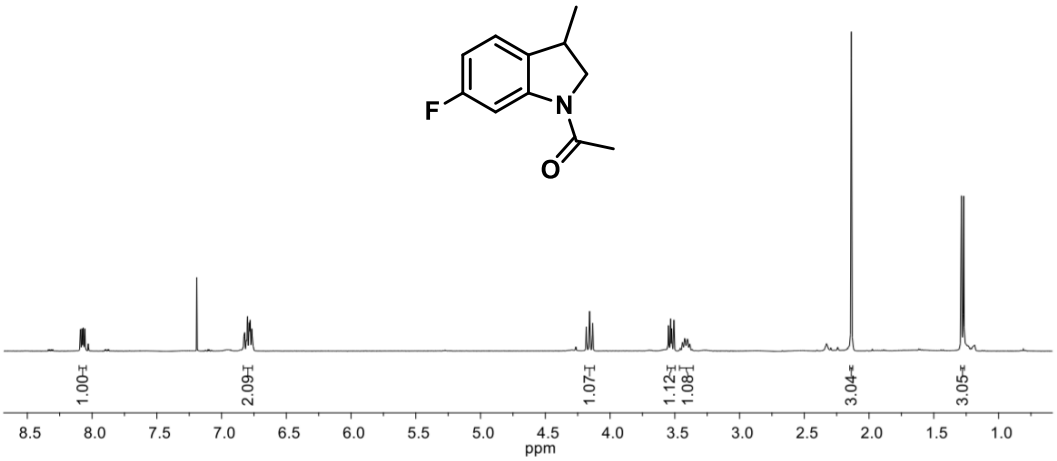

Figure 54: ^{1}H NMR (400 MHz, $CDCl_3$) Spectrum of compound **2c**.

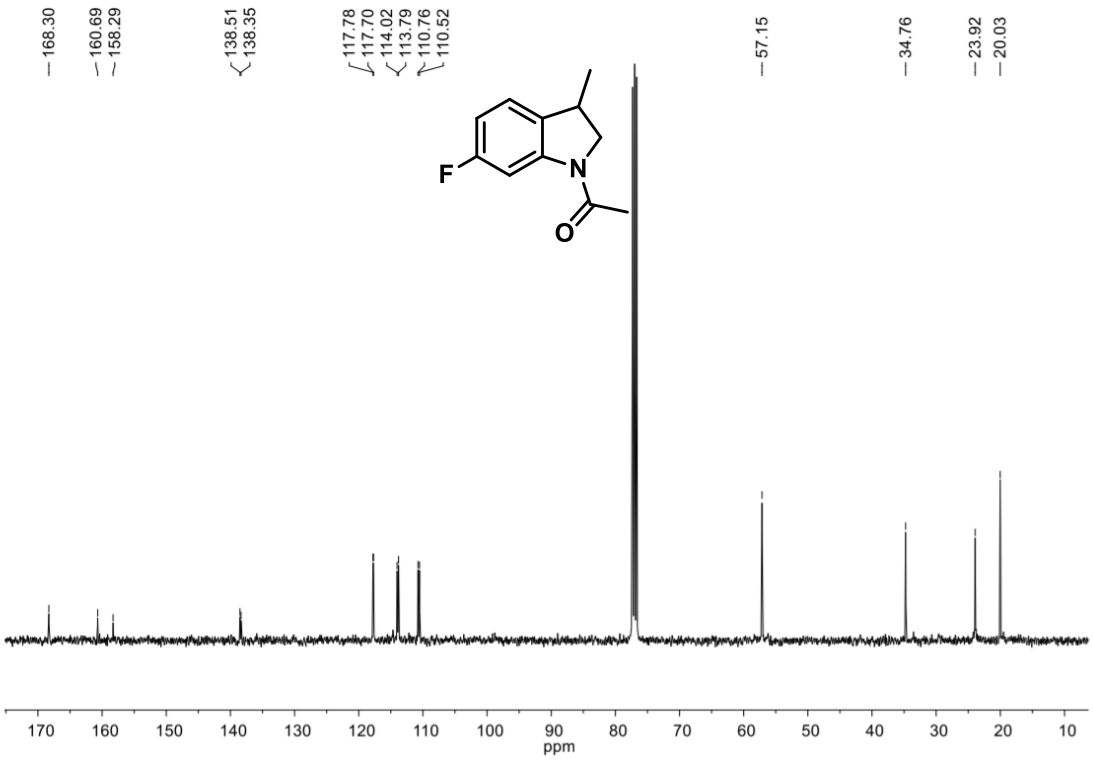

Figure 55: ^{13}C NMR (100 MHz, $CDCl_3$) Spectrum of compound **2c**.

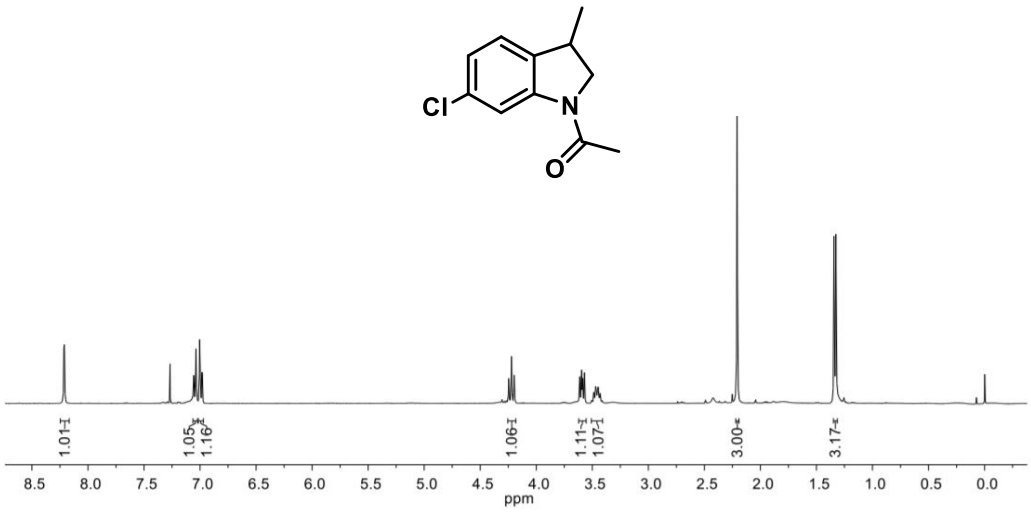

Figure 56: ^{1}H NMR (400 MHz, $CDCl_3$) Spectrum of compound **2d**.

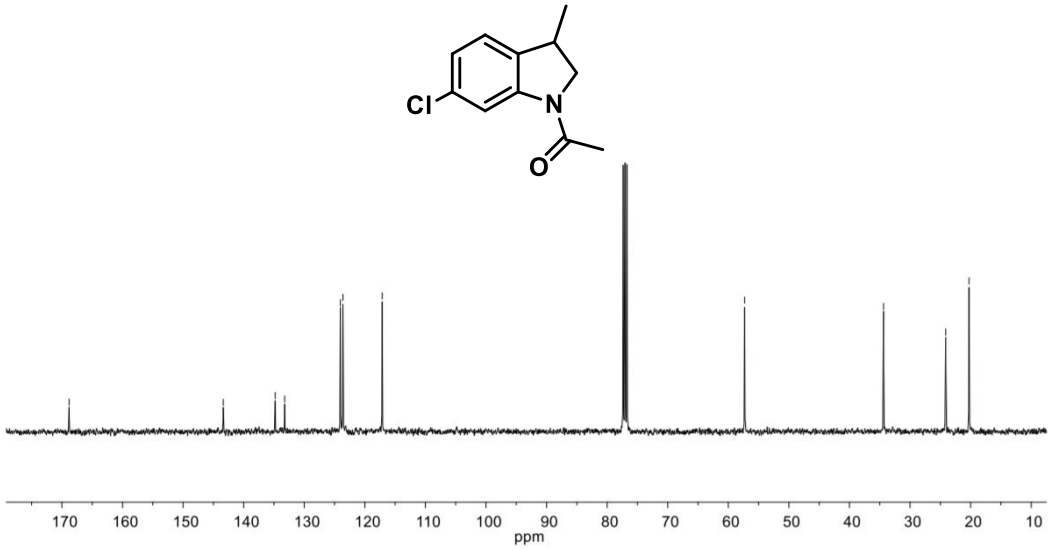

Figure 57: ^{13}C NMR (100 MHz, $CDCl_3$) Spectrum of compound **2d**.

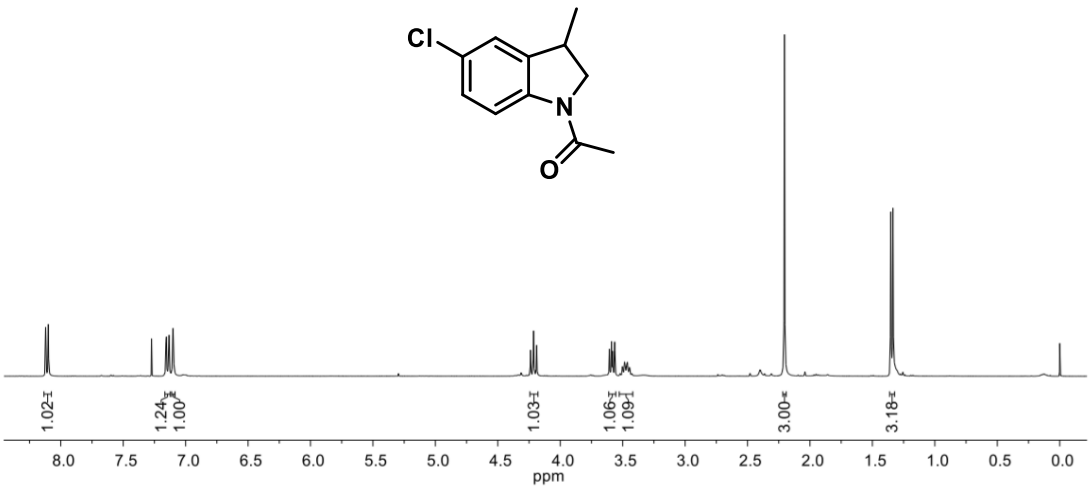

Figure 58: ^{1}H NMR (400 MHz, $CDCl_3$) Spectrum of compound **2e**.

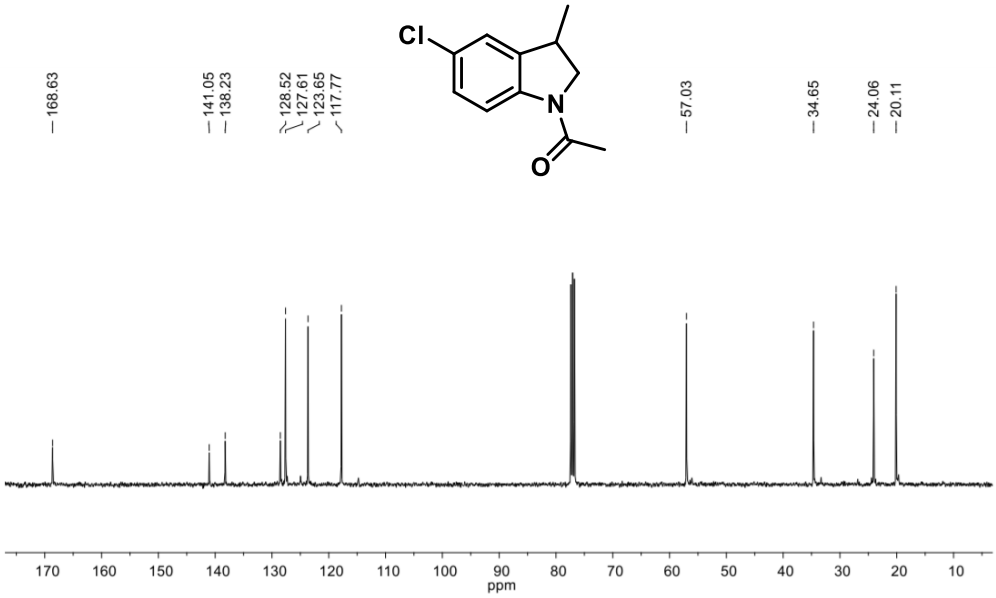

Figure 59: ^{13}C NMR (100 MHz, $CDCl_3$) Spectrum of compound **2e**.

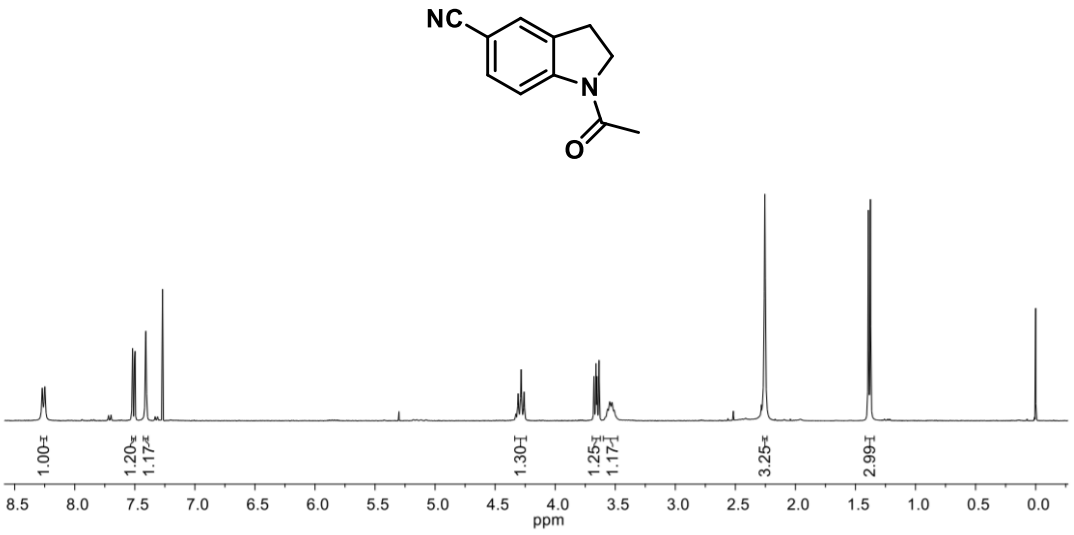

Figure 60: ^{1}H NMR (400 MHz, $CDCl_3$) Spectrum of compound **2f**.

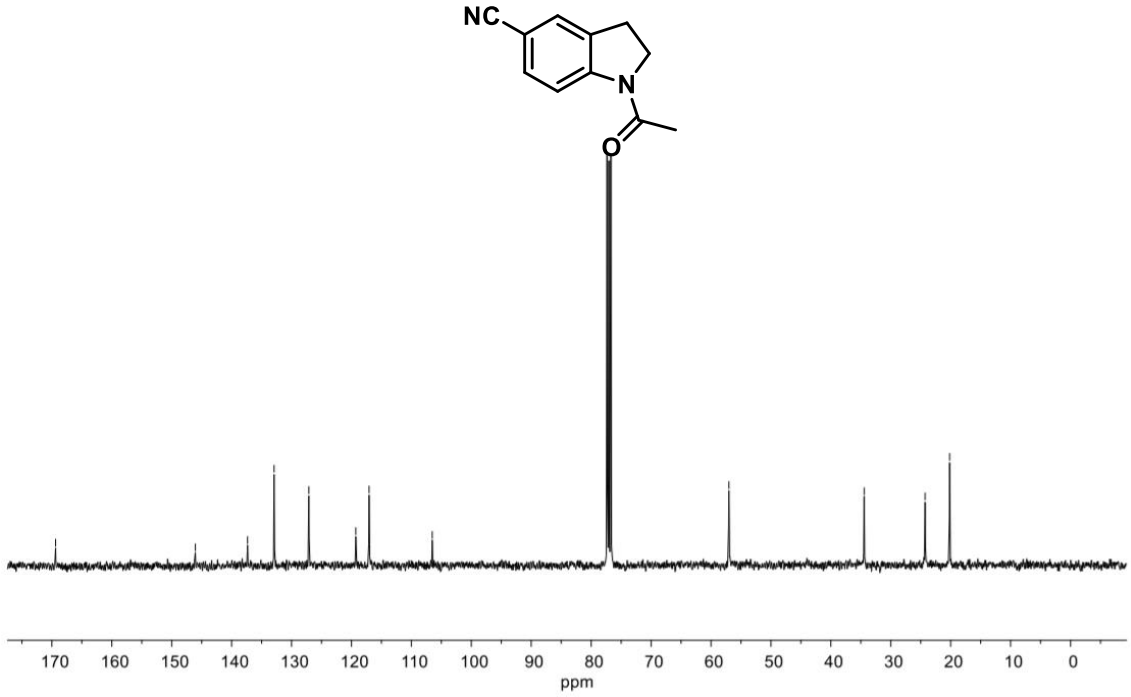

Figure 61: ^{13}C NMR (100 MHz, $CDCl_3$) Spectrum of compound **2f**.

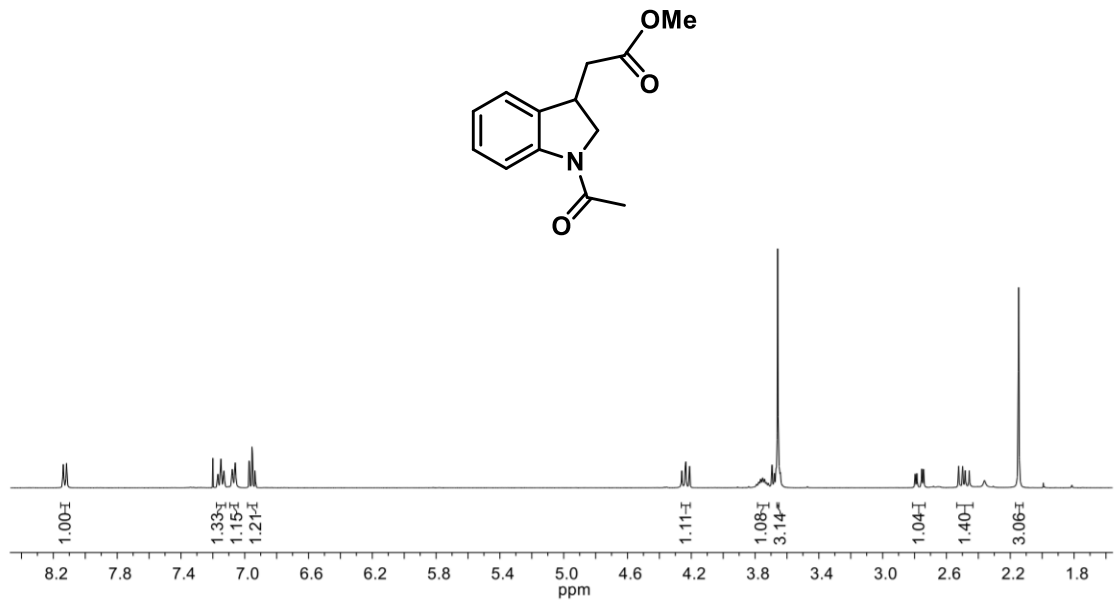

Figure 62: ^{1}H NMR (400 MHz, $CDCl_3$) Spectrum of compound **2g**.

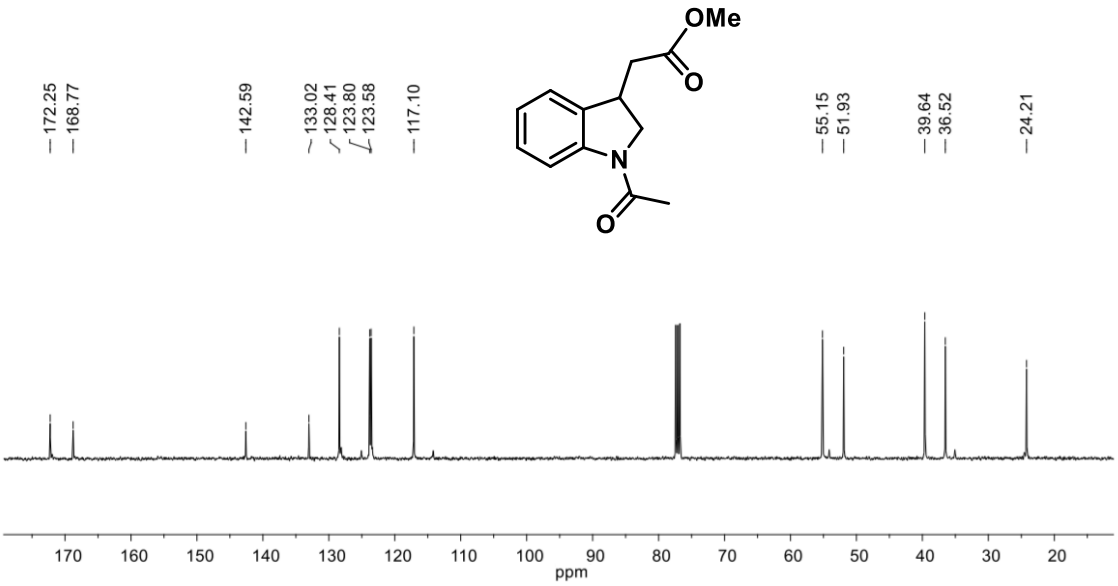

Figure 63: ^{13}C NMR (100 MHz, $CDCl_3$) Spectrum of compound **2g**.

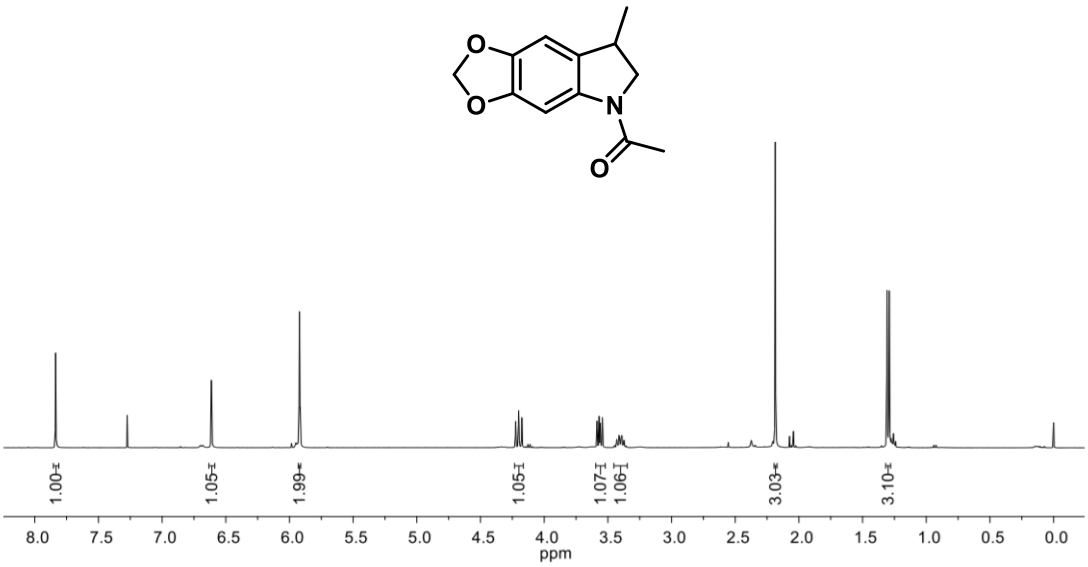

Figure 64: ^{1}H NMR (400 MHz, $CDCl_3$) Spectrum of compound **2h**.

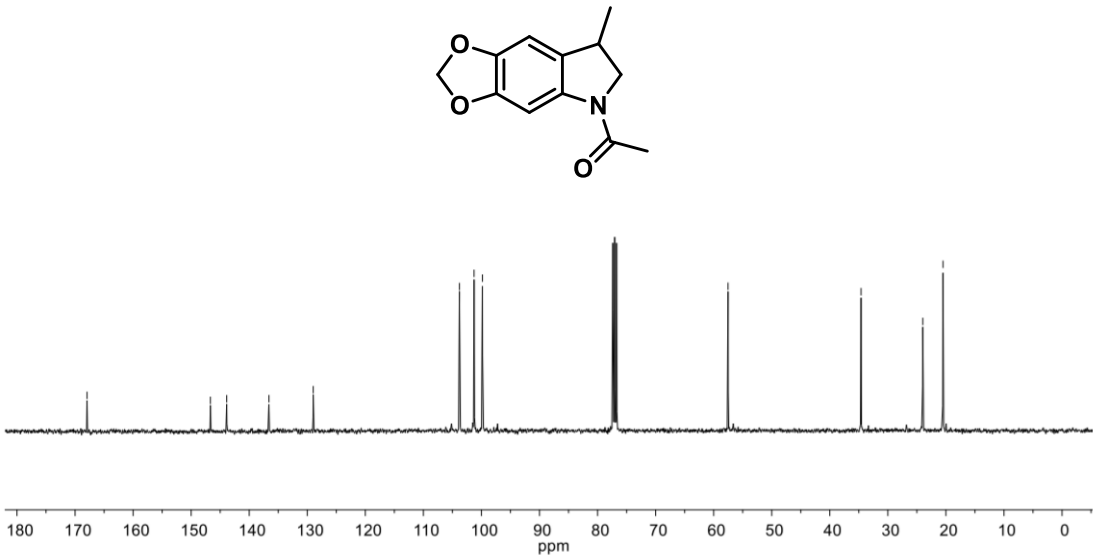

Figure 65: ^{13}C NMR (100 MHz, $CDCl_3$) Spectrum of compound **2h**.

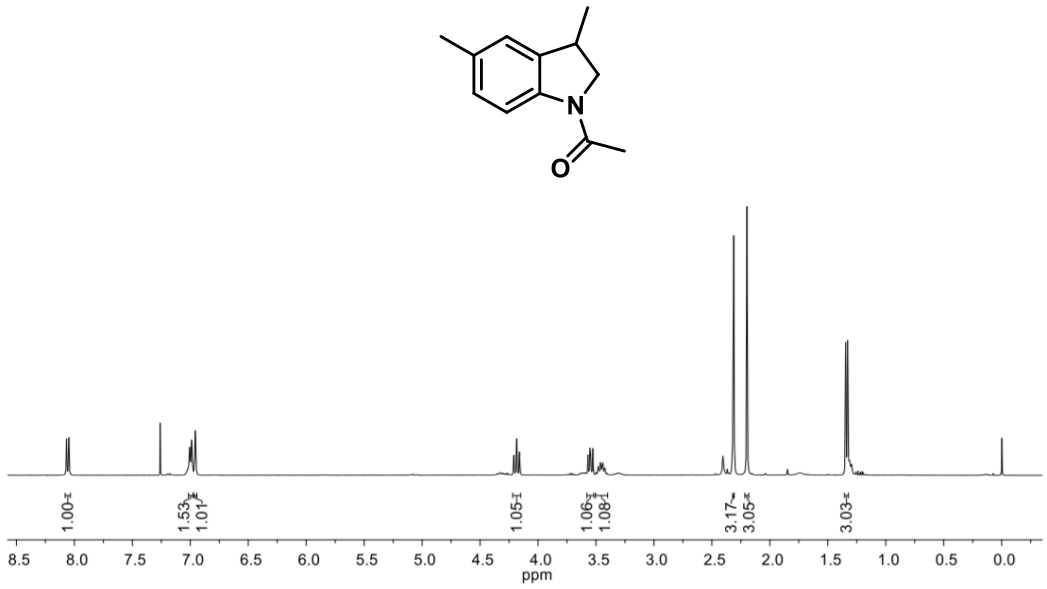

Figure 66: ^{1}H NMR (400 MHz, $CDCl_3$) Spectrum of compound **2j**.

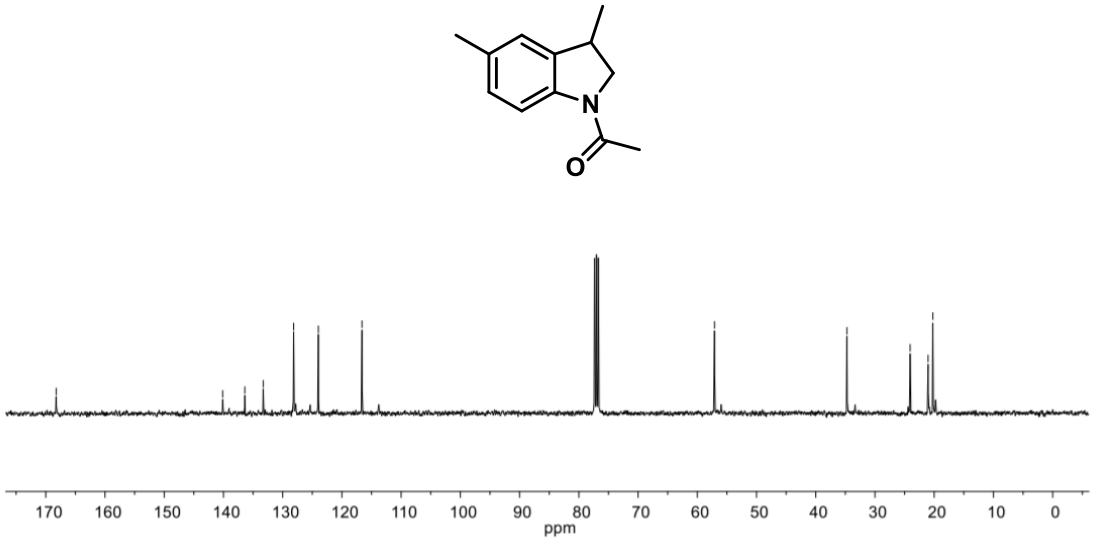

Figure 67: ^{13}C NMR (100 MHz, $CDCl_3$) Spectrum of compound **2j**.

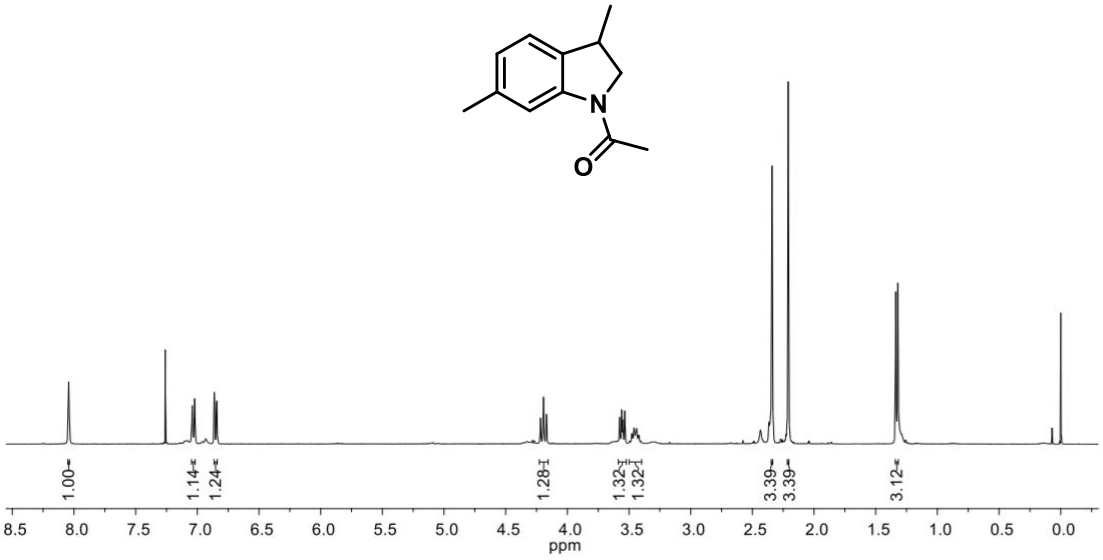

Figure 68: ^{1}H NMR (400 MHz, $CDCl_3$) Spectrum of compound **2k**.

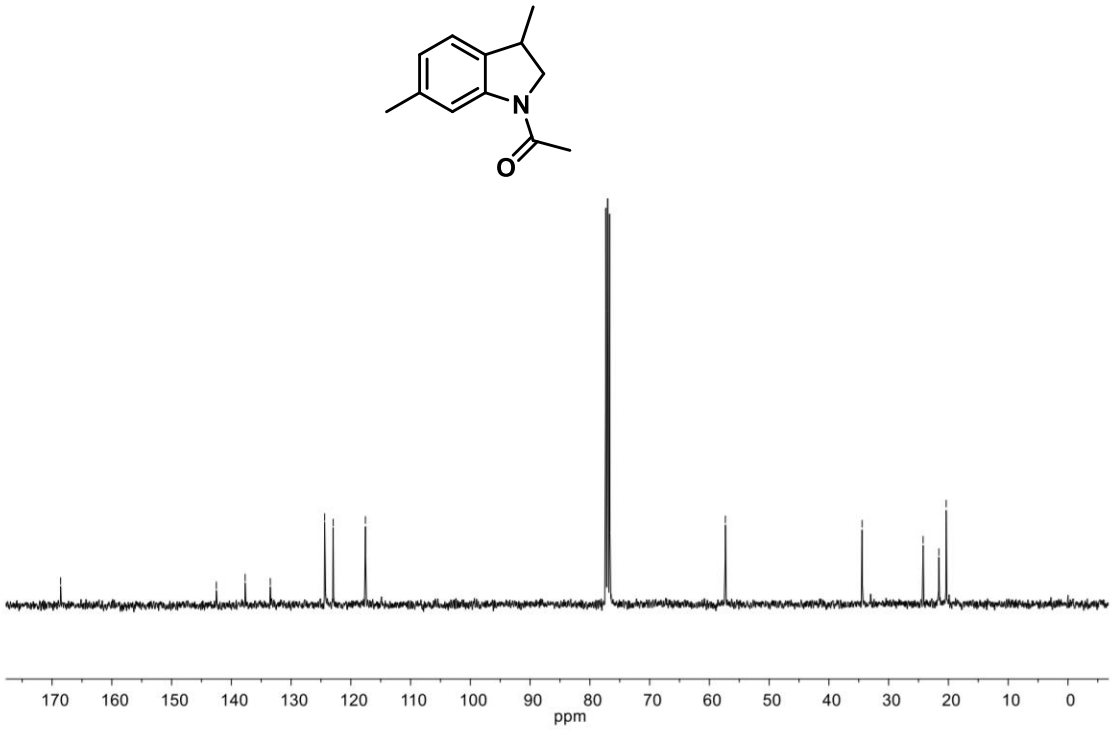

Figure 69: ^{13}C NMR (100 MHz, $CDCl_3$) Spectrum of compound **2k**.

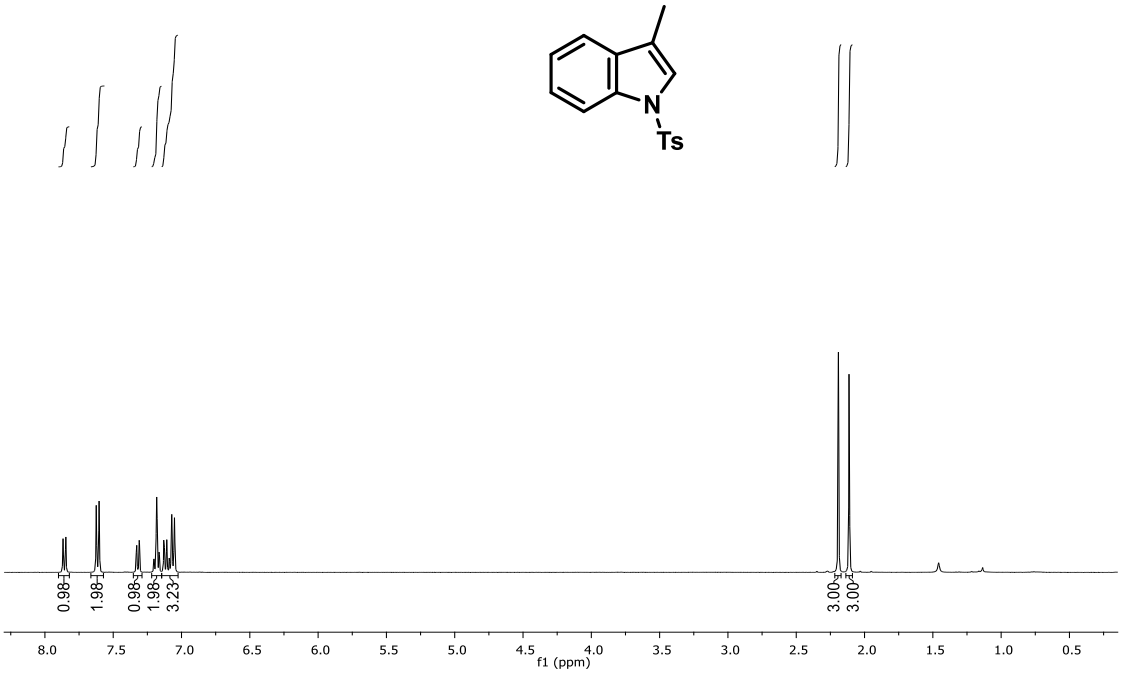

Figure 70: ^{1}H NMR (400 MHz, $CDCl_3$) Spectrum of compound **4a**.

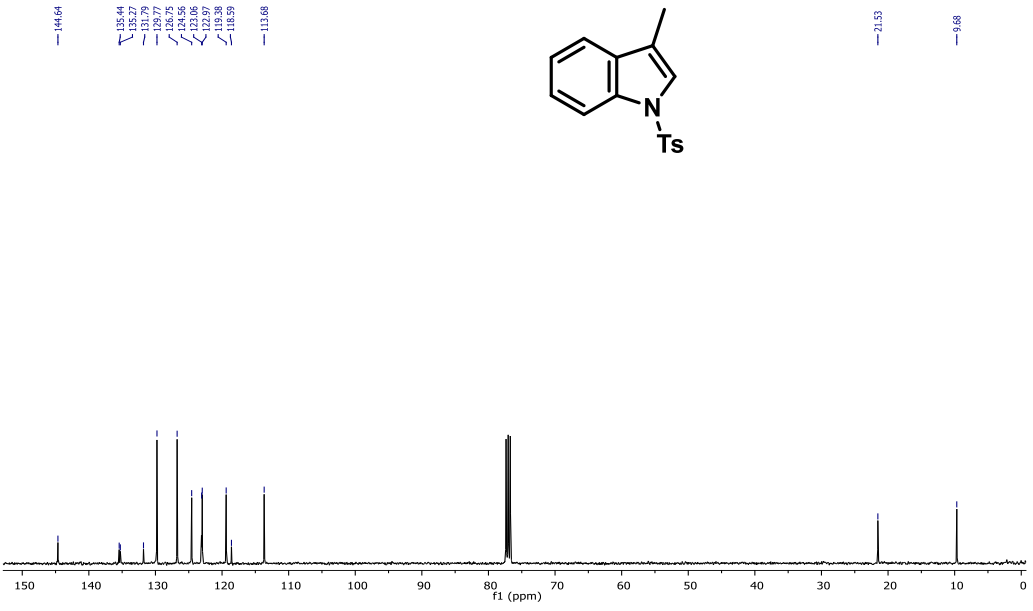

Figure 71: ^{13}C NMR (100 MHz, $CDCl_3$) Spectrum of compound **4a**.

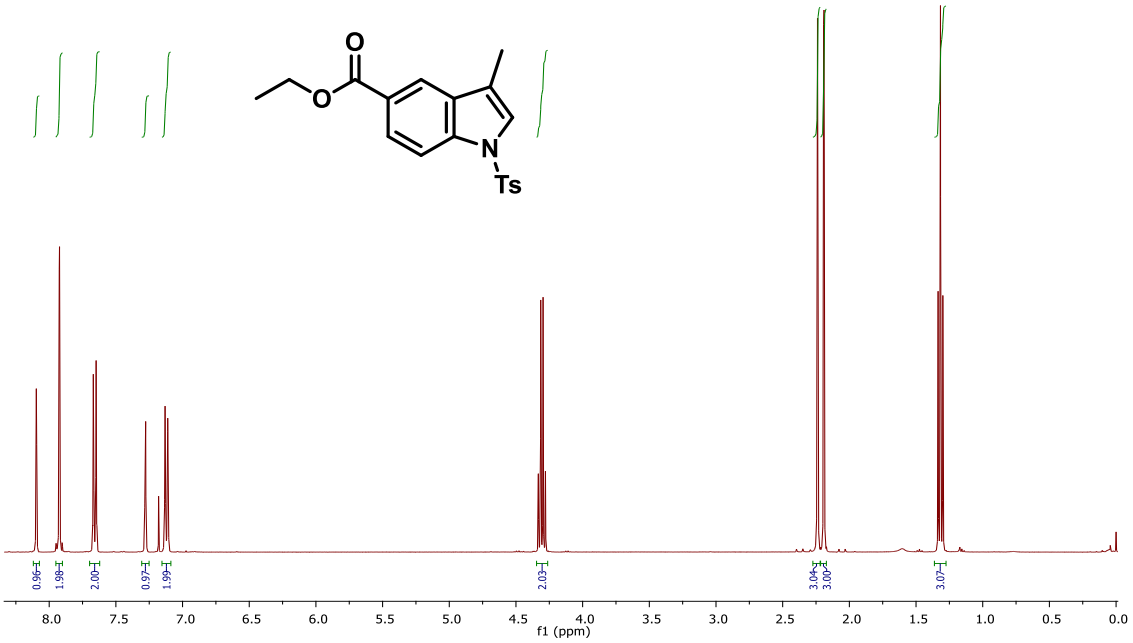

Figure 72: ^{1}H NMR (400 MHz, $CDCl_3$) Spectrum of compound **4b**.

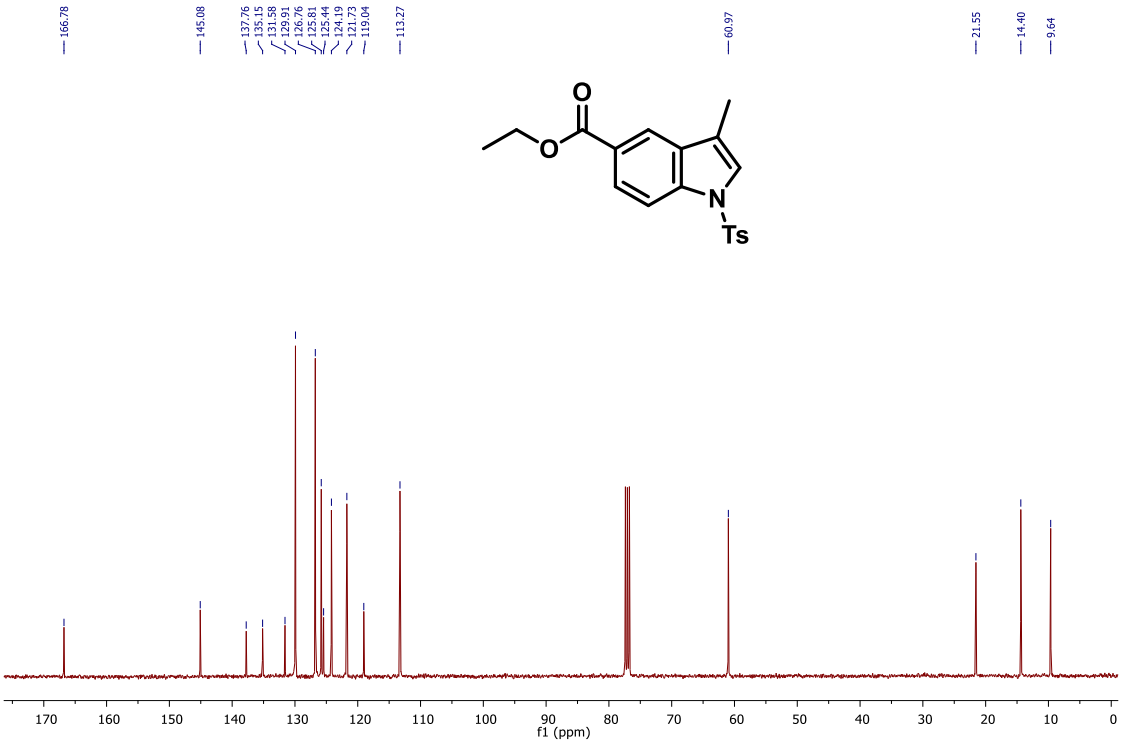

Figure 73: ^{13}C NMR (100 MHz, $CDCl_3$) Spectrum of compound **4b**.

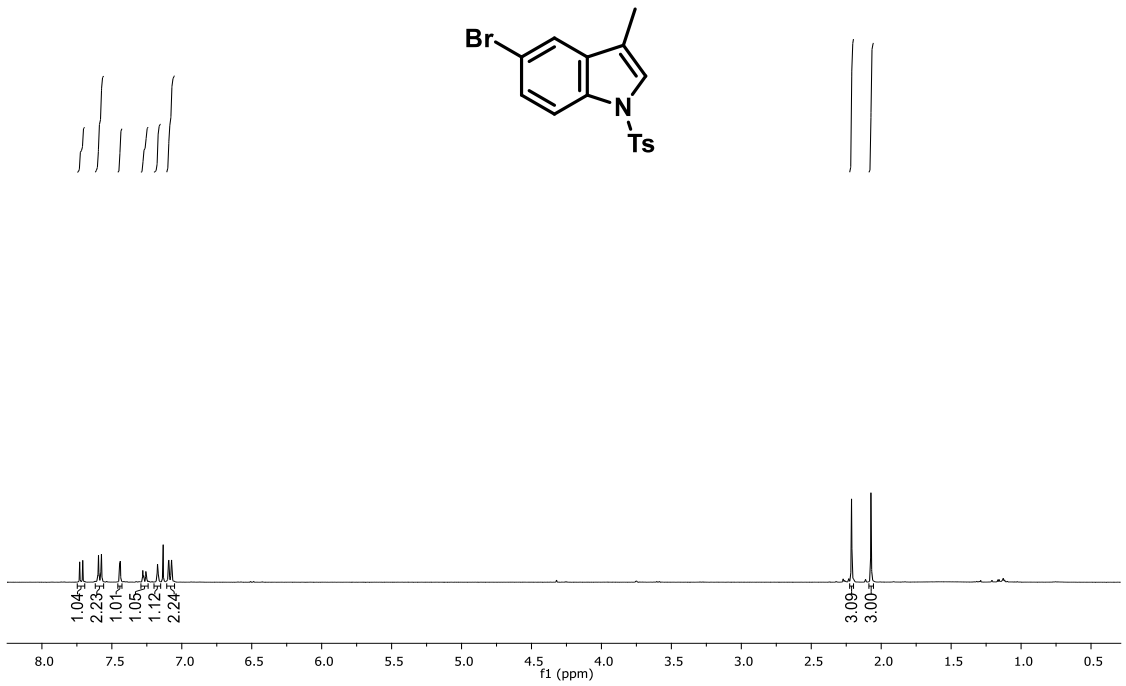

Figure 74: ^{1}H NMR (400 MHz, $CDCl_3$) Spectrum of compound **4c**.

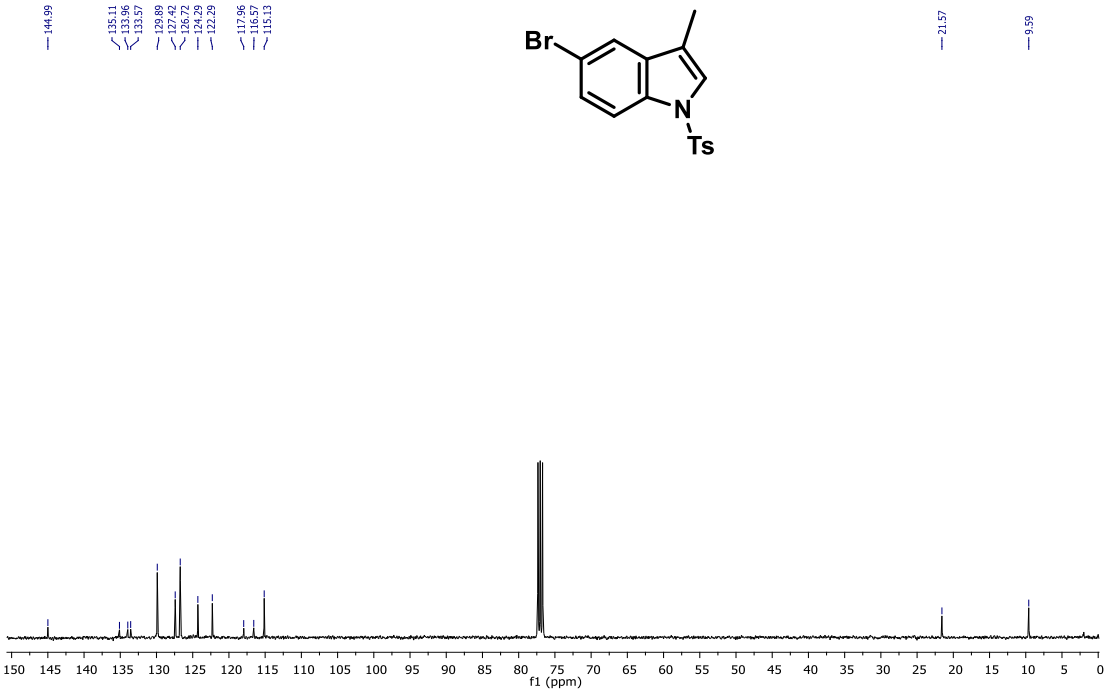

Figure 75: ^{13}C NMR (100 MHz, $CDCl_3$) Spectrum of compound **4c**.

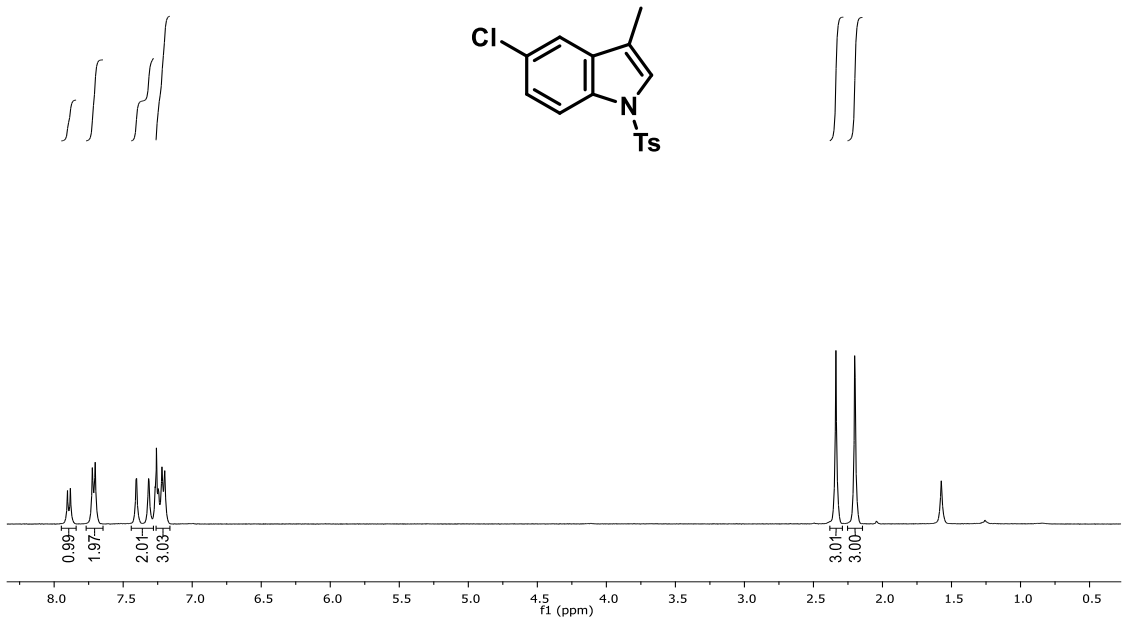

Figure 76: ^{1}H NMR (400 MHz, $CDCl_3$) Spectrum of compound **4d**.

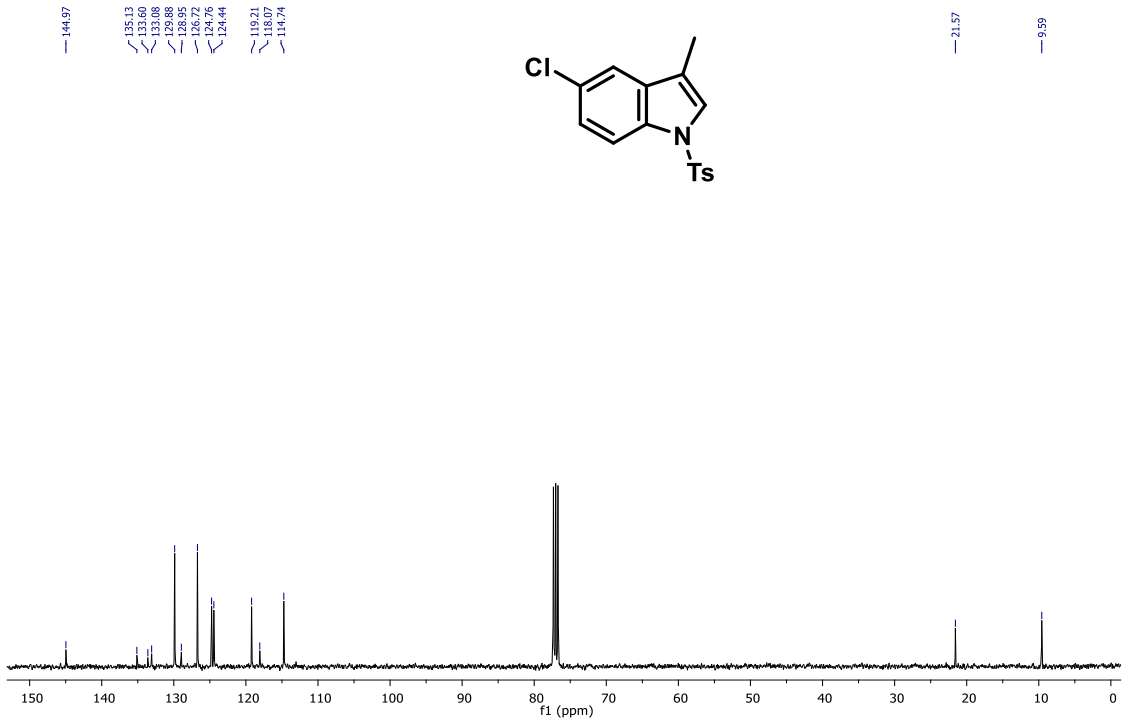

Figure 77: ^{13}C NMR (100 MHz, $CDCl_3$) Spectrum of compound **4d**.

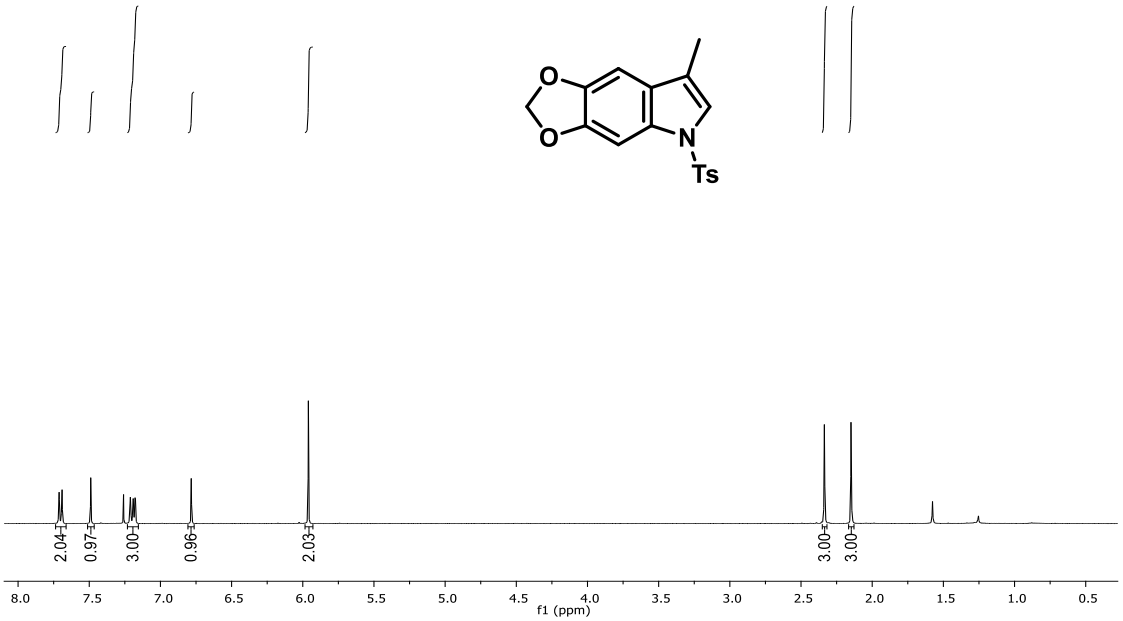

Figure 78: ^{1}H NMR (400 MHz, $CDCl_3$) Spectrum of compound **4e**.

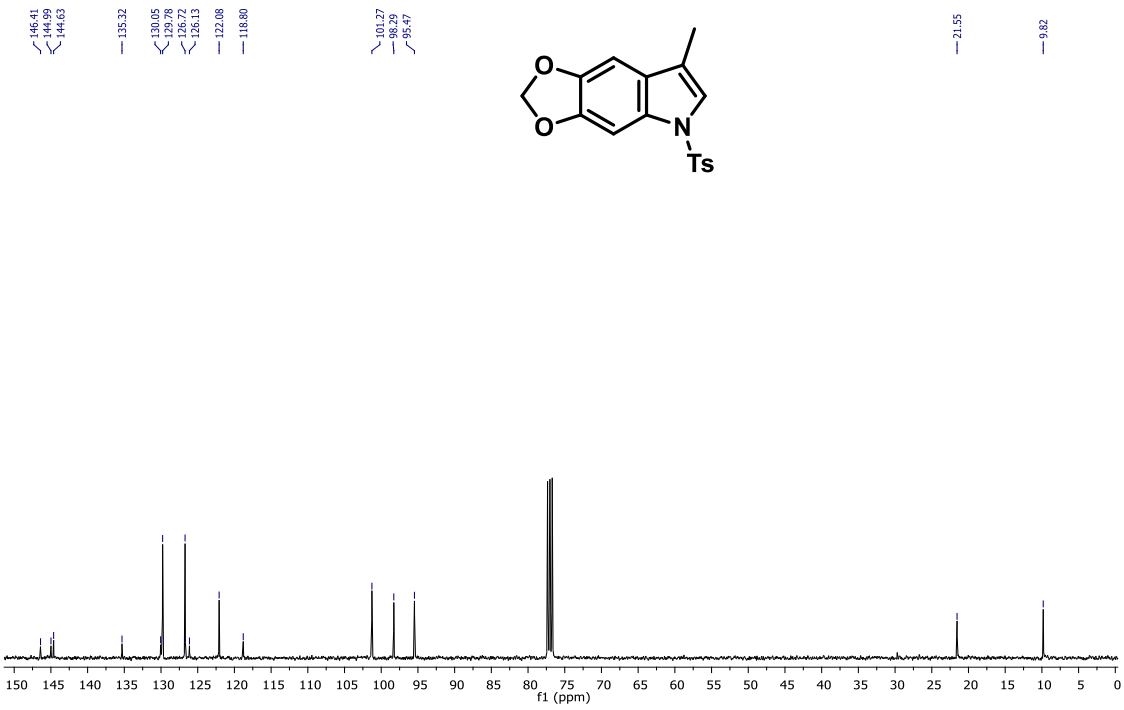

Figure 79: ^{13}C NMR (100 MHz, $CDCl_3$) Spectrum of compound **4e**.

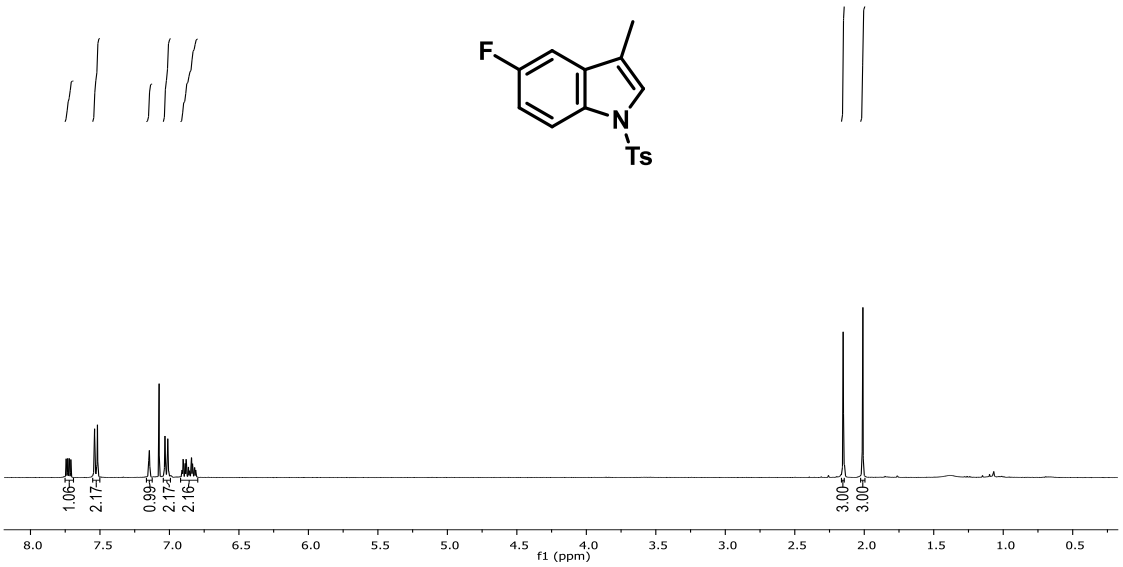

Figure 80: ^{1}H NMR (400 MHz, $CDCl_3$) Spectrum of compound **4f**.

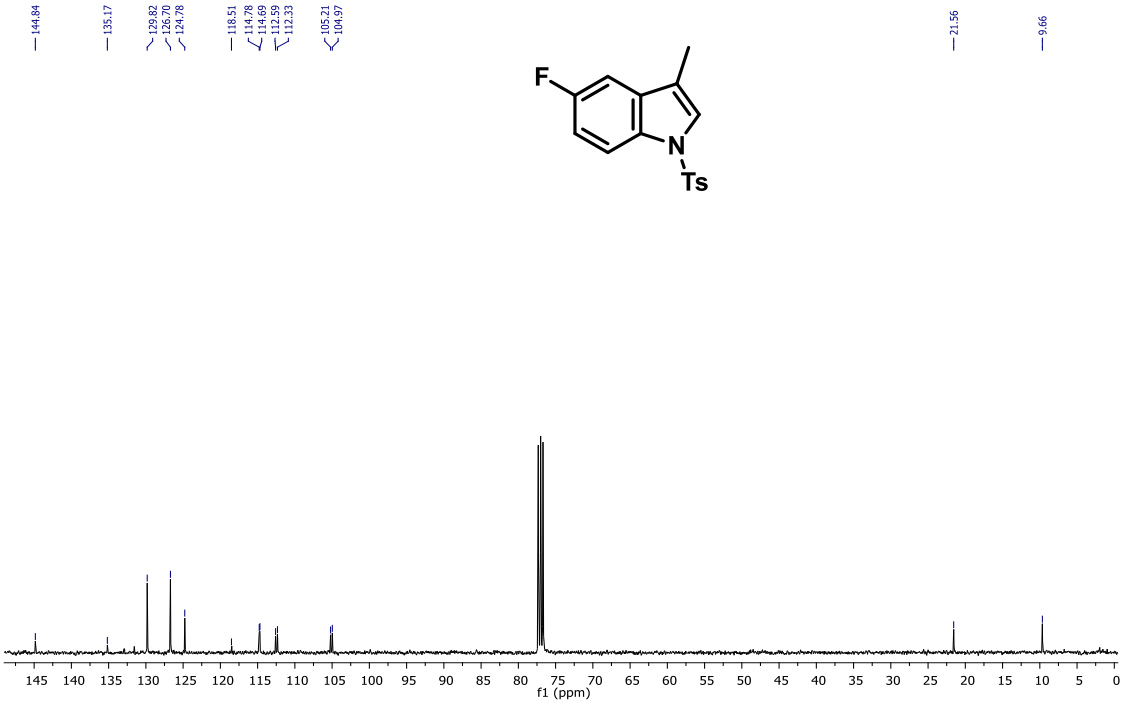

Figure 81: ^{13}C NMR (100 MHz, $CDCl_3$) Spectrum of compound **4f**.

4.5. References

(1) SINGH, T. P.; SINGH, O. M. Recent Progress in Biological Activities of Indole and Indole Alkaloids. *Mini-Reviews Med. Chem.* **2017**, *18* (1), 9–25. https://doi.org/10.2174/1389557517666170807123201.

(2) MA, Y.-M.; LIANG, X.-A.; KONG, Y.; JIA, B. Structural Diversity and Biological Activities of Indole Diketopiperazine Alkaloids from Fungi. *J. Agric. Food Chem.* **2016**, *64* (35), 6659–6671. https://doi.org/10.1021/acs.jafc.6b01772.

(3) MAIER, M. E. Design and synthesis of analogues of natural products. *Org. Biomol. Chem.* **2015**, *13* (19), 5302–5343. https://doi.org/10.1039/C5OB00169B.

(4) TABER, D. F.; TIRUNAHARI, P. K. Indole synthesis: a review and proposed classification. *Tetrahedron* **2011**, *67* (38), 7195–7210. https://doi.org/10.1016/j.tet.2011.06.040.

(5) AND, G. R. H.; KUETHE*, J. T. Practical Methodologies for the Synthesis of Indoles. **2006**. https://doi.org/10.1021/CR0505270.

(6) MIELCZAREK, M.; DEVAKARAM, R. V; MA, C.; YANG, X.; KANDEMIR, H.; PURWONO, B.; BLACK, D. S.; GRIFFITH, R.; LEWIS, P. J.; KUMAR, N. Synthesis and biological activity of novel bis-indole inhibitors of bacterial transcription initiation complex formation. *Org. Biomol. Chem.* **2014**, *12* (18), 2882–2894. https://doi.org/10.1039/c4ob00460d.

(7) FUWA, H.; SASAKI, M. Synthesis of Indoles and Indolines from α-Phosphoryloxy Enecarbamates. *Synfacts* **2007**, *2007* (11), 1143–1143. https://doi.org/10.1055/s-2007-991293.

(8) NAGARAJU, K.; MA, D. Oxidative coupling strategies for the synthesis of indole alkaloids. *Chem. Soc. Rev.* **2018**, *47* (21), 8018–8029. https://doi.org/10.1039/C8CS00305J.

(9) FUKUYAMA, T.; CHEN, X.; PENG, G. A Novel Tin-Mediated Indole Synthesis. *J. Am. Chem. Soc.* **1994**, *116* (7), 3127–3128. https://doi.org/10.1021/ja00086a054.

(10) JIANG, H.; BAK, J. R.; LÓPEZ-DELGADO, F. J.; JØRGENSEN, K. A. Practical metal- and additive-free methods for radical-mediated reduction and cyclization reactions. *Green Chem.* **2013**, *15* (12), 3355. https://doi.org/10.1039/c3gc41520a.

(11) DA SILVA, G. P.; ALI, A.; DA SILVA, R. C.; JIANG, H.; PAIXÃO, M. W. Tris(trimethylsilyl)silane and visible-light irradiation: A new metal- and additive-free photochemical process for the synthesis of indoles and oxindoles. *Chem. Commun.* **2015**, *51* (82), 15110–15113. https://doi.org/10.1039/c5cc06329a.

(12) CAIUBY, C. A. D.; ALI, A.; SANTANA, V. T.; DE LUCAS, F. W. S.; SANTOS, M. S.; CORRÊA, A. G.; NASCIMENTO, O. R.; JIANG, H.; PAIXÃO, M. W. Intramolecular radical cyclization approach to access highly substituted indolines and 2,3-dihydrobenzofurans under visible-light. *RSC Adv.* **2018**, *8* (23), 12879–12886. https://doi.org/10.1039/c8ra01787e.

(13) KÖNIG, B. Photocatalysis in Organic Synthesis - Past, Present, and Future. *European J. Org. Chem.* **2017**, *2017* (15), 1979–1981. https://doi.org/10.1002/ejoc.201700420.

(14) GILMORE, K.; SEEBERGER, P. H. Continuous Flow Photochemistry. *Chem. Rec.* **2014**, *14* (3), 410–418. https://doi.org/10.1002/tcr.201402035.

(15) HUNT, G.; TORABI, M.; GOVONE, L.; KARIMI, N.; MEHDIZADEH, A. Two-dimensional heat and mass transfer and thermodynamic analyses of porous microreactors with Soret and thermal radiation effects—An analytical approach. *Chem. Eng. Process. - Process Intensif.* **2018**, *126*, 190–205. https://doi.org/10.1016/J.CEP.2018.02.025.

(16) LAROCK, R. C.; YUM, E. K. Synthesis of indoles via palladium-catalyzed heteroannulation of internal alkynes. *J. Am. Chem. Soc.* **1991**, *113* (17), 6689–6690. https://doi.org/10.1021/ja00017a059.

(17) TASKER, S. Z.; JAMISON, T. F. Highly Regioselective Indoline Synthesis under Nickel/Photoredox Dual Catalysis. *J. Am. Chem. Soc.* **2015**, *137* (30), 9531–9534. https://doi.org/10.1021/jacs.5b05597.

(18) YAYLA, H. G.; PENG, F.; MANGION, I. K.; MCLAUGHLIN, M.; CAMPEAU, L.-C.; DAVIES, I. W.; DIROCCO, D. A.; KNOWLES, R. R. Discovery and mechanistic study of a photocatalytic indoline dehydrogenation for the synthesis of elbasvir. *Chem. Sci.* **2016**, *7* (3), 2066–2073. https://doi.org/10.1039/C5SC03350K.

(19) SANTANDREA, J.; KAIROUZ, V.; COLLINS, S. K. Continuous Flow Science in an Undergraduate Teaching Laboratory: Photocatalytic Thiol–Ene Reaction Using Visible Light. *J. Chem. Educ.* **2018**, *95* (6), 1073–1077. https://doi.org/10.1021/acs.jchemed.7b00639.

(20) ZOLLER, J.; FABRY, D. C.; RONGE, M. A.; RUEPING, M. Synthesis of Indoles Using Visible Light: Photoredox Catalysis for Palladium-Catalyzed C□H Activation. *Angew. Chemie Int. Ed.* **2014**, *53* (48), 13264–13268. https://doi.org/10.1002/anie.201405478.

(21) YANG, X.; LIU, W.; LI, L.; WEI, W.; LI, C.-J. Photo-induced Carboiodination: A Simple Way to Synthesize Functionalized Dihydrobenzofurans and Indolines. *Chem. - A Eur. J.* **2016**, *22* (43), 15252–15256. https://doi.org/10.1002/chem.201603608.

(22) LOUIE, J.; HARTWIG, J. F. Palladium-catalyzed synthesis of arylamines from aryl halides. Mechanistic studies lead to coupling in the absence of tin reagents. *Tetrahedron Lett.* **1995**, *36* (21), 3609–3612. https://doi.org/10.1016/0040-4039(95)00605-C.

(23) ADAM F. LITTKE; CHAOYANG DAI, AND; FU, G. C. Versatile Catalysts for the Suzuki Cross-Coupling of Arylboronic Acids with Aryl and Vinyl Halides and Triflates under Mild Conditions. **2000**. https://doi.org/10.1021/JA0002058.

(24) TOJO, G.; FERNÁNDEZ, M. Permanganate. In *Oxidation of Primary Alcohols to Carboxylic Acids*; Springer New York: New York, NY, 2007; pp 1–12. https://doi.org/10.1007/0-387-35432-8_1.

(25) KRIEBLE, V. K.; NOLL, C. I. The Hydrolysis of Nitriles with Acids. *J. Am. Chem. Soc.* **1939**, *61* (3), 560–563. https://doi.org/10.1021/ja01872a005.

(26) GANDHAMSETTY, N.; JEONG, J.; PARK, J.; PARK, S.; CHANG, S. Boron-

Catalyzed Silylative Reduction of Nitriles in Accessing Primary Amines and Imines. *J. Org. Chem.* **2015**, *80* (14), 7281–7287. https://doi.org/10.1021/acs.joc.5b00941.

(27) NICOLAOU, K. C.; ESTRADA, A. A.; ZAK, M.; LEE, S. H.; SAFINA, B. S. A Mild and Selective Method for the Hydrolysis of Esters with Trimethyltin Hydroxide. *Angew. Chemie* **2005**, *117* (9), 1402–1406. https://doi.org/10.1002/ange.200462207.

5. Conclusion and final remarks

Three different continuous flow system were setup. The designed systems offer a powerful tool for “greener processes” by improving product selectivity, energy saving, waste minimization, and reduction of time-consuming. The purification steps are:

-One-pot assembly of organocatalysts from a renewable source, resulting in a polyfurfuryl polymer, enabling the continuous production ofγ-nitroaldehyde in moderate yield and enantioselectivity, but excellent diastereoselectivity.

-The synthesis of 1,4,5-trisubstituted 1,2,3-triazoles with solid catalysis under batch and flow conditions with online monitoring of reaction proved to be an efficient strategy.

-The synthesis of indoles and indolines was achieved by using a metal free protocol ally to near visible-light (black light) irradiation and the use of TTMSS as a carbon-radical promoter. Flow conditions helps to decrease reaction time and increase selectivity.

Finally, we intend to use these systems as a platform to make sequential reactions in continuous flow, thus obtaining compounds with greater structural complexity.

Another possibility would be the use of online monitoring and purification system for high-throughput screening of biologically active compounds.